6-25-2018

Azido- and Triazolyl-modified Nucleoside/tide Analogues: Chemistry, Fluorescent Properties, and Anticancer Activities

Zhiwei Wen

zwen001@fiu.edu

FLORIDA INTERNATIONAL UNIVERSITY

Miami, Florida

AZIDO- AND TRIAZOLYL-MODIFIED NUCLEOSIDE/TIDE ANALOGUES:

CHEMISTRY, FLUORESCENT PROPERTIES, AND ANTICANCER ACTIVITIES

A dissertation submitted in partial fulfillment of

the requirements for the degree of

DOCTOR OF PHILOSOPHY

in

CHEMISTRY

by

Zhiwei Wen

2018

To: Dean Michael R. Heithaus
      College of Arts, Sciences and Education

This dissertation, written by Zhiwei Wen, and entitled Azido- and Triazolyl-modified Nucleoside/tide Analogues: Chemistry, Fluorescent Properties, and Anticancer Activities, having been approved in respect to style and intellectual content, is referred to you for judgment.

We have read this dissertation and recommend that it be approved.

_____
Kevin O'Shea

_____
Kathleen Rein

_____
David Becker

_____
Anthony J. McGoron

_____
Stanislaw F. Wnuk, Major Professor

Date of Defense: June 25, 2018

The dissertation of Zhiwei Wen is approved.

_____
Dean Michael R. Heithaus
College of Arts, Sciences and Education

_____
Andrés G. Gil
Vice President for Research and Economic Development
and Dean of the University Graduate School

Florida International University, 2018

DEDICATION

I would like to dedicate this dissertation to my wife Bixia Zhu, my parents Suhui Wen and Sanju Zhou, and my mentor Dr. Stanislaw F. Wnuk for their support.

感谢碧霞一直来的支持，感谢你一直陪我走南闯北，漂洋过海。让我不管到哪里，都有一个家。感谢我的父母一直来的理解和鼓励。子曰："父母在，不远游，游必有方"。望时机成熟，可常伴左右。

ACKNOWLEDGMENTS

Writing this dissertation gave me not only a chance to summarize my motivating anticancer research but also a good time to reflect on the help and support I have got from people around me during pursuing my Ph.D. at FIU in this five years.

I would first like to thank my mentor Dr. Stanislaw Wnuk for his outstanding supervision, support, friendship, and trust in me. I feel proud and lucky to get opportunity to be involved in the research on bioorganic chemistry of nucleoside/tides with applications in anticancer medicine, which I have my passion and enthusiasm for. I do appreciate everything, related to not only my research but also my personal life and future career development, he has done for me. Words cannot describe how thankful I am.

ABSTRACT OF THE DISSERTATION

AZIDO- AND TRIAZOLYL-MODIFIED NUCLEOSIDE/TIDE ANALOGUES:

CHEMISTRY, FLUORESCENT PROPERTIES, AND ANTICANCER ACTIVITIES

By

Zhiwei Wen

Florida International University, 2018

Miami, Florida

Professor Stanislaw F. Wnuk, Major Professor

Two classes of C5 azido-modified pyrimidine nucleosides were synthesized and explored as radiosensitizers. The 5-azidomethyl-2'-deoxyuridine (AmdU) was prepared from thymidine and converted to its cytosine counterpart (AmdC). The 5-(1-azidovinyl) modified 2'-deoxyuridine (AvdU) and 2'-deoxycytidine (AvdC) were prepared employing regioselective Ag-catalyzed hydroazidation of 5-ethynyl pyrimidine substrates with TMSN$_3$. AmdU and AmdC were converted to 5'-triphosphates AmdUTP and AmdCTP, and incorporated into DNA-fragments via polymerase-catalyzed reaction during DNA replication and base excision repair. Radiation-mediated prehydrated electrons formed in homogeneous aqueous glassy (7.5 M LiCl) systems in the absence of oxygen at 77 K led to site-specific formation of π-type aminyl radicals (RNH•) from AmdU, AmdC, AvdU, and AvdC. The ESR spectral studies and DFT calculations showed RNH• undergo facile conversion to thermodynamically more stable σ-type iminyl radicals, R=N•. For AmdU, conversion of RNH• to R=N• was bimolecular involving α-azidoalkyl radical as intermediate; however, for AvdU, RNH• tautomerized to R=N•. Our work provides the first evidence for the formation of RNH• attached to C5 position of azidopyrimidine

nucleoside and its facile conversion to R=N• under reductive environment. These aminyl and iminyl radicals can generate DNA damage via oxidative pathways. The azido-nucleosides were successfully applied as radiosensitizers in EMT6 cancer cells in both hypoxic and normoxic conditions. To explore the generation and reactivity of 2'-deoxyguanosin-N2-yl radical (dG(N2-H)•) postulated to generate from guanine moiety towards •OH, 2-azido-2'-deoxyinosine (2-N_3dI) was prepared by conversion of 2-amino group in protected dG into 2-azido via diazotization with *tert*-butyl nitrite followed by displacement with azide and deprotection. The investigation of dG(N2-H)• generated from 2-N_3dI and its subsequent reactions using ESR will be discussed.

Cycloaddition between 5-ethynylpyrimidine or 8-ethynylpurine nucleosides and TMSN$_3$ in the presence of Ag$_2$CO$_3$, CuI, or CuSO$_4$/sodium ascorbate provided *N*-unsubstituted 1,2,3-triazol-4-yl analogues of the parental DNA bases (*i.e.* 5-TrzdU, 5-TrzdC, 8-TrzdA, and 8-TrzdG). These novel triazolyl nucleosides showed excellent fluorescent properties: 8-TrzdA exhibits the highest quantum yield (Φ_F) of 44% while 8-TrzdG had Φ_F of 9%. The 5-TrzdU and 5-TrzdC showed a large Stokes shift of ~110 nm. The application of these fluorescent nucleosides to cell imaging and DNA modifications will also be discussed.

TABLE OF CONTENTS

LIST OF TABLES

LIST OF FIGURES

LIST OF SCHEMES

LIST OF ABBREVIATIONS

2-N$_3$dI	2-azido-2'-deoxyinosine
3'-AZT	3'-azido-3'-deoxythymidine
5-TrzdC	5-(1H-1,2,3-triazol-4-yl)-2'-deoxycytidine
5-TrzdU	5-(1H-1,2,3-triazol-4-yl)-2'-deoxyuridine
8-TrzdA	8-(1H-1,2,3-triazol-4-yl)-2'-deoxyadenosine
8-TrzdG	8-(1H-1,2,3-triazol-4-yl)-2'-deoxyguanosine
Ac	acetyl
AIBN	azobisisobutyronitrile
AmdC	5-azidomethyl-2'-deoxycytidine
AmdCTP	5-azidomethyl-2'-deoxycytidine 5'-triphosphate
AmdU	5-azidomethyl-2'-deoxyuridine
AmdUMP	5-azidomethyl-2'-deoxyuridine 5'-monophosphate
AmdUTP	5-azidomethyl-2'-deoxyuridine 5'-triphosphate
Ar	aromatic (NMR)
AvdC	5-(1-azidovinyl)-2'-deoxycytidine
AvdU	5-(1-azidovinyl)-2'-deoxyuridine
β	beta
BER	base excision repair
Boc	*tert*-buyloxycarbonyl
br	broad (NMR)
calcd	calculated (HRMS)

CEP	*N,N*-diisopropylamino-2-cyanoethoxyphosphinyl
CEPCl	*N,N*-diisopropylamino-2-cyanoethoxychlorophosphine
CuAAC	copper-catalyzed [3+2] azide-alkyne cycloaddition
ºC	degrees Celsius
d	doublet (NMR)
DBU	1,8-diazabicyclo[5.4.0]undec-7-ene
DCM	dichloromethane
dG(N2−H)•	2'-deoxyguanosin-N2-yl radical
diAcAmdU	3',5'-di-*O*-acetyl-5-azidomethyl-2'-deoxyuridine
DIAD	diisopropyl azodicarboxylate
DIPEA	*N,N*-diisopropylethylamine
DMAP	4-dimethylaminopyridine
DMF	*N,N*-dimethylformamide
DMSO	dimethylsulfoxide
DMT	4,4'-dimethoxytrityl
DMTCl	4,4'-dimethoxytrityl chloride
DNA	Deoxyribonucleic acid
dsDNA	double-stranded DNA
EC_{50}	concentration to reduce virus-induced cytopathogenicity by 50%
EDC	(*N*-dimethylaminopropyl)-*N'*-ethyl-carbodiimide
EPR	electron paramagnetic resonance
ESR	electron spin resonance
g	gram(s)

h	hour(s)
HCMV	human cytomegalovirus
HEL	human embryonic lung
HFCCs	hyperfine coupling constants
HIV	human immunodeficiency virus
HPLC	high performance liquid chromatography
HRMS	high resolution mass spectroscopy
HSV	herpes simplex virus
Hz	hertz
IC_{50}	half maximum inhibitory concentration
J	coupling constant in Hz (NMR)
L	liter(s)
m	milli; multiplet (NMR)
M	moles per liter
min	minute(s)
mol	mole(s)
MS	mass spectrometry
m/z	mass to charge ratio (MS)
NAs	nucleoside/tide analogues
NBS	*N*-bromosuccinimide
NPE	*p*-nitrophenethyl
NPEOH	*p*-nitrophenethyl alcohol

ODN	oligodeoxynucleotide
%	percentage
$POCl_3$	phosphoryl chloride
pol I	DNA polymerase I
pol β	DNA polymerase β
$PO(OMe)_3$	trimethyl phosphate
q	quartet (NMR)
quin	quintet (NMR)
R_f	retention factor
RNA	ribonucleic acid
RP	reverse phase (HPLC)
rt	room temperature
s	second(s); singlet (NMR)
SPAAC	strain-promoted alkyne-azide cycloadditions
ssDNA	single-stranded DNA
t	triplet (NMR)
TBA	tributylamine
TBAF	tetra-*n*-butylammonium fluoride
TBAPP	tributylammonium pyrophosphate
TBDMS	*tert*-butyldimethylsilyl
TBDMS-Cl	*tert*-butyldimethylsilyl
t-Bu	*tert*-butyl
TEA	trimethylamine

TFA	trifluoroacetic acid
THF	tetrahydrofuran
TK^+	wild-type thymidine kinase
TK^-	thymidine kinase--deficient
TLC	thin layer chromatography
TMS	trimethylsilyl
t_R	retention time (HPLC)
μ	micro
UV	ultraviolet
VZV	Varicella Zoster virus

1. INTRODUCTION

1.1. Anticancer nucleoside/tide analogues

Globally, cancer is the second most common cause of death and is responsible for one out of every six deaths. The cancerous cells undergo uncontrolled growth, avoid programmed cell death, as well as invade into tissues and form metastases. It was estimated that there will be around 1.7 million new cancer cases and around 600 thousand deaths caused by cancer in USA in 2018 (Table 1).[1] Cancer, a genetic disease, arises from the changes to genes, which would be inherited from parents, unrepaired errors during cell divisions, or DNA damages from certain environmental exposure (like unhealthy diet, tobacco, *etc.*)

Table 1. Estimated new cases of cancer and deaths in USA, 2018

	Estimated New Cases	Estimated Deaths
All Sites	1,735,350	609,640
Digestive system	319,160	160,820
Genital system	286,390	62,330
Breast	268,670	41,400
Respiratory system	253,290	158,770
Urinary system	150,350	33,170
Others	457,490	153150

Types of treatments of cancer include surgery, radiotherapy, chemotherapy, immunotherapy, hormone therapy, targeted therapy, and stem cell transplant. As a chemist, I am most interested in the chemotherapy, radiotherapy, and their combination. Among the anticancer drugs, nucleoside/tide analogues (NAs) have been approved by US Food and Drug Administration (FDA) and European Medicines Agency (EMA) and been in clinical use for the treatment of various cancers for about 49 years since the first approved nucleoside analogue, *i.e.,* cytarabine, for the treatment of acute myeloid leukemia.[2] Some

currently approved NAs as anticancer agents are summarized in Figure 1, in which the

modifications to the natural nucleoside/tides were highlighted in red. The approval of some

new nucleoside/tide analogues drugs in the past decade proves that nucleoside/tide

analogues still have excellent potential for the cancer treatment.

Cytarabine (1)
Pfizer, **1969**
Acute myeloid leukaemia
Acute lymphocytic leukaemia
Lymphomas

Fludarabine (2)
Genzyme, **1991**
Chronic lymphocytic leukaemia
Non-Hodgkins lymphoma
Acute myeloid leukaemia

Cladribine (3)
Janssen-Cilag, **1993**
Hairy cell leukaemia

Gemcitabine (4)
Eli Lilly and Co, **1996**
Non-small lung cancer
Pancreatic cancer
Bladder cancer
Breast cancer

Clofarabine (5)
Genzyme, **2004**
Acute lymphocytic leukaemia

Nelarabine (6)
SmithKline Beecham, **2005**
T-cell acute lymphoblastic leukaemia

Capecitabine (7)
Hoffmann-La Roche, **1998**
Metastatic breast cancer
Metastatic colorectal cancer

Floxuridine (8)
Hospira, **1970**
Advanced colon cancer
kidney cancer
stomach cancer

Deoxycoformycin (9)
Hospira Inc, **1991**
Hairy cell leukemia
Chronic lymphocytic leukemia

Azacitidine (10)
Celgene, **2004**
Myelodysplastic syndrome

Decitabine (11)
Eisai Inc. and Janssen Cilag, **2006**
Myelodysplastic syndrome
acute myeloid leukemia

Figure 1. Approved anticancer nucleoside/tide drugs

The differences between the nucleoside/tide analogues and their counterpart are tiny

(Figure 1). Like gemcitabine **4**, its difference from its counterpart deoxycytidine is the two

fluorine atoms at C2' position instead of two hydrogen atoms. Nevertheless, this tiny

2

difference endows the NAs with anticancer properties.[3] As demonstrated in Figure 2, firstly the NAs are taken up into cells through nucleoside transporters, organic anion/cation transporters, or peptide transporters.[2] Then, the nucleosides mimic natural nucleosides and are metabolically phosphorylated by nucleoside kinase, nucleoside monophosphate kinase and nucleoside diphosphate kinase. The NAs would interact with and inhibit important proteins. Nucleotides may also be incorporated into DNA/RNA and block the division of cancer cells. The inhibition of important proteins (enzymes) and incorporation into DNA would both lead to the apoptosis of tumor cells. [2,3]
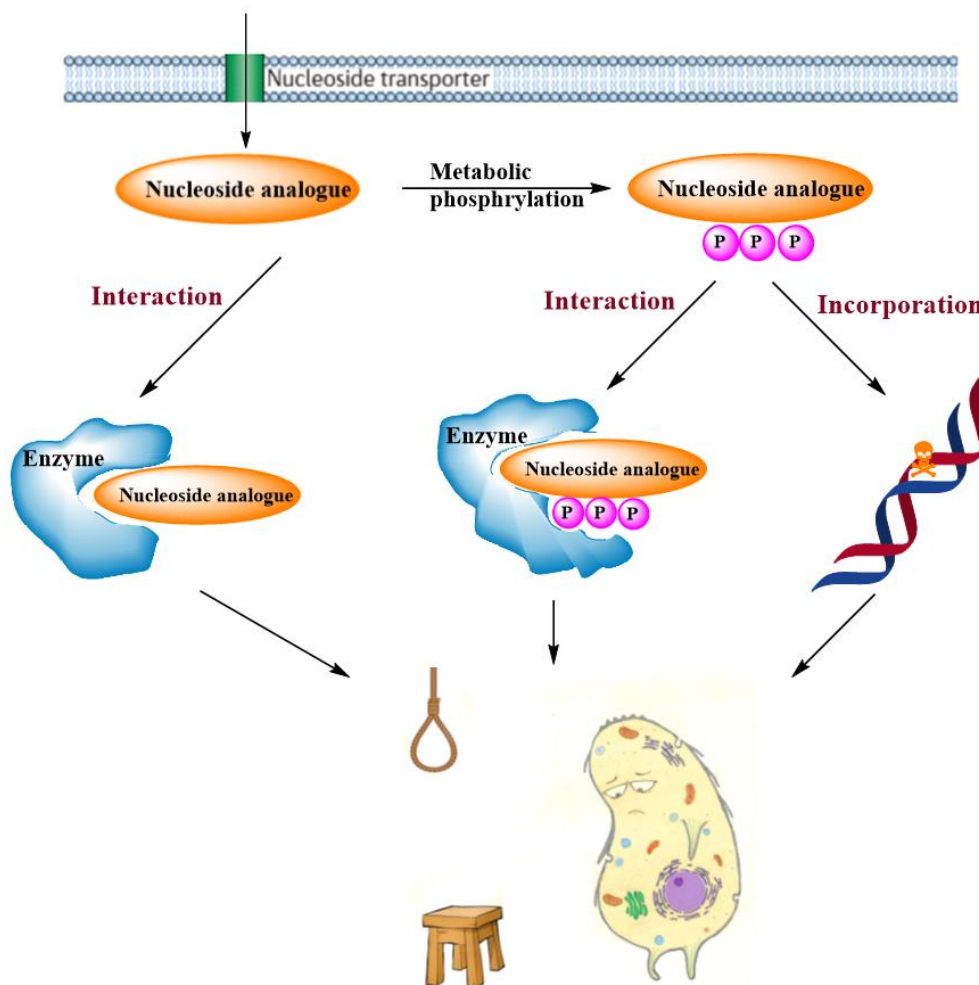
Figure 2. General mechanisms of anticancer activities of nucleoside/tide analogues

1.2. Cancer radiosensitization

1.2.1. Radiotherapy

Radiotherapy and its combination with other treatments (*e.g.,* surgery, chemotherapy) are applied for the treatment of most common types of cancers to cure or control tumors.[4,5] Even though new types of cancer treatment with better selectivity against cancerous cells,[6] like immunotherapy and targeted therapy, are emerging, almost half of all the cancer patients are still treated with radiotherapy.[7]

The mechanism of ionizing radiation during the radiotherapy is illustrated in Scheme 1. The interaction of ionizing radiation with materials inside cancerous cells includes direct and indirect effects.[7,8] Water in the cells undergo radiolysis to give ionized water cation ($H_2O^{\bullet+}$) and electrons. The water cation reacts with another water to yield reactive oxygen species (ROS) hydroxyl radicals (HO•), which is related to oxidative DNA damage.[9] The electron generated from water radiolysis is solvated to offer prehydrated electron e^-_{aq}, which further interact with oxygen to give superoxide ($O_2^{\bullet-}$) or with hydronium (H_3O^+) to give hydrogen atom (H•). The electrons are related to the reductive DNA damage. Approximately, the electrons with low energy are responsible for 67% of DNA damage, while the highly reactive HO• is responsible for the remaining 33%.[10] This DNA damage caused by the radicals generated from the radiolysis of water is named as indirect effect (Scheme 1). On the other hand, the ionizing radiation would also directly ionize the base or backbones of DNA fragments, which is named as direct effect.

DNA damage from the ionizing radiation includes damage to base or sugar, single/double-strand breaks, cross-linking of DNA and other biomolecules like DNA or

proteins, and so on. The DNA lesion frequency is revealed in Table 2.[11] The DNA damage results in the death of cancerous cells.[12-14]
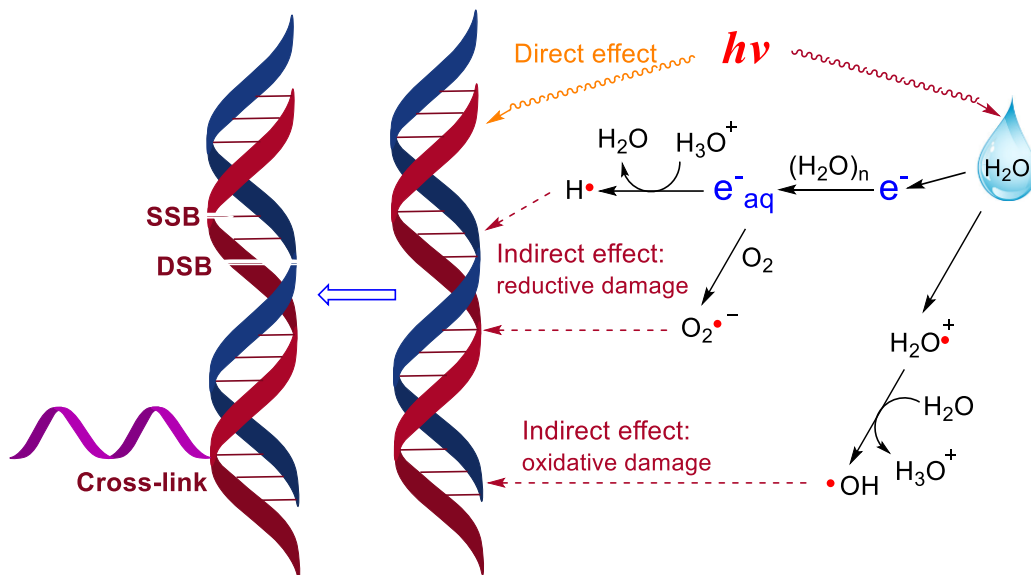
Scheme 1. The rationale for the direct/indirect effects of irradiation in radiotherapy

Table 2. The approximate number of DNA lesions per Gy per cell induced by ionizing radiation

DNA damage induced by ionizing radiation	Approximate number/Gy in one cell
DNA DSB (double-strand breaks)	40
DNA SSB (single-strand breaks)	1000
DNA-DNA cross-links	30
DNA-protein cross-links	150
Damage at base	2,000
Damage at sugar-phosphate backbone	1,000

1.2.2. Radiosensitizers (Radiosensitizing agents)

A high dose of ionizing radiation leads to both acute and cumulative side effects,[15] thus it is significant to enhance the radiosensitiveness of tumor cells during radiotherapy to lower the dose of radiation required for same surviving fraction. Radiosensitizers have been developed to enhance the sensitiveness of cancerous cells to radiotherapy.[3,16] Radiotherapy

employing radiosensitizers is used for most cancer patients and improves the survival compared to radiotherapy alone.[3] Radiosensitizers include small molecules, macromolecules, and nanomaterials.[8] The most conventional radiosensitizers include halogenated nucleosides, gemcitabine, and platinum analogues.[3,7]

The C5 halogenated pyrimidine bases and nucleosides are well-investigated as radiosensitizers in cancer radiotherapy.[3,7,17,18] 5-Bromo-2'-deoxyuridine (5-BrdU, **12**, Figure 3) has been recognized as a radiosensitizing agent with potential clinical applications.[17] However, owing to toxicity of 5-BrdU, it did not show any increase in patient survival during phase III clinical trials and the trials were called off.[19] On the other hand, 5-fluorouracil (5-FU, **13**, Figure 3) via protracted venous infusion has become a typical treatment of rectal[20] and pancreatic cancers.[21] The radiosensitizing effect of 5-fluorouracil is believed to derive from its inhibition of thymidylate synthase, which stops the DNA replication. The complex protracted venous infusion lasting for one to two months may lead to infection and/or thrombosis. As a consequence, capecitabine (**7**, Xeloda, Figure 1) was developed as a prodrug suitable for oral taken.[22] Capecitabine is used for the treatment of colorectal cancer, breast cancer, oesophageal cancer, and gastric cancer.[23]
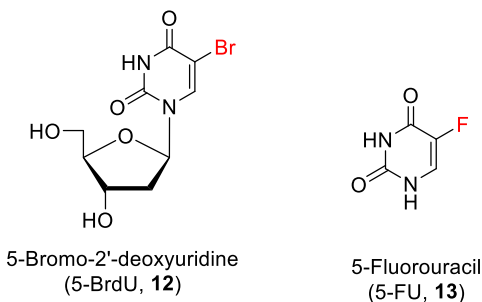
Figure 3. Structures of C5 halogenated pyrimidine bases and nucleosides

Gemcitabine (**4**, Figure 1) was explored as radiosensitizer to enhance the sensitiveness of human colon carcinoma cells to radiation.[24] The radiosensitizing effect of gemcitabine is a result of inhibition of ribonucleotide reductase, which depletes the dATP pools. The cells progressing into S phase suffer from the depletion of dATP and the consequent misincorporation and misrepair of wrong bases, which generate DNA lesions that lead to the cell apoptosis.[3]

In addition to the nucleoside-based radiosensitizers, there are various non-nucleosides-based radiosensitizing agents, among which platinum analogues have been applied clinically as a radiosensitizers to treat various cancerous tumors.[3]

Cisplatin (**14**)   Carboplatin (**15**)   Oxaliplatin (**16**)
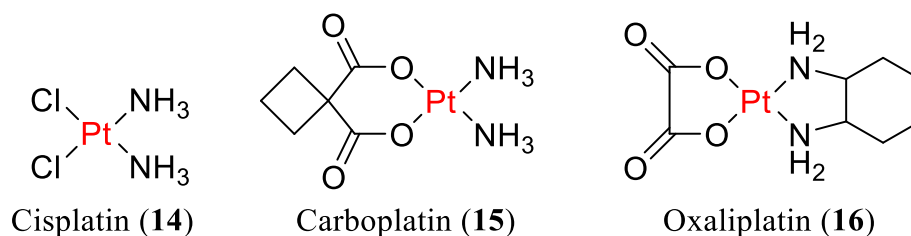
Figure 4. Platinum analogues applied clinically as a radiosensitizers

Cisplatin analogues (Figure 4) are well known to interfere with DNA replication by forming 1,2-intrastrand crosslinks with two adjacent guanine/guanine (90%) along DNA fragment as well as with adjacent guanine and adenine, which induces apoptosis of fast proliferating cells (Figure 5).[25] The mechanisms of the radiosensitizing effect of cisplatin analogues include formation of more toxic platinum intermediates from the interaction between the cisplatin and free radicals induced by irradiation (Irradiated hypoxic solutions of cisplatin were more toxic than unirradiated solutions),[26] enhanced uptake of carboplatin into cells induced by irradiation,[27] and repression of DNA repair.[28]
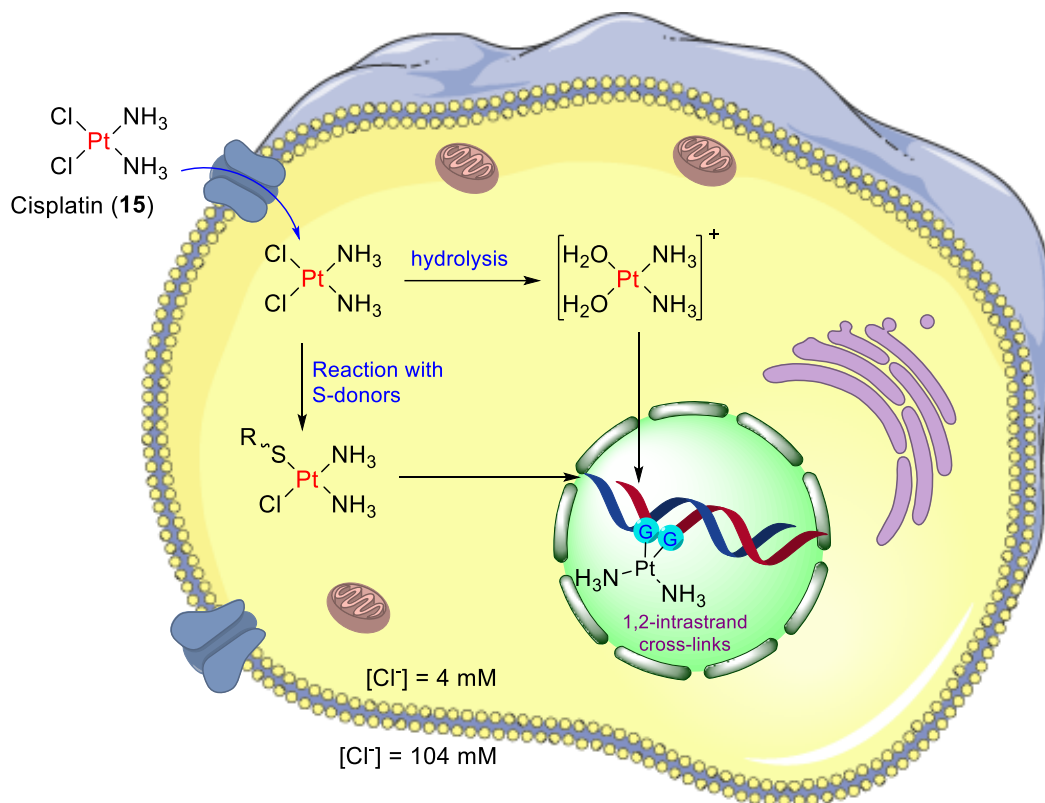
Figure 5. Mechanism of the anticancer activity of cisplatin

1.2.3. Hypoxia and hypoxia-selective radiosensitizers

Tumor cells replicate quickly and require nutrients from blood vessels. As solid tumors grow, angiogenesis allows the generation of new vascular beds to support the cancerous cells.[29] Nevertheless, the morbid tumor vascular bed formed during the angiogenesis is twisting and irregular and thus lacks the ability to deliver blood to every part of the tumors. As a consequence, solid tumors encompass regions with transient and chronic low concentration of oxygen, which is named as transient hypoxia and chronic hypoxia, respectively.[30-32]

The partial pressure of oxygen (pO_2) in human tumors is less than 5 mmHg, while the pO_2 in the surrounding normal cells is higher than 30 mmHg. As discussed in section 1.2.1

8

and shown in Scheme 1, oxygen is essential for the sensitiveness of cancerous cells in radiotherapy. The tumor cells under hypoxic microenvironment are resistant to radiotherapy and chemotherapy.[30] On the other hand, the existence of hypoxia, unique features of solid tumors that is not found in normal cells, offers an chance for tumor-selective therapy.

One of the strategies exploiting the tumor hypoxia is to design prodrugs activated by hypoxia. Tirapazamine (17, TPZ, Scheme 2), the first developed specific cytotoxin for hypoxia, was demonstrated for its antitumor activity.[33] The mechanism for the hypoxia-selectivity of TPZ 17 was shown in Scheme 2.[30] TPZ 17 undergoes one-electron reduction by reductases or aquated electron from radiolysis of water to give tirapazamine radicals (TPZ•). TPZ• further decays to hydroxyl radical (HO•) or benzotriazinyl radical (BTZ•), which poisons the topoisomerase II and leads to DNA double-strand breaks.[33]
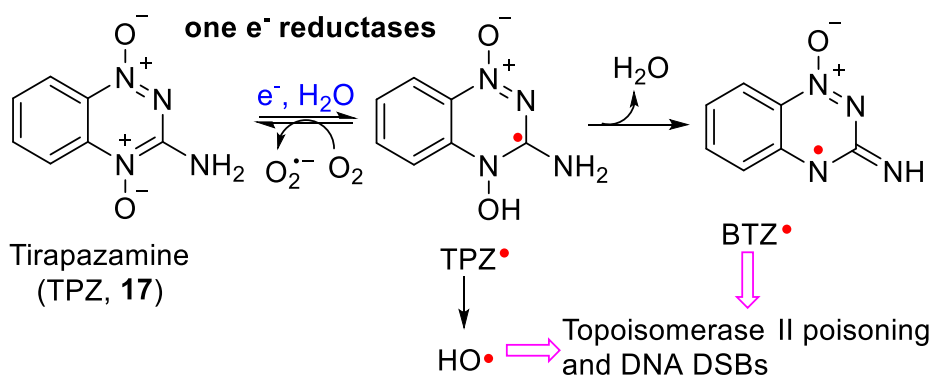
Scheme 2. The mechanism for the hypoxia-selectivity of tirapazamine

However, the cells under hypoxic condition usually lack reductase enzymes and cofactors. Thus, developing radiosensitizers activated by irradiation-induced prehydrated electron is more attractive than activation by enzymes. Cobalt(III) complexes,[34] nitrobenzyl quaternary ammonium salts,[35] and oxypropyl-substituted 5-fluorouracil

derivatives[36] (Figure 6) were demonstrated to be capably triggered by ionizing radiation under hypoxic conditions. Nevertheless, none of the compounds has yet shown undisputed radiosensitizations in hypoxic tumors. As a result, more effort and research should be dedicated to the development of new hypoxia-selective radiosensitizers activated by irradiation.

Cobalt(III)
(8-hydroxyquinoline)
complexes

Wilson, W. R. and coworkers,
Radiat. Res. **2004**, *162*, 315-325.

Nitrobenzyl quaternary
ammonium salts

Wilson, W. R. and coworkers,
Radiat. Res. **2002**, *158*, 753-762.

Oxypropyl-substituted
5-fluorouracil derivatives

Nishimoto, S.-i. and coworkers,
Jpn. J. Cancer Res. **2000**, *91*, 433-438.
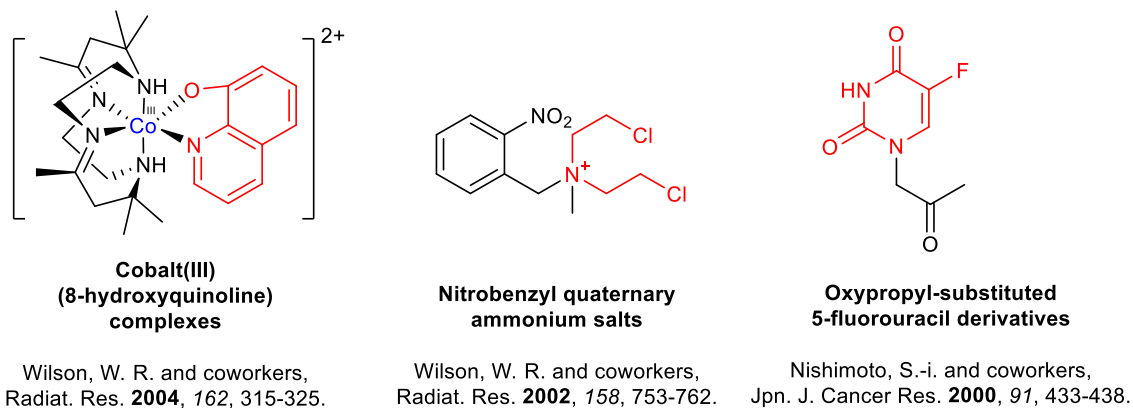
Figure 6. Radiosensitizers activated by irradiation-induced prehydrated electron

1.3. Azido-modified nucleoside/tide analogues as biological probe for click reaction

Because of the various novel properties, azido modified small molecules and biomacromolecules have been designed and investigated for a variety of applications including serving as biological probes for cycloaddition click reaction for bioconjugation, anticancer and antiviral agents, and potential radiosensitizers.[37-42]

The absence of azides in almost all creatures and their inert reactivity with water, amines, oxidant, or other functional groups abundant in biological systems endow the azides with exquisite bioorthogonality. The bioorthogonal ligations employing azides include Staudinger ligation of azides with phosphines as wells as click reactions between azides and strain-promoted alkyne or terminal alkyne catalyzed by copper (Table 3).[43]

10

Table 3. Azido-modified biomolecules for labeling and tracking

Chemical Reporter	Reactive partner (R' = probe)	Ligation Product
R-N₃ Target R: Nucleic acid Protein Glycan Lipid	Staudinger Ligation	
	Cu-catalyzed Cycloaddition ≡—R', CuI (cat)	
	Strain-promoted Cycloaddition	
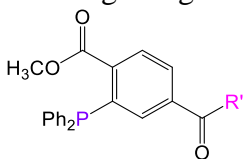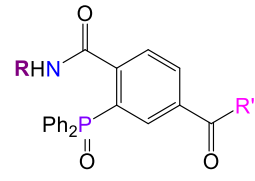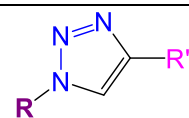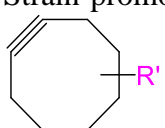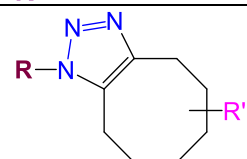
In 2002, Sharpless and Meldal brought the Huisgen [3+2] cycloaddition between azide and alkyne into focus by employing copper as a catalyst.[44,45] The copper-catalyzed [3+2] azide-alkyne cycloaddition (CuAAC) could proceed smoothly under mild reaction condition in aqueous media to form 1,2,3-triazoles, and thus is biocompatible. The toxic copper limits the application of CuAAC in living cells and animals. The strain-promoted azide-alkyne cycloaddition (SPAAC) "click" reactions developed by Bertozzi in 2004[46] expanded the application of [3+2] azide-alkyne cycloaddition in covalent interaction of biomolecule/biomolecule and biomolecule/probe in living systems. Azide as a reactive reporter introduced into a target biomolecule like nucleic acid, protein, glycans, and lipids reacts with probe or other biomolecules modified with terminal alkyne/cyclooctyne via CuAAC or SPAAC to label and track biomolecules.[43,47] CuAAC and SPAAC are broadly used for bioorthogonal conjugation, new drug discovery, and proteomic profiling.[48-51]

The chemically stable 5-azidomethyl-2'-deoxyuridine (AmdU, **18**, Figure 7), as opposed to the highly photolyzable 5-azido-2'-deoxyuridine (5-AdU),[52] serves as a

substrate for the synthesis of clickable triazoles.[40,53-57] AmdU **18** was able to be metabolically incorporated into DNA in living cells for click labeling of DNA.[40]
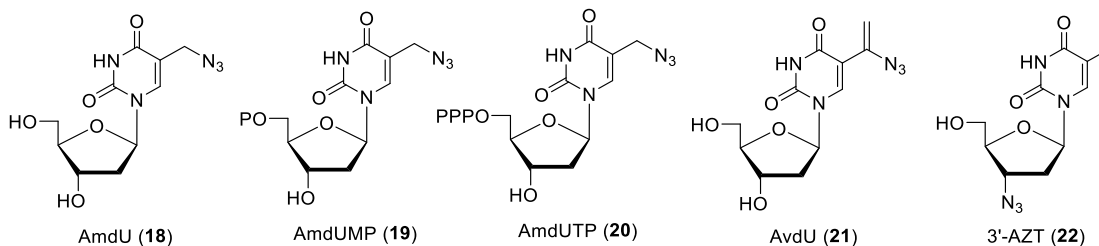
Figure 7. Azido-modified pyrimidine nucleoside/tide analogues

1.4. Anticancer and radiosensitizing properties of azido-modified nucleoside/tide analogues

1.4.1. Anticancer activities of azido-modified nucleoside/tide analogues

Azido-modified pyrimidine nucleoside analogues were reported to exhibit anticancer and antiviral activities. The 3'-azido-3'-deoxythymidine (3'-AZT, **22**, Figure 7), first prepared by Horwitz in 1964,[58] has been widely investigated for its anticancer and antiviral activities. The 3'-AZT has been commonly used to treat HIV positive patients benefit from its antihuman telomerase reverse transcriptase activity[59] and also used as a radiosensitizer for tumors of patients also carrying HIV.[60] The mechanism of the formation of reactive aminyl radical responsible for the radiosensitivity of 3'-AZT will be detailed in section 1.5.

The AmdU **18** and its monophosphate (AmdUMP **19**, Figure 7)[61,62] inhibited thymidylate synthetase activity derived from calf thymus and Ehrlich ascites tumor.[61,63] They also inhibited thymidine kinase activity[64] and consequently affected the growth of murine sarcoma 180 and L1210,[41,62] and the replication of herpes simplex virus type 1 (HSV-1).[41,65,66] The AmdU 5'-triphosphate (AmdUTP, **20**) was found to be a substrate for DNA polymerases and PCR amplification.[57] Moreover, the clickable triazole adducts of

12

5-AdU[67] were incorporated into oligodeoxynucleotides; but, an attempt to synthesize the peptide-siRNA covalent conjugates from AmdU-derived triazole was unsuccessful.[53]

The 5-(1-azidovinyl)-2'-deoxyuridine (AvdU, **21**) proved inhibitory to the replication of HSV-1 and VZV and became highly cytostatic against HSV-1 and HSV-2 TK gene transfected FM3A tumor cells; the cytostatic effect was enhanced by 5-fold after short exposure to UV irradiation at 254 nm.[68] AvdU **21** showed also anti-mycobacterial activities in submicromolar range.[69]

1.4.2. Azido-modified nucleoside/tide analogues as radiosensitizers

The 3'-AZT **22** (Figure 7) has been employed as a radiation sensitizer in radiotherapy of tumors for HIV positive patients.[60] Zhou and his colleagues reported their results on the investigation of the effects of 3'-AZT **22** combining with γ-radiation on telomere length, activity of telomerase, DNA single/double-strand breaks, and of its radiosensitizing effects in human malignant glioma cell line U251.[70] The 3'-AZT **22** suppressed the telomerase activity and slowed down DNA strand breaks repair. The changes in radiosensitivity were quantified by the sensitization enhancement ratio (SER). The 3'-AZT **22** (800 μM) enhanced the radiosensitivity at 2 Gy γ-radiation of U251 cells with SER of 1.37. The 3'-AZT **22** also increased the radiosensitivity of Hep-2 cells.[71]

In addition to the radiosensitizing effect, 3'-AZT **22** was also reported to enhance cytotoxicity of the anticancer drugs in the irradiated cancerous cells. The 3'-AZT **22** was able to enhance the radiosensitizing effects of (*E*)-2'-deoxy-(fluoromethylene)cytidine (FMdC) on human colon cancer cells.[72] Various concentration (25 μM to 100 μM) of **22** was added immediately before irradiation of the cancerous cells treated with FMdC. The combination of FMdC and 3'AZT **22** gave SER ranging from 1.25 to 2.26.

1.5. Formation of aminyl radicals on prehydrated one-electron attachment to azido-modified nucleosides and their subsequent reactions

The formation of neutral and reactive aminyl radicals on prehydrated one-electron attachment to azido-modified nucleosides in γ-irradiated aqueous glassy (7.5 M LiCl) systems was characterized using electron spin resonance spectroscopy (ESR).[42,73] γ-Irradiated chloride ion in glassy system at 77 K produced chlorine radical and electron (Scheme 3), which was solvated to yield aquated electron. Electron attachment to the azido group led to azide anion radical intermediate **I** ($RN_3\bullet^-$), which formed nitrene anion radical intermediate **II** ($RN\bullet^-$) after the loss of N_2. Subsequently, rapid protonation of $RN\bullet^-$ from the solvent led to $RNH\bullet$ formation.
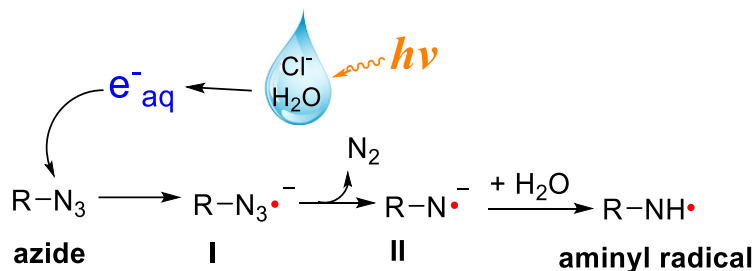
Scheme 3. The mechanism of formation of aminyl radicals on electron attachment to azido compounds in γ-irradiated aqueous glassy system

Radical at C5' position (C5'•) was reported to cause DNA strand breaks and associate unaltered base release.[9] To prove that the ring-opened C4'• is an intermediate in mechanism of C5'• mediated unaltered base release, methyl 2-azido-2-deoxy-α-D-lyxofuranoside (**23**, Scheme 4) as well as other azido-modified pentofuranoses were prepared and used for the ESR study (Scheme 4).[73] In methyl 2-azido-2-deoxy-α-D-lyxofuranoside, the aminyl radical (**I**, Scheme 4) at the 2 position undergoes intramolecular H-abstraction to give C5'• (**II**), which further undergoes intramolecular conversion to the ring-opened C4'• (**III**).

14
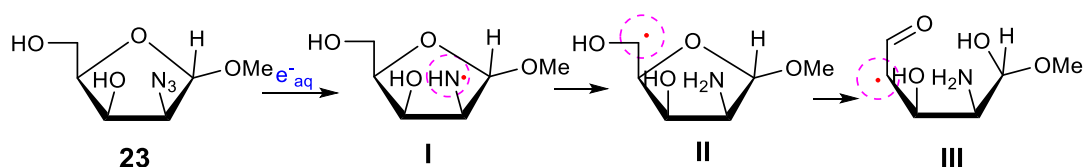
Scheme 4. Formation of aminyl radicals in methyl 2-azido-2-deoxy-α-D-lyxofuranoside and subsequent intramolecular H-atom transfer and ring opening

In 3'-AZT **22**, the aminyl radical at the C3'-site of sugar moiety underwent a bimolecular H-atom abstraction either from the methyl group at C5 to give dUCH$_2$•, from the C5'-atom to give C5'•, or from the C3'-atom to give C3'• of a proximate 3'-AZT (Scheme 5A).[42] On the other hand, the aminyl radical at the C3' site from 3'-azido-2',3'-dideoxyguanosine (3'-AZddG, **24**) resulted in one-electron oxidation of guanine base to give G(N1-H)• (Scheme 5B). The radicals formed at sugar are known to lead to strand breakage in RNA (Scheme 6A) and DNA (Scheme 6B), and further affects the apoptosis of cancer cells.[9,17] The structural DNA damage, like formamidopyrimidines (*e.g.,* FapyG) and 8-oxopurines (*e.g.,* 8-oxoG), formed from the guaninyl radicals are cytotoxic.[74]
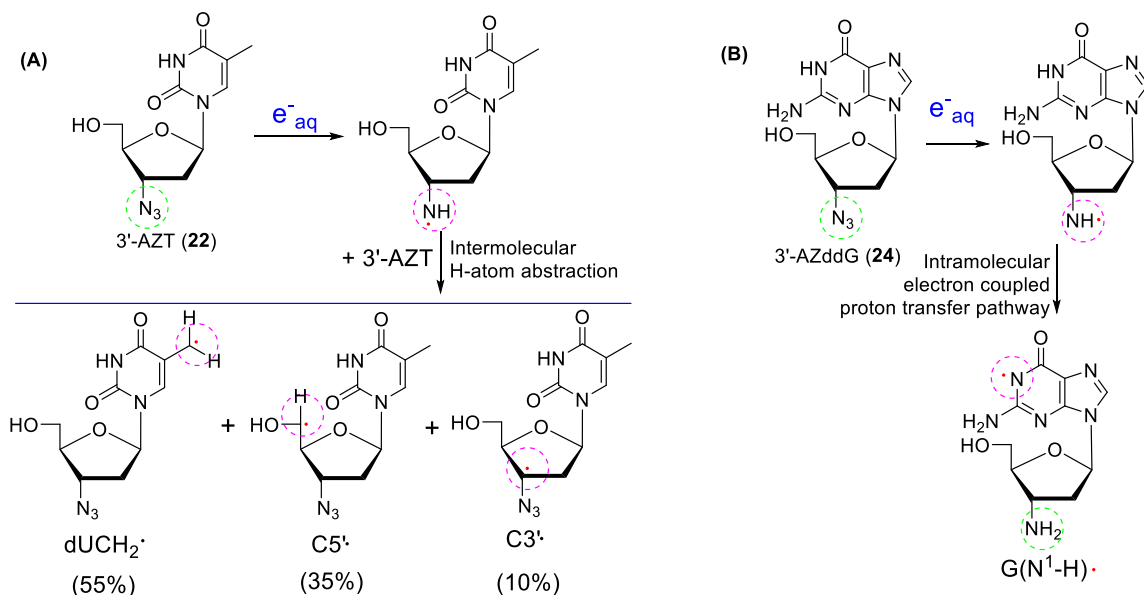
Scheme 5. Prehydrated one-electron attachment to azido group on 3'-AZT(**A**) and 3'-AZddG (**B**): Aminyl radical formation and subsequent reactions

15

(A) RNA breakage

(B) DNA breakage
  i. C1'-radical

  ii. C3'-radical

  iii. C5'-radical
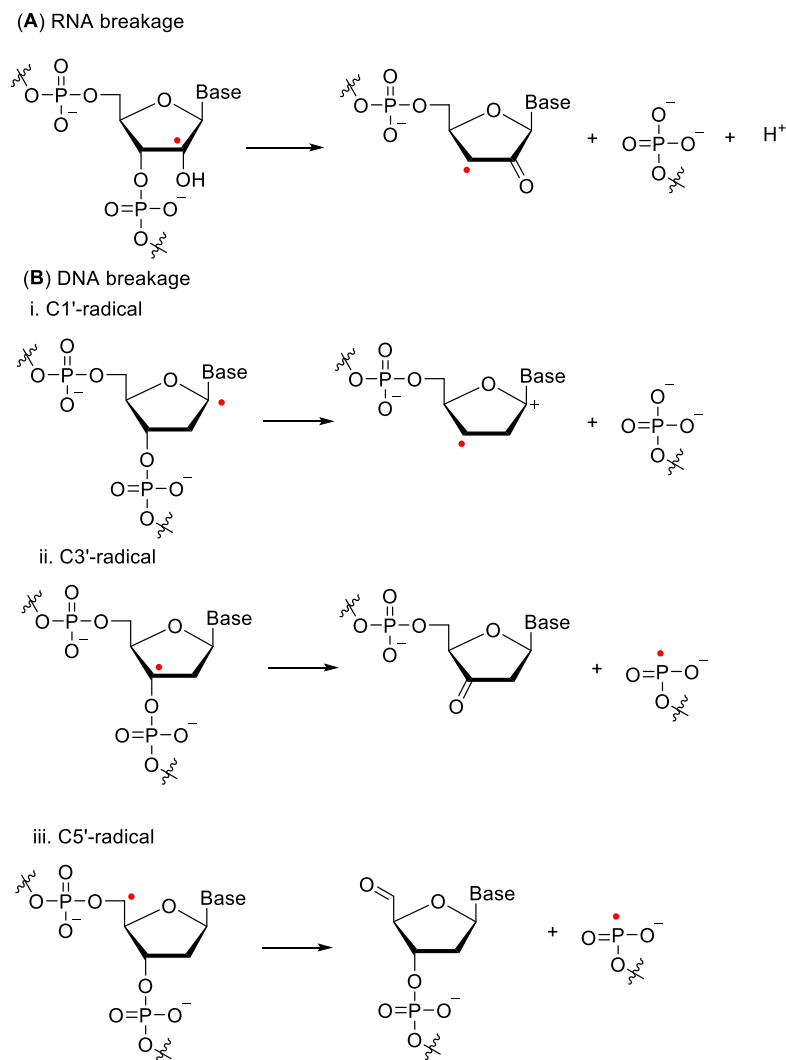
Scheme 6. Mechanism of RNA/DNA single-strand breaks upon generation of sugar radicals

The azido group in 3'-AZT **22** rather than the thymine moiety was proved to be the predominant site of electron capture, as a result of the higher electron affinity of the azido group in **22** than the most electron affinic DNA base, thymine.[42] The formation of the reactive aminyl radicals in γ-irradiated system and their subsequent reactions provides a plausible mechanism for the radiosensitizing effects of 3'-AZT[60,70,72,75] and meanwhile suggest that the azido-modified nucleoside/tide analogues are possible to be explored as potential radiosensitizing agents in hypoxia (bioreductive) microenvironments.

1.6. Electron-hole transfer in DNA

As discussed at section 1.2.1 (Scheme 1), hydroxyl radical HO• generated from ionizing irradiation causes DNA damage by reaction with guanine residues having the lowest oxidation potential.[76,77] Deeper understanding of the pathways for γ-radiolysis damage to nucleic acids and how cancerous cells respond to radiotherapy would help the design of new treatments and improve current-existing therapies. Thus, it is essential to understand reactions of guanine with the reactive radicals, like hydroxyl radical during the radiolysis, and the subsequent reactions.
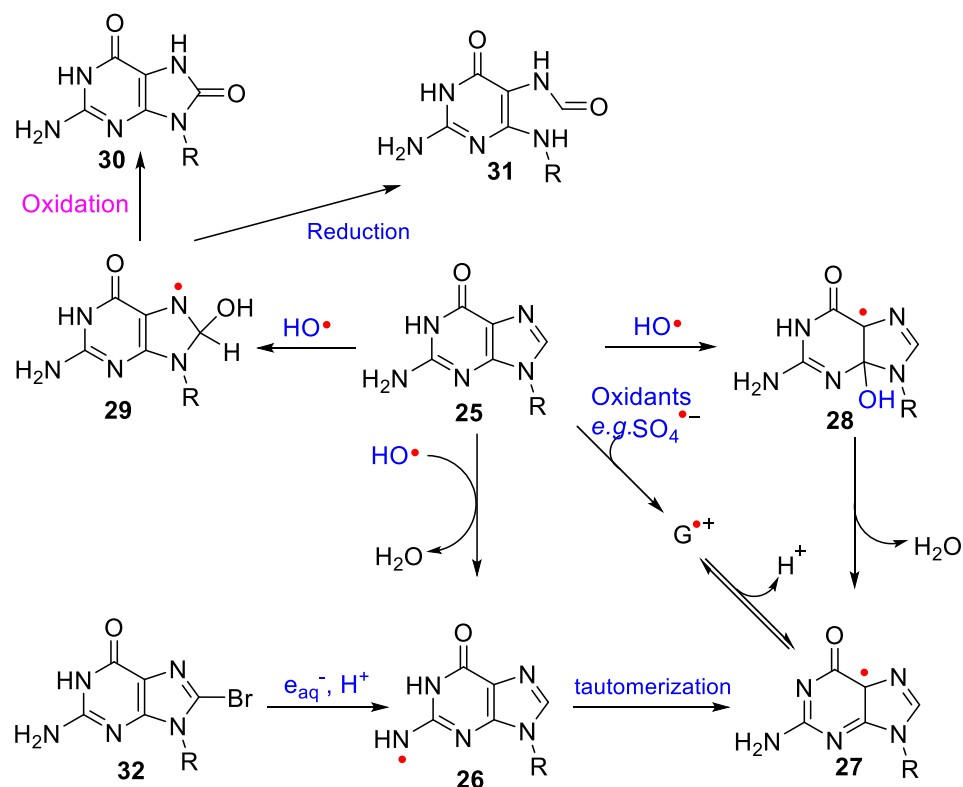
Scheme 7. Radical reactions of guanine with hydroxyl radicals and subsequent reactions

One-electron oxidation of guanine **25** by oxidants leads to the formation of G•+, which undergoes deprotonation to give guanyl radical **27** (Scheme 7).[78] The reaction between the

guanine **25** and hydroxyl radical was studied using optical absorption. On the basis of the absorption, the major radical (65%) was assigned to C5• generated from the addition of HO• at C4, which further dehydrate to yield radical **27**.[79,80] In addition to the **28**, 17% of HO• involves in the addition at C8 to provide radical **29**, which is further converted into 8-oxoG **30** and FapyG **31** via oxidation and reduction, respectively. In 2009, Chatgilialoglu reevaluate the reactivity of guanine towards HO•. Based on the DFT-TD calculations they assign the major radical to guan-N2-yl radical (G(N2-H)•, **26**).[81] The more favored formation of **26** from H-atom abstraction from **25** by HO• than the formation of **28** was further established by a Car-Parrinello molecular dynamics study.[82]

The 8-substituted (*e.g.,* Cl, Br **32**, I, and N_3) guanine derivatives were designed for investigating the formation and tautomerizations of one-electron-oxidized guanine.[77] The pulse radiolysis technique with optical absorption detection and DFT calculations reveal the formation of radicals **26** as well as N3• with iminic and aminic forms, the tautomers of **27**.[77,83,84]

As mentioned in section 1.5, ESR could be applied as a powerful tool to characterize radicals from the reaction between guanine and HO•. Nevertheless, ESR was not popular for identifying the radicals in previous research. An attempt was made to use ESR to investigate the formation of dG(N2−H)• **26** from hydrazine was not successful and the resulting product dG was the evidence for the formation of **26** during the photolysis.[85]

On the basis of the formation of aminyl radicals on prehydrated one-electron attachment to 3'-AZT **22**[42] (detailed at section 1.5), it is possible to explore azido-modified guanine derivatives as efficient precursors for investigation of elusive guanine-based aminyl radical under reducing conditions.

1.7. Fluorescent nucleosides for investigating nucleic acid structure, location, activation, and interactions

The natural purine and pyrimidine bases in nucleic acids have weak fluorescent properties (Figure 8).[86] Modified fluorescent nucleoside analogues with minimal perturbation to the natural DNA/RNA structures have attracted attention for their application to studying the perturbations to the nucleic acids such as abasic site from depurination/depyrimidination,[87] base flipping,[88] interaction between DNA/RNA and ligands,[89,90] and so on.[91,92]
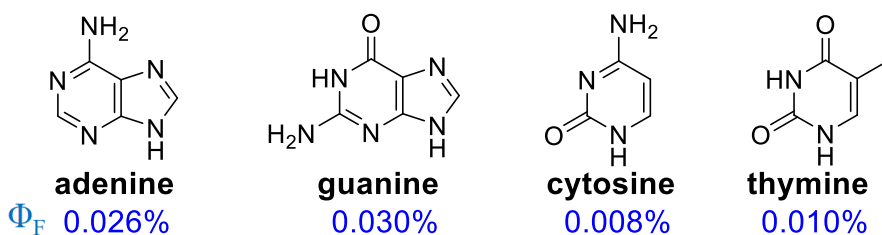
Figure 8. Fluorescence of the natural purine and pyrimidine bases

Recently, Dr. Kool at Stanford University published a comprehensive review in *Nature Chemistry* on the design of various fluorescent nucleobases and their application as powerful tools for investigating DNA and RNA.[93] The modification to purines (Figure 9A) and pyrimidines (Figure 9B) includes substitution, conjugated ring substitution, ring structure modification, conjugated linker extension, and ring fusion. This type of modifications shown in Figure 9 preserves the hydrogen bonding structures (highlighted in red), and thus retains the abilities of paring to their counterparts and some or most of the enzyme recognition. This group of fluorescent nucleobases is named as canonical fluorescent nucleobases.
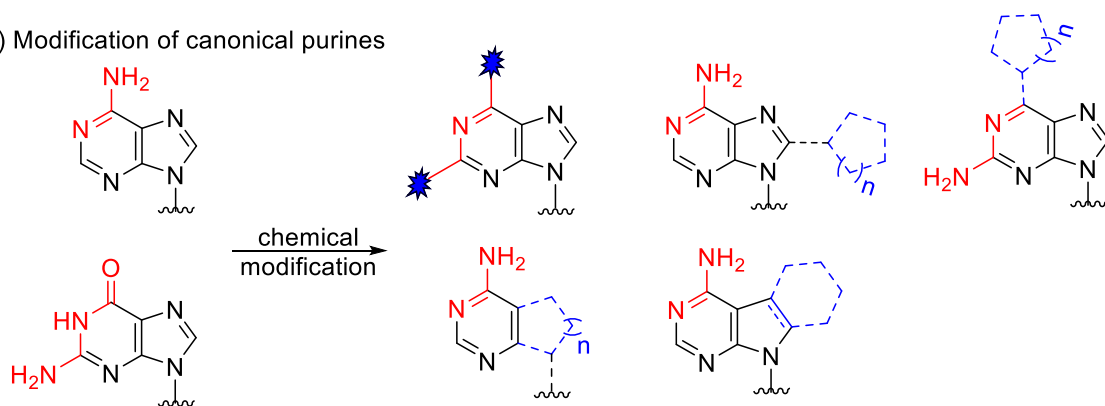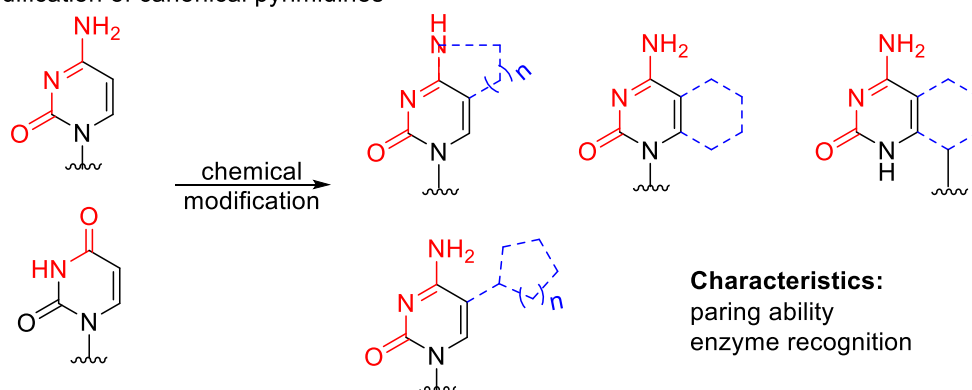
Figure 9. Canonical fluorescent nucleobase analogues

On the other hand, non-canonical fluorescent nucleobases with more varied photophysical properties have also been developed (Figure 10). Since the fluorophore structures are not necessarily confined to the natural nucleobases, theoretically they can be any fluorescent architectures. The more widely varied emissive spectra would allow non-canonical fluorescent nucleobases wider applications in biochemistry and biology. Accompanying the advantages, the shortcomings of non-canonical fluorescent nucleobases consist of the loss of base-paring ability and limited recognition by base-related enzymes.
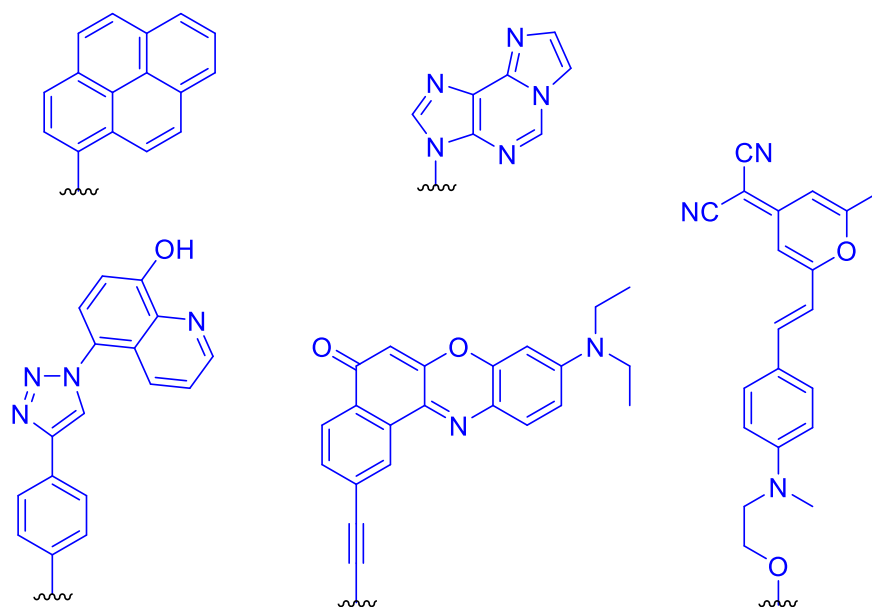
Figure 10. Non-canonical fluorescent nucleobases

The novel fluorescent properties, especially the varied quantum yield under different microenvironments, make fluorescent nucleosides valuable tools for investigating nucleic acid interactions, location, activities, and structure. Some examples are shown in Figure 11. Serva and coworkers employed 2-aminopurine for the study on DNA base flipping (Figure 11A).[88] Kim and coworkers used 8-pyrenylethynyl-2'-deoxyadenosine to detect base mismatch (Figure 11B).[94] Tor and coworkers at UCSD explored the 5-furyl-2'-deoxyuridine to locate abasic sites at DNA duplex (Figure 11C).[87] They also used 5-furyluridine to examine the interaction between RNA fragments and small molecules and to detect small molecules utilizing the increasing fluorescent intensity with increasing concentration of small molecules (Figure 11D).[89] In Dr. Wnuk's lab, the strain-promoted azide-alkyne cycloaddition (SPAAC) "click" reactions were applied to form fluorescent triazoles in cells for cell imaging.[51] The frequency domain fluorescence lifetime imaging microscopy (FD-FLIM) in MCF-7 cells is shown in Figure 11E.

21
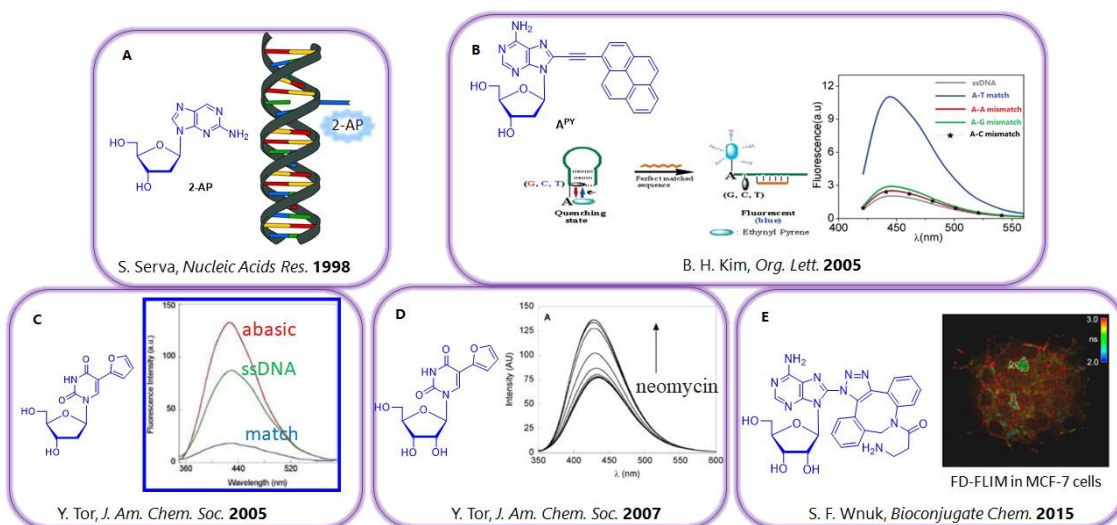
Figure 11. Fluorescent nucleobase serving as powerful tools for investigating the perturbations to nucleic acids

Among the fluorescent nucleosides, I was most interested in the triazolyl adenosine nucleosides because of their complex and interesting different fluorescent properties varied by N1 or C4 of the triazolyl moiety attached to the adenine base. The 2- or 8-azidopurine and 5-azidopyrimidine nucleosides were synthesized and ligated with cyclooctynes via strain promoted click chemistry to form 2- or 8-(1,2,3-triazol-1-yl) ($\Phi_F = 0.6\text{-}10.6\%$) and 5-(1,2,3-triazol-1-yl) pyrimidine ($\Phi_F = 0.9\text{-}1.3\%$) for the application to living cell fluorescent imaging (*e.g.,* **33** in Figure 12).[51] The 2-(1,2,3-triazol-1-yl)adenosine analogues **34** with triazole at C2 position gave relatively higher quantum yield of 20%,[95] while 8-(1,2,3-triazol-1-yl)-7-deazapurine nucleoside analogues **35** showed moderate quantum yields ($\Phi_F = 0.2\text{-}1.4\%$) and a large Stocks shifts.[96] The photo-physical characterization of a series of 2-(4-amino-5-(1*H*-1,2,3-triazol-4-yl)-7H-pyrrolo-[2,3-d]pyrimidin-7-yl) and 2-(4-amino-3-(1H-1,2,3-triazol-4-yl)-1H-pyrazolo[3,4-d]pyrimidin-1-yl) analogues showed that compounds with a nitrogen atom in position 8 showed an approximately ten-fold increase in quantum yield ($\Phi_F = \sim5\%$) and decreased Stokes shift compared to

analogues with a carbon atom in position 8 (Φ_F = ~0.6%).[97] The 8-(1*H*-1,2,3-Triazol-4-yl)adenosine derivatives **37** and **38** with the base attached to C4 position of triazole had promising quantum yield as high as 64%.[98] It is noteworthy that the 8-(1,2,3-triazol-1-yl) adenosines **33** and **36** display fluorescence properties with significantly lower quantum yields than the 8-(1,2,3-triazol-4-yl) adenosines **37** and **38**.[99]
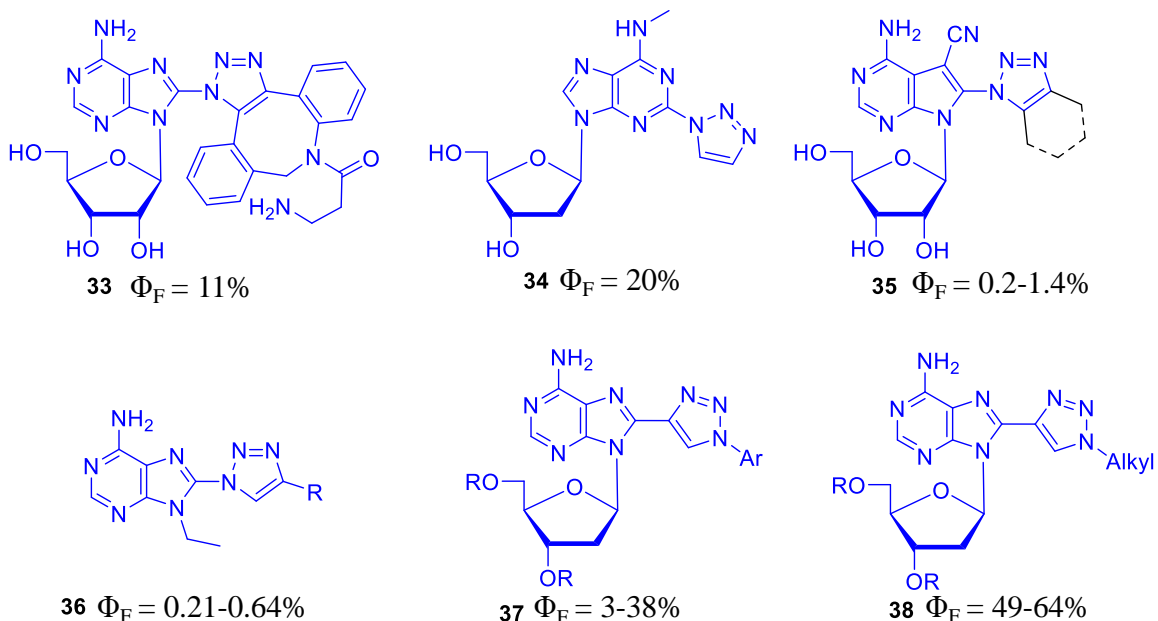
Figure 12. Structure and the fluorescent properties of *N*-substituted triazoles

According to the criteria[87] of designing new fluorescent nucleosides: (*i*), sensitiveness to the microenvironment, (*ii*) absorption and emission at long wavelengths, (*iii*), high emission quantum efficiency, (*iv*) minimalistic modification, *N*-unsubstituted 1*H*-1,2,3-triazol-4-yl modified adenine analogues as well as the other three nucleic acid bases would have novel fluorescent properties.

The 5-(1*H*-1,2,3-triazol-4-yl)-2'-deoxyuridine (5-TrzdU, **39**, Scheme 8) was synthesized by general CuAAC click reaction to give **40** followed by POM-deprotection (Scheme 8).[100] The 5-TrzdU was also prepared via nucleobase-exchange reaction catalyzed

by thymidine phosphorylase from thymidine (**41**) to 1*H*-1,2,3-triazol-4-yl.[101] The 5-TrzdU incorporated into DNA via solid-phase ODN synthesis stacks in the major groove and increases the stability of the DNA duplex.[100]
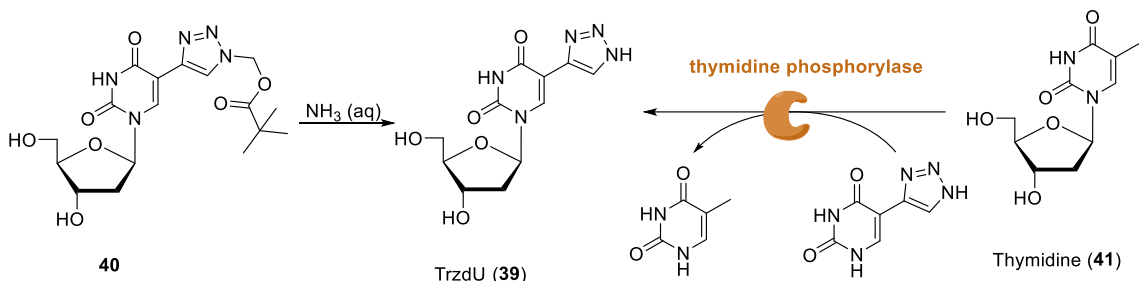
Scheme 8. Strategies for the synthesis of 5-TrzdU

The strategies developed for the synthesis of *N*-unsubstituted triazoles (Scheme 9) includes the [3+2] cycloaddition of terminal alkynes and trimethylsilyl azide (TMSN$_3$) using CuI as catalyst,[102] Pd[103] or *p*-toluenesulfonic acid[104] catalyzed cyclization between activated alkene and sodium azide, and deprotection of *N*-substituted triazole intermediates prepared by general CuAAC click reactions.[96,105,106] All of these reaction conditions may be applied to synthesize the *N*-unsubstituted triazoles-modified nucleosides.

(A) Direct reaction with terminal alkyne

a) Y. Yamamoto, *Eur. J. Org. Chem.* **2004**

$$R-\!\!\!\equiv + \text{TMS-N}_3 \xrightarrow[\text{100 °C}]{\text{CuI, DMF/H}_2\text{O}} \text{triazole (R, NH)}$$
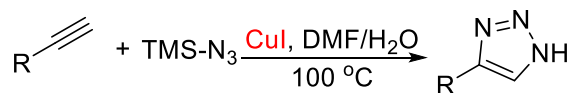
(B) Direct reaction with activated alkene

b) F. Aznar, *Angew. Chem. Int. Ed.* **2006**

$$\text{Br}-\!\!\!=\!\!\!-R + \text{NaN}_3 \xrightarrow[\text{90-100 °C}]{\substack{[\text{Pd}_2(\text{dba})_3], \text{ xantphos} \\ \text{DMSO or dioxane}}} \text{triazole (R, NH)}$$

c) Z.-H. Guan, *Org. Lett.* **2014**

$$\text{O}_2\text{N}-\!\!\!=\!\!\!-R + \text{NaN}_3 \xrightarrow[\text{60 °C}]{p\text{-TsOH, DMF}} \text{triazole (R, NH)}$$
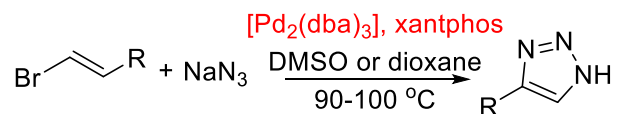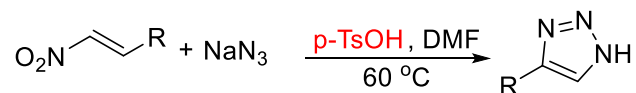
(C) CuAAC click reaction followed by deprotection

d) V. V. Fokin, *Org. Lett.* **2008**

$$R-\!\!\!\equiv + \text{NaN}_3 \xrightarrow[\substack{\text{Na-ascorbate} \\ \text{AcOH, 1,4-dioxane} \\ \text{r.t.}}]{\text{HCHO, CuSO}_4} \text{(triazoles, CH}_2\text{OH)} \xrightarrow{\text{NaOH}} \text{triazole (R, NH)}$$
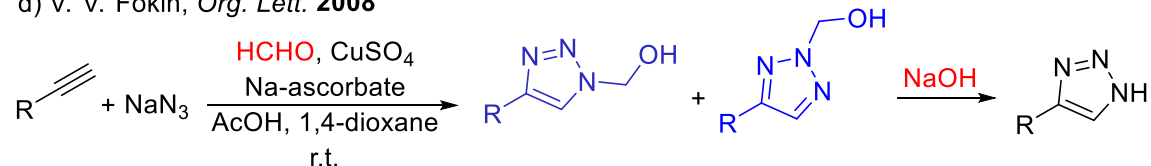
e) D. Y. Chi, *Tetrahedron* **2017**

$$R-\!\!\!\equiv + \text{Ph}\overset{\text{O}}{\underset{}{\text{C}}}\text{N}_3 \xrightarrow[\substack{\text{Na-ascorbate} \\ t\text{-BuOH/H}_2\text{O} \\ \text{r.t.}}]{\text{CuSO}_4} \text{(triazole, CH}_2\text{C(O)Ph)} \xrightarrow[\substack{\text{pyridine, PhCF}_3 \\ \text{80 °C}}]{\text{Cu(OAc)}_2, \text{O}_2} \text{triazole (R, NH)}$$
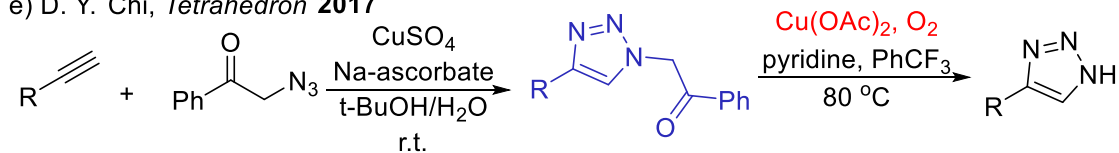
f) T. E. Nielsen, *Org. Lett.* **2010**
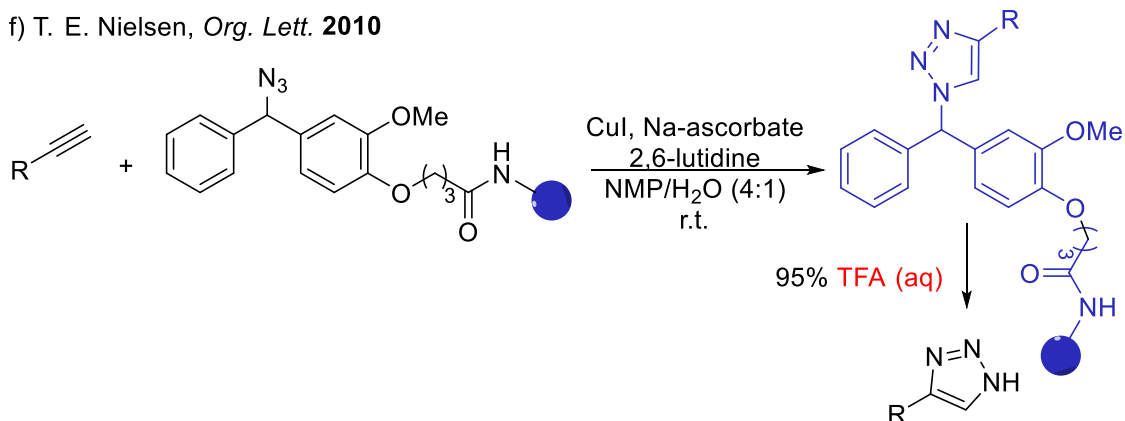
Scheme 9. Reported strategies for the synthesis of *N*-unsubstituted triazoles

25

1.8. Concept of prodrugs

The anticancer activity of drugs would be limited by their inadequate diffusion into cancerous cells, especially into cells of a solid tumor under hypoxic condition.[107] Designing chemically modified prodrugs, which are inactive, bio-reversible derivatives of active drug molecules, is a promising strategy to enhance pharmacokinetics of drug delivery. As shown in Figure 13, first prodrugs can pass through the physiological membranes more easily than the drugs. After entering the cells, the prodrugs undergo an enzymatic and/or chemical transformation and then the active parent drug can be released. Around 20% of all small molecular drugs approved in 2000-2008 were prodrugs.[108] Even though designing a new prodrug can be challenging, the prodrug approach shows a practical path to minimize some undesirable properties of investigational drugs or commercially available drugs. Designing proTides is another gorgeous strategy that skips the metabolic phosphorylation and meanwhile increases the uptake of drugs.[109]
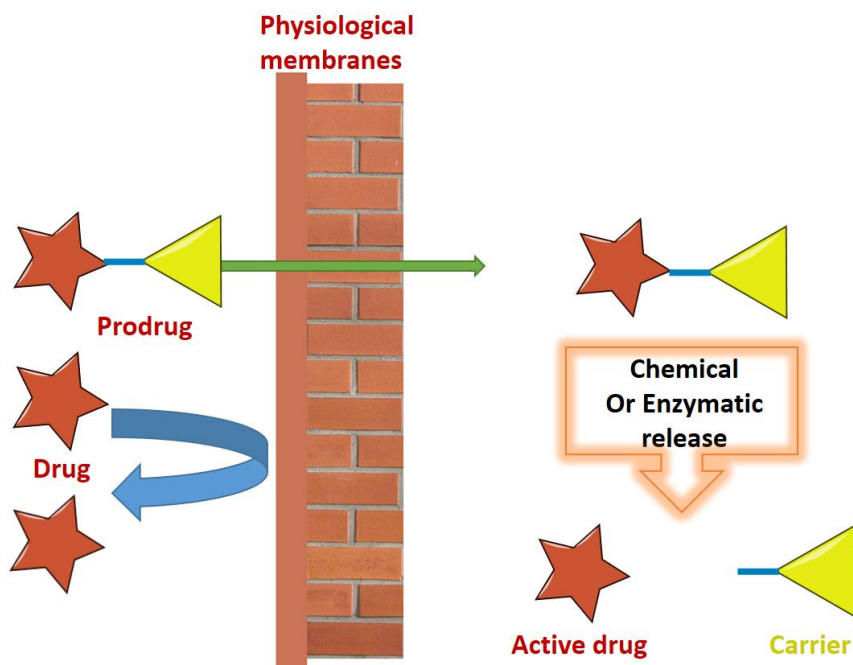
Figure 13. A simplified illustration of the prodrug concept

2. RESEARCH OBJECTIVES

The discovery of copper-catalyzed [3+2] azide-alkyne cycloaddition (CuAAC) developed by Sharpless and Meldal in 2002[44,45] as well as strain-promoted azide–alkyne cycloaddition (SPAAC) "click" reactions developed by Bertozzi in 2004[46] led to the application of azide as a reactive reporter introduced into a target biomolecule like nucleic acid, protein, glycans, and lipids to label and track biomolecules.[43,47] Click chemistry is now widely used for bioorthogonal conjugation, new drug discovery, and proteomic profiling.[48-51] However, in my dissertation I have explored the application of the azide group beyond the click chemistry. On the basis of the original discovery from Sevilla's group[42] on the formation of neutral and reactive aminyl radicals upon one-electron attachment to the azido group in 3'-AZT, I have investigated C5 azido-modified pyrimidine nucleosides as precursors to the reactive aminyl radicals. I also planned to investigate their application as anticancer radiosensitizing agents.

Objective 1: Exploring C5 azido-modified pyrimidine nucleosides as radiosensitizers

The first objective of my dissertation was to investigate if C5 azido-modified pyrimidine nucleosides (AmdU **18**, AvdU **21**, AmdC **42**, AvdC **43**, Figure 14) can act as radiosensitizers under both normoxic and hypoxic microenvironments. To serve as useful radiosensitizing agents, the C5 azido-modified pyrimidine nucleosides are required to a) be easily synthesized chemically and be stable under biological environment, b) be able to generate active radicals under normoxic and/or hypoxic condition, c) be able to be incorporated into DNA and not block further polymerization, d) and eventually show radiosensitizing effect in cancerous cells.
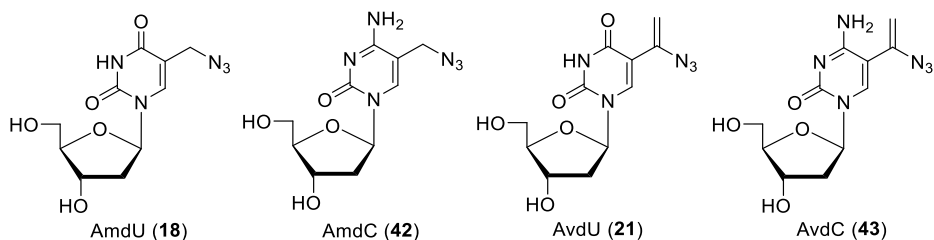
Figure 14. 2'-Deoxyuridine and 2'-deoxycytidine with azidomethyl and azidovinyl modified at C5

Initially, I chose to synthesize and explore the chemistry and biochemistry of AmdU **18**. Contrary to the 5-azido-2'-deoxyuridine, in which the azido group is attached directly to the pyrimidine base, AmdU **18** was reported to be stable in aqueous solution.[40] AmdU was also reported to be able to be enzymatically[57] and metabolically[40] incorporated into DNA. AmdU could be conveniently prepared by bromination of protected thymidine and subsequent displacement of bromide with sodium azide.[40] The 5-Azidomethyl-2'-deoxycytidine (AmdC, **42**), in turn, could be obtained by conversion of the uracil ring in the protected AmdU to cytosine. Another class of C5 azido-modified pyrimidine nucleosides I explored were 5-azidovinyl derivatives of 2'-deoxyuridine (AvdU, **21**) and 2'-deoxycytidine (AvdC, **43**) in which azido group is attached to sp^2 hybridized carbon. The synthesis of AvdU **21** and AvdC **43** could be accomplished via silver-catalyzed hydroazidation of 5-ethynyl pyrimidines nucleoside substrates.

The formation of aminyl radicals on electron attachment to azido-modified nucleosides in γ-irradiated aqueous glassy (7.5 M LiCl) systems and the subsequent reactions would be characterized using electron spin resonance (ESR). Unlike elongation terminator 3'-AZT **22**, the 5-azidomethyl (**18** and **42**) and 5-azidovinyl (**21** and **43**) pyrimidine nucleosides with modification moieties at the 5-postion of pyrimidine bases were expected not only

28

able to be metabolically/enzymatically incorporated into DNA but also allow DNA elongation after incorporation during the DNA replication. To test this hypothesis, the corresponding C5 azido-modified nucleoside triphosphates will be synthesized and evaluated for their ability for polymerase-catalyzed incorporation and further extension during DNA replication and base excision repair (BER). The radiation response of cells in the presence of azido-modified nucleosides in vitro will be examined in both aerobic and hypoxic condition of selected cancerous cells.

Objective 2: 2-Azido-2'-deoxyinosine as probe to investigate elusive guanine-based aminyl radical

The second objective of my dissertation was to explore the generation and reactivity of 2'-deoxyguanosyl radical **45** postulated to be generated during the ambident reactivity of the guanine moiety in 2'-deoxyguanosine (dG) towards hydroxyl radicals (HO•) by direct hydrogen abstraction from the NH$_2$ moiety rather than the addition at C4 position[81] (Figure 15). Based on the previous knowledge that one-electron reduction of azido group generates aminyl radicals,[42,73] I proposed that 2-azido-2'-deoxyinosine (2-N$_3$dI, **44**) could serve as convenient substrate for the generation of elusive guaninyl aminyl radical **45**. If successful, the structure of radical **45**, its tautomers, and subsequent reactions will be investigated to understand nucleic acid damage pathways induced by γ-radiolysis.
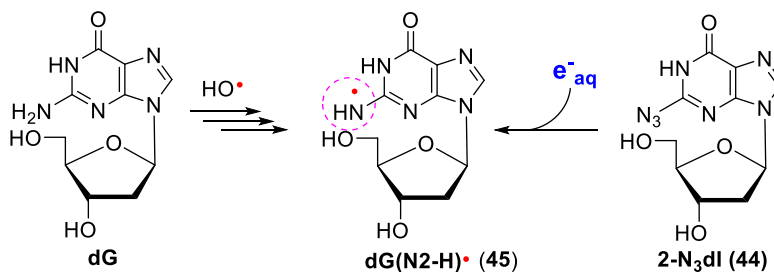
Figure 15. A plausible generation of 2'-deoxyguanosin-N2-yl radical (dG(N2-H)•) from 2-azido-2'-deoxyinosine

Synthesis of the 2-N₃dI **44** could be accomplished by conversion of 2-amino group in the protected 2'-deoxyguanosine into 2-azido group via diazotization reaction with *tert*-butyl nitrite followed by nucleophilic displacement with azide and deprotection. The formation of 2-aminyl radical from 2-N₃dI **44** and subsequent radical transfers will be characterized using electron spin resonance (ESR).

Objective 3: *N*-unsubstituted 1,2,3-triazol-4-yl nucleosides: Chemistry and fluorescent properties

Fluorescent nucleosides serve as powerful molecular tools for investigating nucleic acid structures, activities, locations, and interaction with other biomolecules or small molecules.[93] The *N*-alkyl/aryl substituted 1,2,3-triazol-4-yl adenine showed higher quantum yield than 1,2,3-triazol-1-yl adenine.[98,99] In light of the criteria of designing new fluorescent nucleosides, *i.e.,* high emission quantum efficiency and minimalistic modification, the third objective of my dissertation was to synthesize *N*-unsubstituted 8-(1*H*-1,2,3-triazol-4-yl)-2'-deoxyadenosine (8-TrzdA, **46**). I also plan to expand this goal to other three nucleosides of natural DNA and prepare 8-(1*H*-1,2,3-triazol-4-yl)-2'-deoxyguanosine (8-TrzdG, **47**), 5-(1*H*-1,2,3-triazol-4-yl)-2'-deoxycytidine (5-TrzdC, **48**), and 5-(1*H*-1,2,3-triazol-4-yl)-2'-deoxyuridine (5-TrzdU, **39**) (Figure 16).
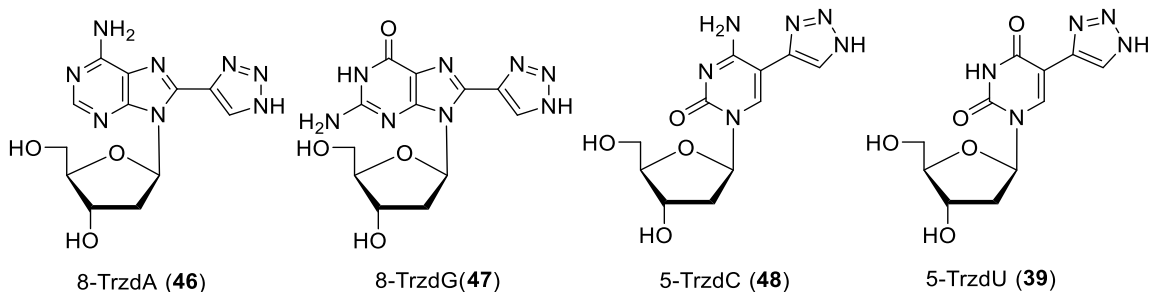
Figure 16. Fluorescent *N*-unsubstituted 1,2,3-triazol-4-yl nucleosides

From several strategies developed for the synthesis of *N*-unsubstituted 1,2,3-triazoles, I expect Yamamoto's procedure for the cycloaddition of alkynes with TMSN$_3$ catalyzed by CuI[102] should provide C5-pyrimidine and C8-purine triazol-4-yl nucleosides. Other catalysts, like CuSO$_4$/sodium ascorbate and Ag$_2$CO$_3$ will be also tried to optimize the cycloaddition between alkynyl nucleosides and TMSN$_3$. The *N*-unsubstituted 1,2,3-triazol-4-yl nucleosides (**46-48** and **39**) would be converted to 5'-triphosphates and their incorporation into DNA by polymerase-catalyzed reactions will be investigated. If triazolyl derivatives show good fluorescent properties they will be also explored for the potential application in cell imaging and investigating the perturbations to nucleic acids.

Objective 4: Antiviral and cytostatic evaluation of 5-(1-halo-2-sulfonylvinyl) and 5-(2-furyl)uracil nucleoside prodrugs

My fourth objective was to evaluate the antiviral and cytostatic activities of the prodrugs recently synthesized in Dr. Wnuk's lab, uracil nucleosides substituted at C5 with 1-halo-2-sulfonylvinyl (Figure 17, **49**)[110] or heteroaren-2-yl scaffolds (Figure 17, **50**).[111] In order to have a comprehensive biological evaluation of these uracil nucleosides analogues, I planned to increase uptake of compounds into cells by improving the lipophilicity of these compounds by esterification of the hydroxy group at sugar (Figure 17, **51**) and/or incorporation of a permanent long lipophilic alkyl chain in the furan ring (Figure 17, **52**).
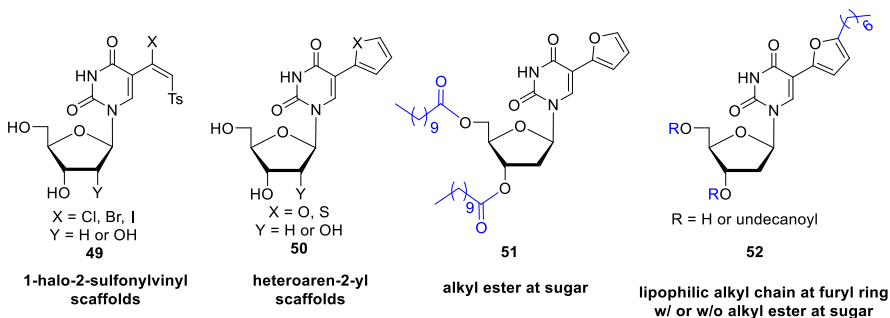
Figure 17. 5-(1-Halo-2-sulfonylvinyl) and 5-(2-furyl) uracil nucleosides prodrugs

31

3. RESULTS AND DISCUSSION

3.1. Pyrimidine nucleosides with azidomethyl and azidovinyl modification at C5 position: Chemistry and biology

3.1.1. Synthesis of AmdU, AmdC, and their phosphoramidite analogues

The 5-azidomethyl-2'-deoxyuridine (AmdU, **18**) was synthesized from thymidine **41** by successive (a) protection of sugar hydroxyl with *tert*-butyldimethylsilyl group (to give **53**), (b) *i*, bromination with *N*-bromosuccinimide (NBS); followed by *ii*, displacement of bromide with NaN_3 (to give **54**), and (c) desilylation with *tetra*-n-butylammonium fluoride (TBAF) with overall 45% yield (Scheme 10).[40,54] The ^{1}H NMR data of **18** were in good agreement with those published [*e.g.,* δ 4.06 (s, 2H, CH_2N_3)].[40] Treatment of **54** with 2,4,6-triisopropylbenzenesufonyl chloride (TIPBSCl), in the presence of triethylamine (TEA)/ 4-dimethylaminopyridine (DMAP) followed by *in situ* displacement of the resulting aryl sulfate with NH_4OH provided **55.** Subsequent desilylation with TBAF provided 5-azidomethyl-2'-deoxycytidine (AmdC, **42**) in 76% overall yield from **54** (Scheme 10). Treatment of AmdU **18** with acetyl anhydride in the presence of DMAP/TEA in ACN at room temperature for 1 h gave more lipophilic 3',5'-di-*O*-acetyl-AmdU **56** (70%).
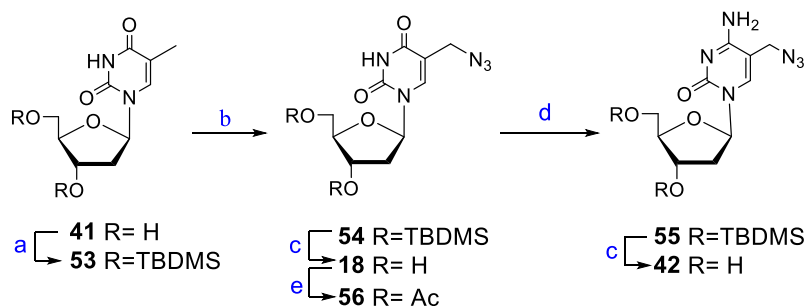
Reagents and conditions: (a) TBDMSCl, imidazole, 50 ºC, overnight. (b) (*i*) NBS, azobisisobutyronitrile (AIBN), benzene, reflux, 1 h; (*ii*) NaN_3, DMF, 60 ºC, 1 h. (c) TBAF, THF, rt, 4 h. (d) (*i*) TIPBSCl, TEA, DMAP, CH_2Cl_2, rt, 1h; (*ii*) aq. NH_4OH/THF, rt overnight. (e) acetic anhydride, DMAP, TEA, ACN, rt, 1 h.

Scheme 10. Synthesis of AmdU **18** and AmdC **42**

Since the synthesis of AmdU required multistep procedure (including protection and deprotection steps), I attempted synthesis of AmdU directly from thymidine *via* direct C-H activation of the methyl group (Scheme 11) using C-H azidation protocols reported for the synthesis of alkyl azide.[112] Thus, treatment of thymidine **41** with tosyl azide **57** in the presence of $Na_2S_2O_8$ and base showed that all the starting material was converted to a new spot on TLC, which had same R_f as AmdU. Potassium iodide and sodium thiosulfate solutions were used to quench excess oxidant $Na_2S_2O_8$. The reaction residue was column chromatographed to give a new product which was confirmed to be 5-(dimethoxymethyl)-2'-deoxyuridine **58**[113] rather than AmdU **18**. The presence of two methoxy group at the 3.22 and 3.24 ppm in ^{1}H NMR and downfield shifted signal for acetal carbon at 97.9 ppm in ^{13}C NMR was diagnostic for structure **58**. The spectroscopic data for **58** were also in agreement with the reported data for acetal **58** prepared by reaction of 2'-deoxyuridine-5-aldehyde with MeOH.[113] Modification of the procedure shown in Scheme 11 (like removing the tosyl azide **57**) would provide a convenient one-step synthesis of 5-(dimethoxymethyl)-2'-deoxyuridine **58**, which can serve as precursor to 5-formyl-2'-deoxyuridine. Compound **58** showed anti-orthopoxvirus activity in micromolar range.[113]
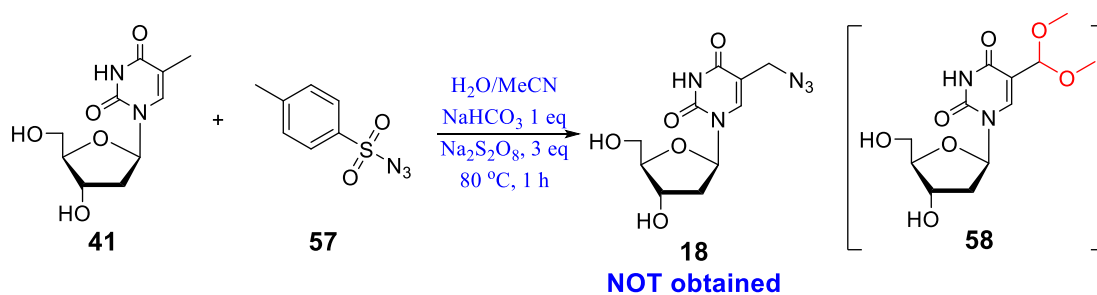
Scheme 11. Attempted one-step synthesis of AmdU

To study the formation of aminyl radicals and their subsequent reactions along DNA fragments, I made an attempt to introduce AmdU **18** into oligonucleotides using solid-

phase oligodeoxynucleotides (ODN) synthesis (Scheme 12). Such a phosphoramidite approach is believed to be not applicable for the synthesis of azido-modified ODN presumably due to Staudinger reduction.[114] The synthesis of phosphoramidite precursor 5'-(4,4'-dimethoxytrityl)-3'-(*N,N*-diisopropylamino-2-cyanoethoxychlorophosphinyl)-AmdU (5'-DMT-3'-CEP-AmdU, **60**) for solid-phase ODN synthesis is shown in Scheme 12. Thus, AmdU **18** was selectively tritylated with 4,4'-dimethoxytrityl chloride (DMTCl) at the 5'-position to give 5'-DMT-protected AmdU **59**. The phosphitylation at the 3'-position of **59** with *N,N*-diisopropylamino-2-cyanoethoxychlorophosphine in the presence of *N,N*-diisopropylethylamine (DIEA) was completed in 10 min to give two phosphoramidite diastereomers **60**. The DCM solution of **60** after extraction was dried over anhydrous Na_2SO_4 and used for solid-phase ODN synthesis without any further treatment.
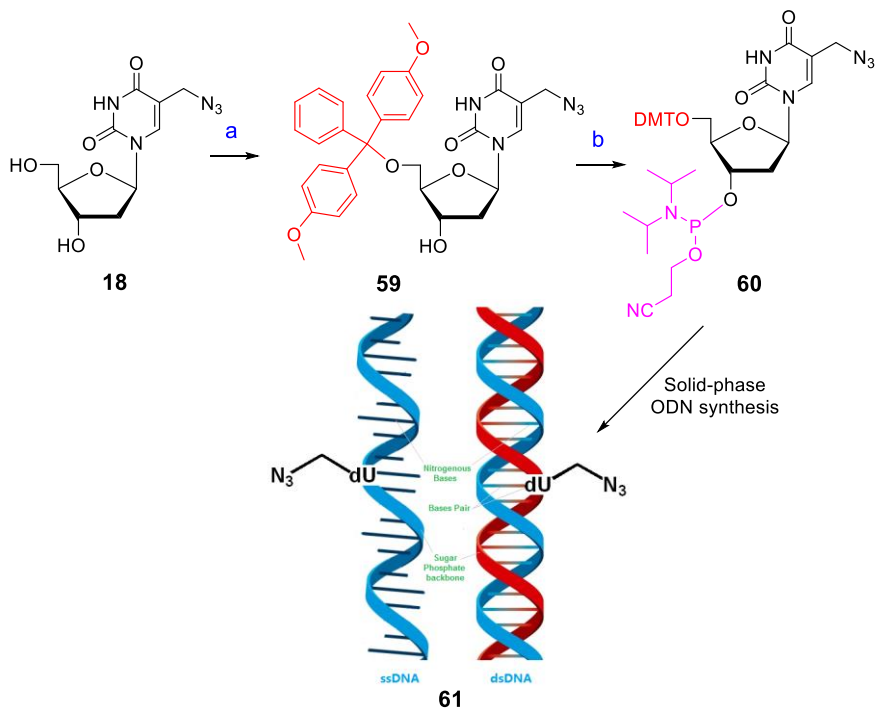
Reagents and conditions: (a) DMTCl, pyridine, rt, 2 h; (b) 2-Cyanoethyl *N,N*-diisopropylchlorophosphoramidite, DIPEA, DCM, rt, 10 min.
Scheme 12. Synthesis of AmdU phosphoramidite precursor for potential solid-phase preparation of azido-modified DNA fragments

For NMR and HRMS characterization, the solvent after extraction was removed under high vacuum [ice/acetone bath (-10 $^{\circ}$C)]. The residue was column chromatographed (hexane/EtOAc/TEA) to give 5'-DMT-3'-CEP-AmdU **60** as a separable mixture of two diastereomers with 75.6% isolated yield as white solid. The structure of the phosphoramidite **60** was confirmed by ^{1}H NMR, ^{13}C NMR, ^{31}P NMR as well as HRMS (see experimental section for completed data). The ^{1}H NMR and ^{31}P NMR of one of the two diastereomers (first eluted from column) is shown in Figure 18. The single ^{31}P peak at 148.8 ppm (Figure 18, B) indicates that phosphoramidite were obtained as single diastereomers after column chromatography. Interestingly, contrary to AmdU where methylene protons for CH_2N_3 group in ^{1}H NMR resonates as singlet at δ 4.06, diastereotopic protons in CH_2N_3 group of **60** were split into two doublets (δ 3.32 and 3.57, $^2J = 13.4$ Hz; Figure 18A).

The CH_2Cl_2 solution of phosphoramidite **60** can be stored under -20 $^{\circ}$C for over two months. However, it decomposes within 24 h when stored in a solid form even under low temperature (-20 $^{\circ}$C) or in solution at ambient temperature. Figure 19 showed formation of new peaks resulting from decomposition of **60** (CD_2Cl_2/rt/15 h) in both ^{1}H NMR (δ 5.67-6.28 ppm: presumed signal from the terminal olefin CH_2=CHCN) and ^{31}P NMR (δ 12.70, 14.34) spectra. Phosphoramidite **60** was also found to be unstable (removal of DMT-group) in $CHCl_3$, and thus during any process, $CHCl_3$ would be avoided.

It is noteworthy that **60** is one of the *first* examples of azidonucleoside phosphoramidite building blocks which we attempted to employ for the synthesis of azido-modified DNA fragments using solid-phase ODN synthesis.
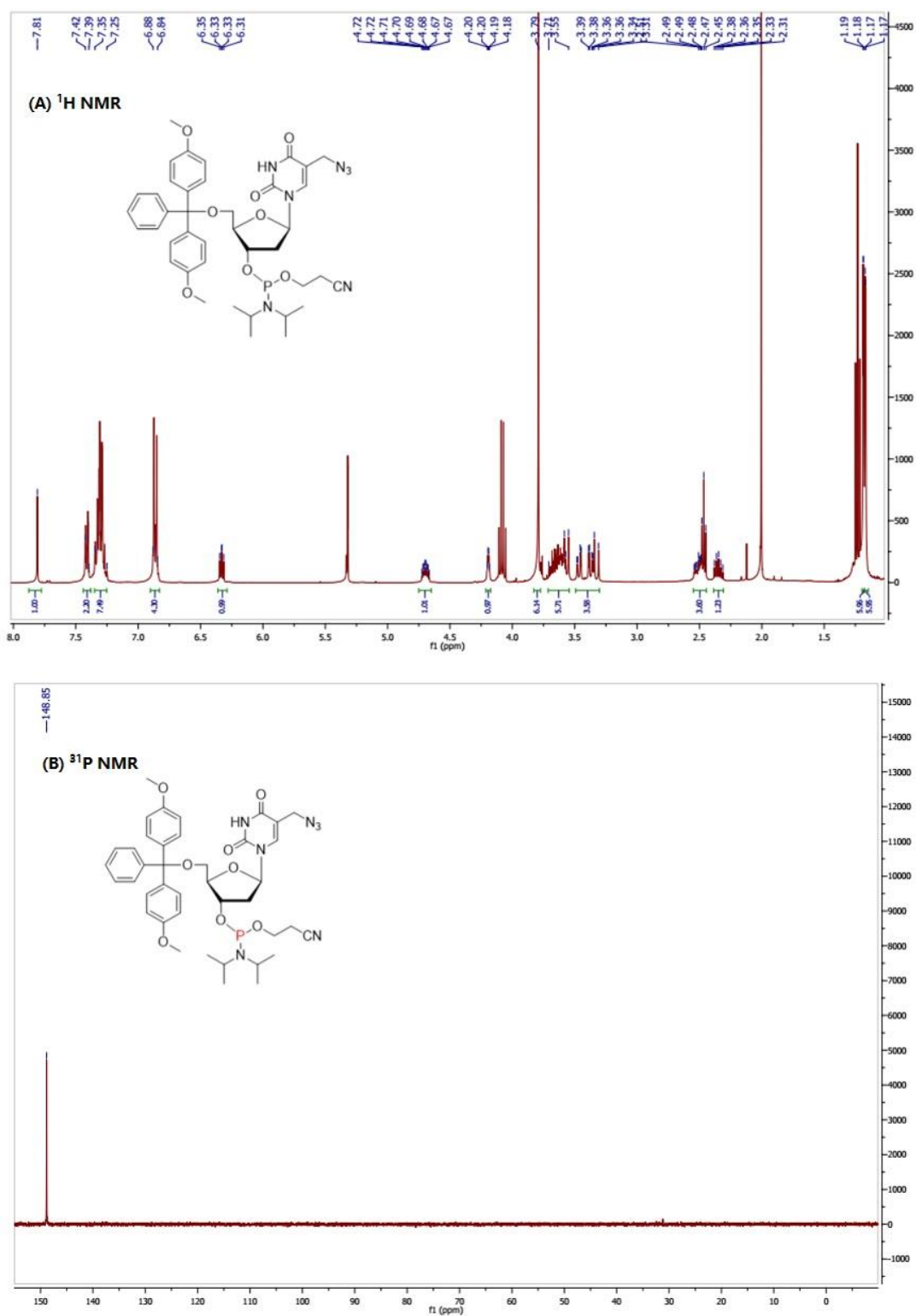
Figure 18. [1]H (**A**) and ^{31}P (**B**) NMR spectra of AmdU phosphoramidite **60** single diastereomer
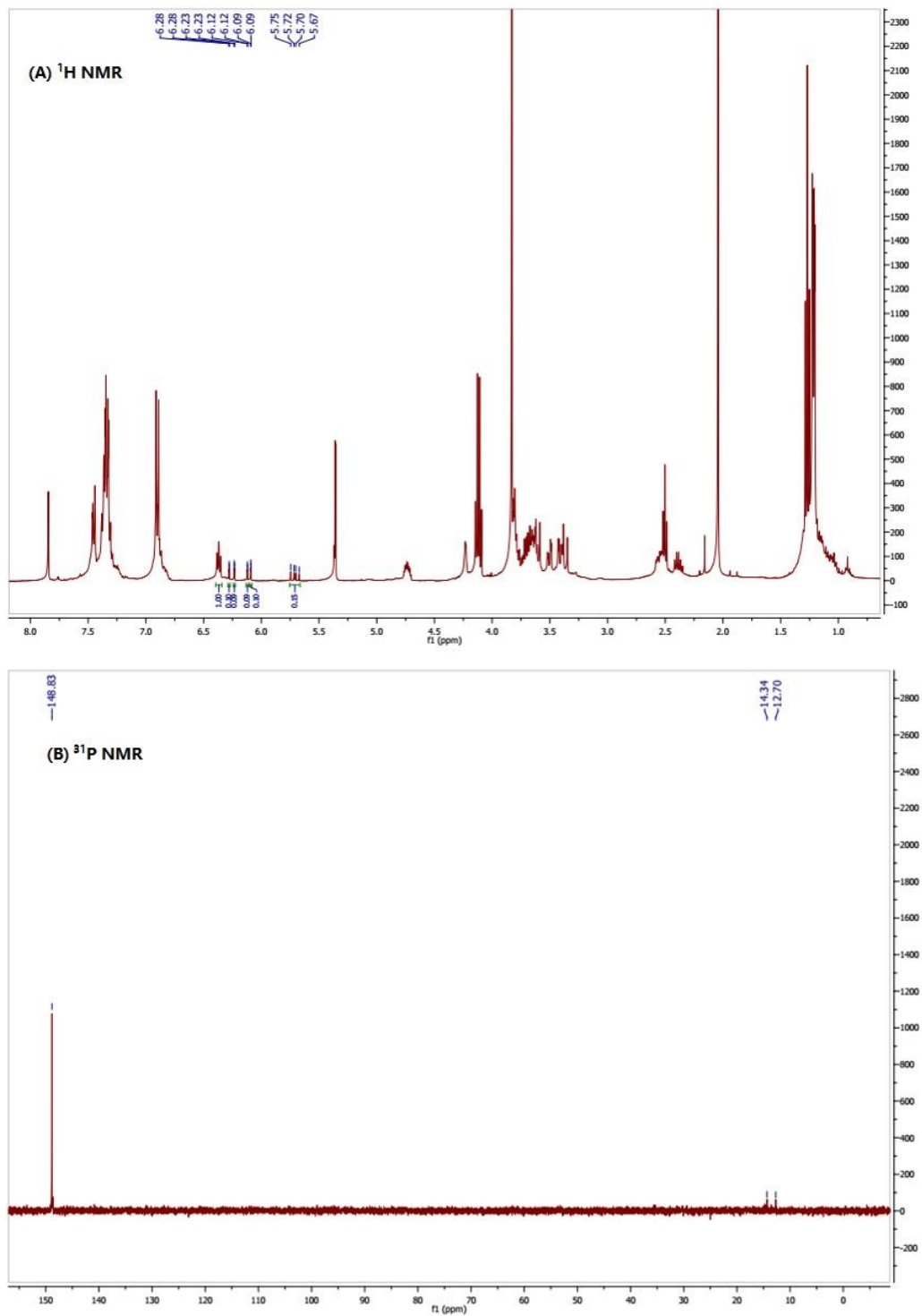
Figure 19. [1]H (**A**) and ^{31}P (**B**) NMR spectra showing decomposition of phosphoramidite **60** (in CD$_2$Cl$_2$ at room temperature for 15 h)

3.1.2. Synthesis of AvdU and AvdC by Ag₂CO₃ catalyzed hydroazidation

From several methods developed for the synthesis of vinyl azides,[37,115-117] I adopted hydroazidation of alkyne with trimethylsilyl azide (TMSN$_3$) in the presence of Ag$_2$CO$_3$ as catalyst.[115] Thus, reaction of readily available acetyl-protected 5-ethynyl-2'-deoxyuridine[110,118] **62** with TMSN$_3$ in the presence of Ag$_2$CO$_3$ produced regioselectively α-vinyl azide **64** in 52% yield (Scheme 13). Deacetylation of **64** yielded 5-(1-azidovinyl)-2'-deoxyuridine (AvdU, **21**) in 90% yield. Peaks of the two terminal olefin protons at δ 5.00 ppm and 5.91 ppm in ¹H NMR and two vinylic carbons at δ 101.3 and 137.4 ppm in ¹³C NMR were diagnostic for structure **21**.
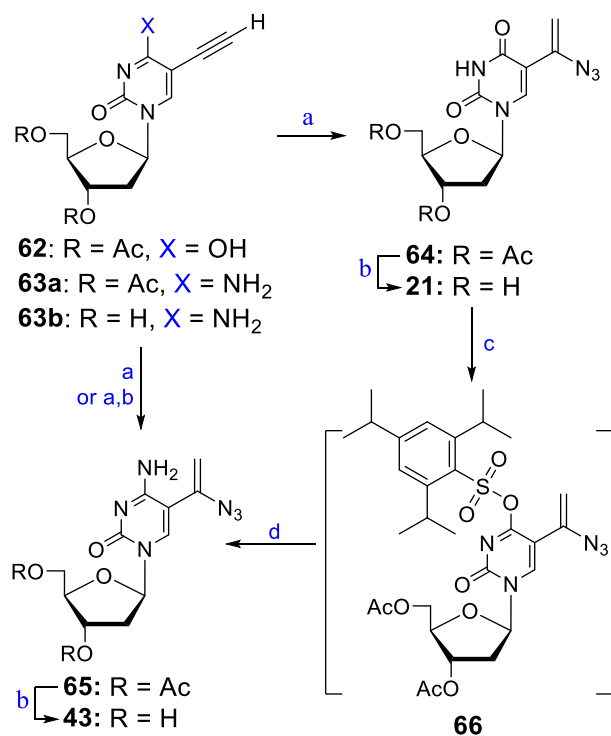
Reagents and conditions: (a) TMSN$_3$, Ag$_2$CO$_3$, H$_2$O, DMF, 80 ºC, 1 h; (b) NH$_3$/MeOH, 0 ºC to rt, overnight. (c) TIPBS-Cl, DMAP, TEA, CH$_2$Cl$_2$, rt, 1 h; (d) aq. NH$_3$, THF, rt, overnight.

Scheme 13. Strategies for the synthesis of 5-(1-azidovinyl)-2'-deoxyuridine (AvdU, **21**) and 5-(1-azidovinyl)-2'-deoxycytidine (AvdC, **43**).

Hydroazidation of the 3',5'-di-*O*-acetyl-5-ethylnyl-2'-doxycytidine **63a**[119] with TMSN$_3$/Ag$_2$CO$_3$ gave desired vinyl azide **65** in addition to a fluorescent by-product, which was characterized as 3',5'-di-*O*-acetyl-5-(1*H*-1,2,3-triazol-4-yl)-2'-deoxycytidine (diAc-5-TrzdC, **83**, see Table 5 at section 3.3.1.1). The chemistry of these 1,2,3-triazol-4-yl analogues will be further discussed at section 3.3. Deacetylation of **65** provided 5-(1-azidovinyl)-2'-deoxycytidine (AvdC, **43**) in 51% overall yield from **63a**. AvdC **43** was also obtained in a 34% yield by hydroazidation of the unprotected 5-ethynyl-2'-deoxycytidine[120] **63b**. A third method to prepare AvdC **43** was developed via conversation of uracil ring in **64** to a cytosine counterpart. Thus, treatment of **64** with 2,4,6-triisopropylbenzenesulfonyl chloride (TIPBSCl) followed by treatment of the resulting 4-*O*-TIPBS-protected intermediate **66** with aq. NH$_3$ afforded AvdC **43.**

The vinylazides were reported to be involved in thermal- and photo-induced reactions,[121] thus the decomposition of AvdU **21** under UV was carried out to investigate the potential application of AvdU **21** as a UV-activated/enhanced drug (Scheme 14). The UV-induced reaction was performed in a dark box equipped with a 254 nm UV lamp (UVG-11, 4 W, 0.16 Amps). After 1.5 h UV irradiation, AvdU **21** in the MeOH solution was all converted to two major products, which were characterized by NMR to be 5-formyl-2'-deoxyuridine **67** and 5-azirinyl-2'-deoxyuridine **68**. This result would support the reported enhancement of the cytotoxicity of AvdU by UV light.[68]
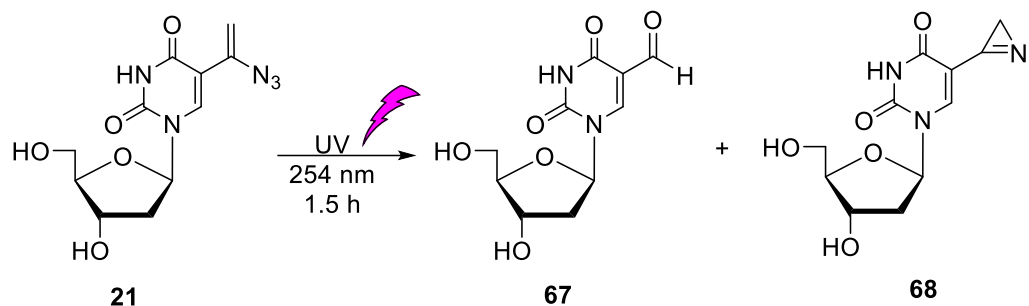
Scheme 14. Decomposition of AvdU under 254 nm UV

Synthesis 3'-CEP-5'-DMT-AvdU **70** (Scheme 15) was also attempted following the procedure developed for AmdU (Scheme 12). Treatment of AvdU **21** with DMTCl in pyridine provided 5'-DMT-AvdU (**69**, 60%). After the phosphitylation, the desired phosphoramidite diastereomers could be observed on TLC with 90% conversion. However attempted purification on silica gel column resulted in excessive decomposition most probably as a result of the higher reactivity of the vinyl azide,[121] as compared to the alkyl azides, towards Staudinger reduction.
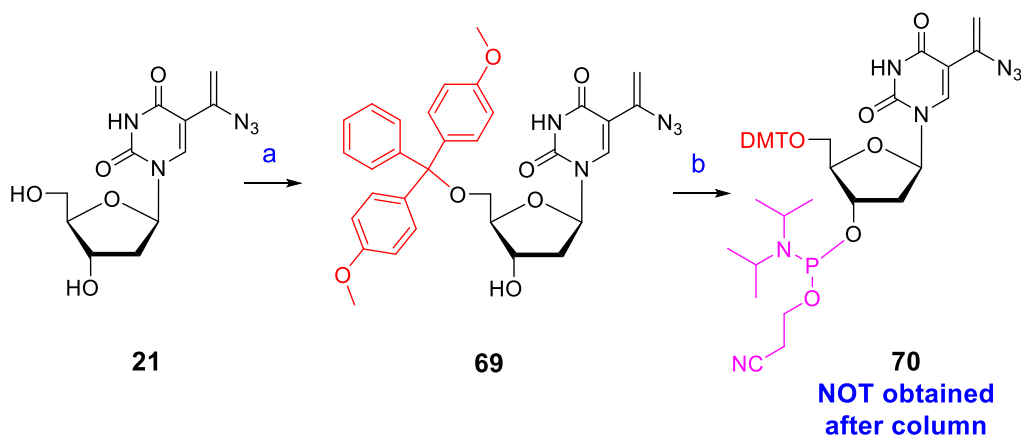
Reagents and conditions: (a) DMTCl, pyridine, rt, 2 h; (b) 2-Cyanoethyl *N,N*-diisopropylchlorophosphoramidite, DIPEA, DCM, rt, 10 min.

Scheme 15. Attempted 3'-phosphitylation of AvdU **21**

3.1.3. Polymerase-catalyzed incorporation of AmdU 5'-triphosphate and AmdC 5'-triphosphate into DNA

3.1.3.1. Synthesis of C5 azido-modified pyrimidine nucleotides

I attempted to synthesize C5 azido-modified pyrimidine nucleotide to investigate their polymerase-catalyzed incorporations into DNA. Moreover, these nucleotides can be used to study the effect of phosphate moiety on the subsequent radical reactions of the initial aminyl radicals generated from the azido group.

For the triphosphorylation, tributylammonium pyrophosphate (TBAPP, **73**), one of the necessary starting materials, was prepared by modified ion-exchange procedure using DOWEX[R] 50WX2 hydrogen form (Scheme 16).[122] Sodium pyrophosphate **71** aqueous solution (0.5 M, pH = 9) was passed through DOWEX resin (15 g resin per 1mmol sodium pyrophosphate) to give pyrophosphoric acid **72** aqueous solution (pH = 1), into which 2 equivalents of tributylamine (TBA) was added. The resulting mixture was stirred at rt until homogeneous solution (pH = 4-5) was obtained. Water was evaporated and coevaporated with acetonitrile to dry. The residue was dried under high vacuum for 24 h to give TBAPP **73** as a pale solid, into which argon was filled and DMF was added to prepare 0.5 M solution for the triphosphorylation. The Dowex Resins can be recycled by washing the column with 2 column volumes of 5% (1.5 M) HCl and then with sufficient DI water until the pH return to be around 6.
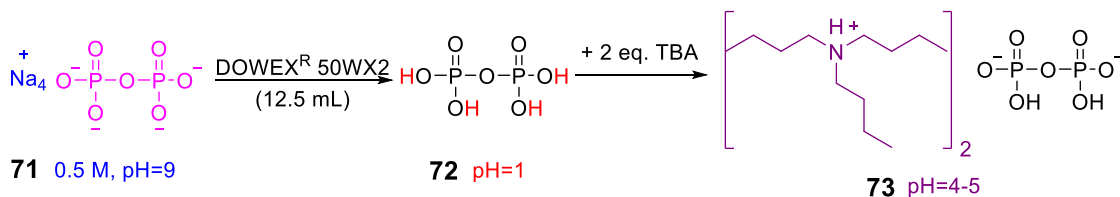
Scheme 16. Preparation of tributylammonium pyrophosphate (TBAPP)

AmdU 5'-monophosphate (AmdUMP, **19**, 70%, Scheme 17) was prepared via the phosphorylation of AmdU **18** with POCl$_3$ employing modified Yoshikawa protocols[123,124] in the presence of proton sponge followed by quenching of the crude reaction mixture with triethylammonium bicarbonate buffer (TEAB) and purification on a DEAE-Sephadex column. The reaction of AmdU **18** with POCl$_3$ in the presence of proton sponge followed by addition of 0.5 M TBAPP in DMF and then tributylamine (TBA) yielded AmdU 5'-triphosphate (AmdUTP, **20**, 76%, Scheme 17) after DEAE-Sephadex purification. The phosphates were characterized by ^{1}H, ^{13}C, ^{31}P NMR as well as HR-MS (see experimental section for the data). The ^{31}P NMR showed two doublet peaks at δ -10.80 ($J = 19.8$, γ) and δ -11.64 ($J = 19.8$, α) as well as one triple peak at δ -23.25 ($J = 19.7$, β). The proton sponge was used to accelerate the phosphorylation and provide reaction conditions suitable for acid-labile deoxynucleosides by neutralizing the formed HCl.[123] The AmdC **42** was converted to AmdC 5'-triphosphate (AmdCTP, **74,** 23%) by analogous phosphorylation (Scheme 17).
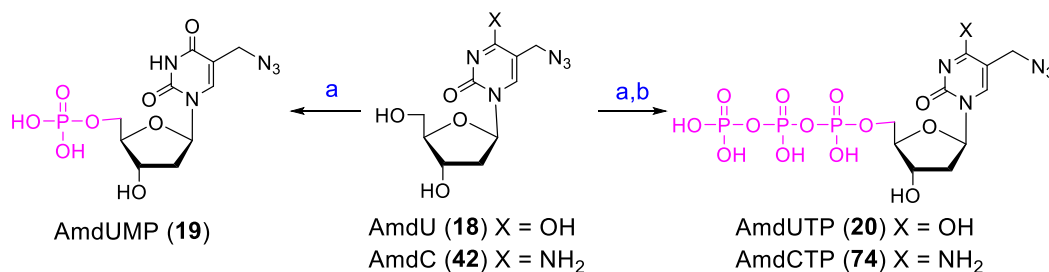
(*a*) PO(OMe)$_3$, POCl$_3$, proton sponge, 0 °C, 30 min; (*b*) TBAPP, TBA, DMF, 0 °C, 2 min.
Scheme 17. Synthesis of AmdUMP, AmdUTP, and AmdCTP

I was planning to synthesize AvdU 5'-triphosphate (AvdUTP **76**, Scheme 18)**,** following the analogous phosphorylation of AvdU **21**, but because of the instabilities of azidovinyl unit in AvdU the reactions provided 5-acetyl-2'-deoxyuridine 5'-triphosphate

75[125] rather than the desired AvdUTP **76**. To circumvent instability of vinylazide moiety in the phosphorylation reactions, post-synthetic route was also designed for the synthesis of **76** (Scheme 19). Thus, 5-ethynyl-2'-deoxyuridine 5'-triphosphate **78** was prepared from **77** (46%) employing analogous phosphorylation conditions. However, the hydroazidation of **78** also yielded 5-acetyl-2'-deoxyuridine 5'-triphosphate **75**. Addition of 10 eq. Et₃N into the hydroazidation reaction to stabilize the product **76** also failed. The presence of two peaks at the 5.04 and 5.54 ppm in the crude ¹H NMR indicated the formation of desired AvdUTP **76**, which was not stable and decompose in the reaction residue. Because of the instabilities of the AvdUTP **76**, the enzymatic incorporation of AvdU **21** into DNA fragment could not be carried out.
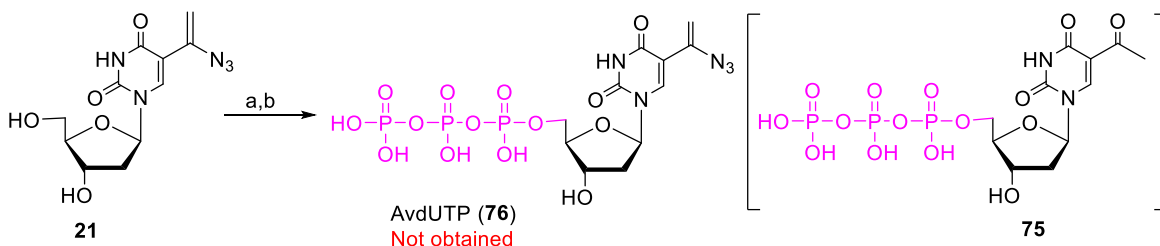
(*a*) PO(OMe)₃, POCl₃, proton sponge, 0 °C, 30 min; (*b*) TBAPP, TBA, DMF, 0 °C, 2 min.
Scheme 18. Attempted synthesis of AvdUTP **76**
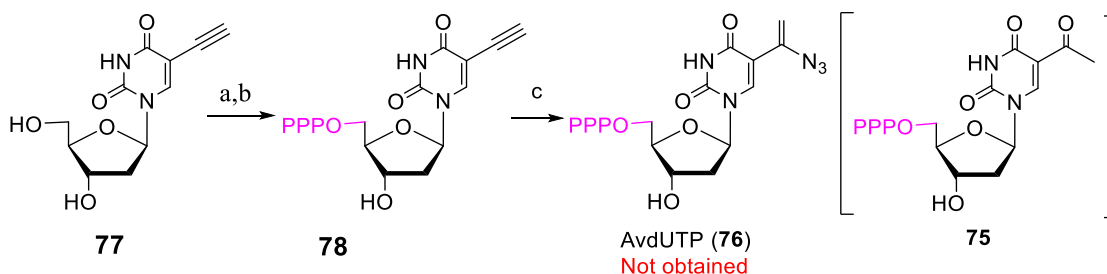
 (*a*) PO(OMe)₃, POCl₃, proton sponge, 0 °C, 30 min; (*b*) TBAPP, TBA, DMF, 0 °C, 2 min. (c) TMSN₃, Ag₂CO₃, H₂O, DMF, 80 °C, 1 h
Scheme 19. Attempted post-synthetic procedure for AvdUTP **76**

3.1.3.2. Polymerase-catalyzed incorporation of AmdUTP and AmdCTP into DNA

Since DNA replication is essential for proliferation of cancer cells, and cancer radiation therapy can induce DNA damage and initiate DNA repair such as base excision repair (BER) during which nucleotides are incorporated into double-strand DNA (dsDNA) by replication and repair DNA polymerases, it is important to determine whether an AmdUTP can also be incorporated into dsDNA during DNA replication and repair. The incorporation of AmdUTP will provide new insights into the potential application of AmdU **18** in cancer treatment. In collaboration with Dr. Liu from our department, I determined the incorporation of an AmdUTP **20** into dsDNA by the *E. coli* Klenow fragment of DNA polymerase I (pol I) and human repair DNA polymerase, DNA polymerase β (pol β) using AmdUTP **20** and synthesized oligonucleotide substrates that mimic the intermediates formed during DNA replication and repair (see section 4.2 for the DNA fragments sequences and other details). The incorporation of an AmdUTP **20** by the Klenow fragment and pol β during DNA leading and lagging strand synthesis, and BER was examined with an open template, one-nucleotide gap substrates, and one-nucleotide substrate containing a 5'-THF (a tetrahydrofuran ring which mimics a sugar residue) at the downstream strand, respectively (Figure 20). The results showed that the Klenow fragment at 0.1-5 U efficiently inserted an AmdUTP **20** with all the substrates to basepair with a template A (Figure 20A, lanes 2-6; Figure 20B, lanes 8-12; Figure 20C, lanes 14-17). With the open template, the Klenow fragment also continuously inserted an AmdUTP **20** to mispair with a template G, T and T, respectively (Figure 20A, lanes 2-6). On the other hand, pol β incorporated only one AmdUTP **20** in the open template substrate at a concentration of 10 nM (Figure 20D, lane 6), whereas it efficiently incorporated one AmdUTP to fill in the

one-nucleotide gap with the gapped substrate at concentrations of 0.5-10 nM (Figure 20E, lanes 8-12). Similarly, AmdUTP **20** was efficiently incorporated into one-nucleotide gap-THF substrate by both pol I (Figure 20C, lanes 14-17) and pol β (Figure 20F, lanes 14-17) at 0.5-5 U and 1-25 nM, respectively.
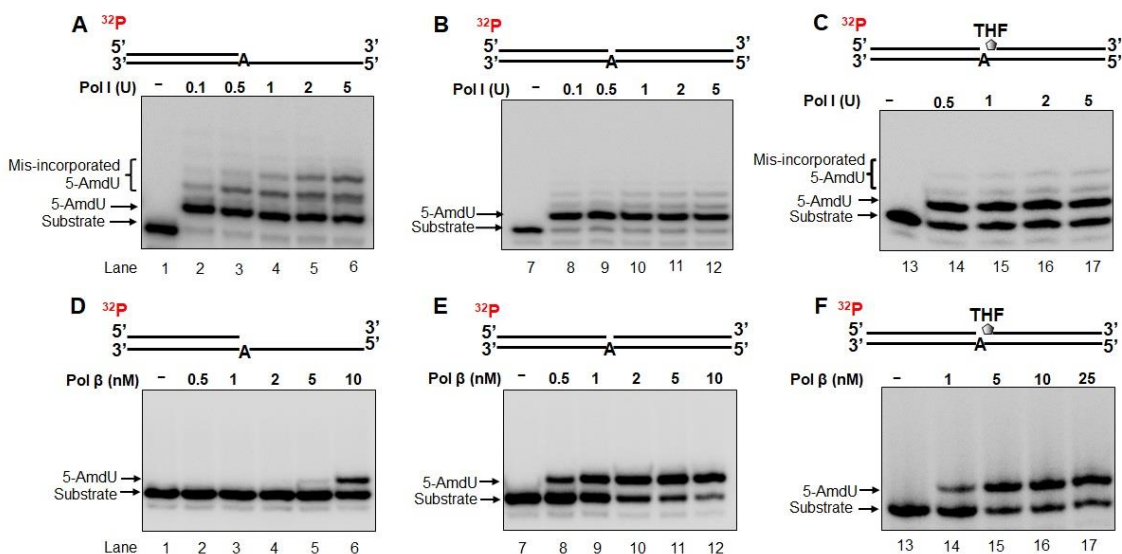
Figure 20. Incorporation of AmdUTP **20** into duplex DNA by pol I and pol β. Measurement of incorporation of an AmdUTP by Klenow fragment on the open template (**A**) and one-nucleotide gap substrate (**B**), and the one-nucleotide gap substrate containing a 5'-THF at the downstream strand (**C**). Measurement of incorporation of an AmdUTP by pol β on the open template (**D**) and one-nucleotide gap substrate (**E**), and substrate containing a 5'-THF at the downstream strand (**F**). Lanes 1, 7, and 13 represent substrate only. Lanes 2-6, 8-12, and 14-17 represent the products resulting from incorporation of an AmdUTP.

Further characterization of incorporation of the nucleotide in the presence of the other three nucleotides dATP, dGTP and dCTP, showed that an AmdUTP **20** inserted by pol I and pol β was further extended by the polymerases. Pol I (0.5-5 U) extended an AmdUTP and continued to perform DNA synthesis to the end of the template with all substrates (Figure 21A-C), whereas pol β at the concentrations of 1-25 nM extended the AmdUTP and further synthesized 9-10 nucleotides (Figure 21D-F). The results indicate that the

polymerase readily inserted the nucleotide into dsDNA and continued to extend the nucleotide during DNA replication and repair.
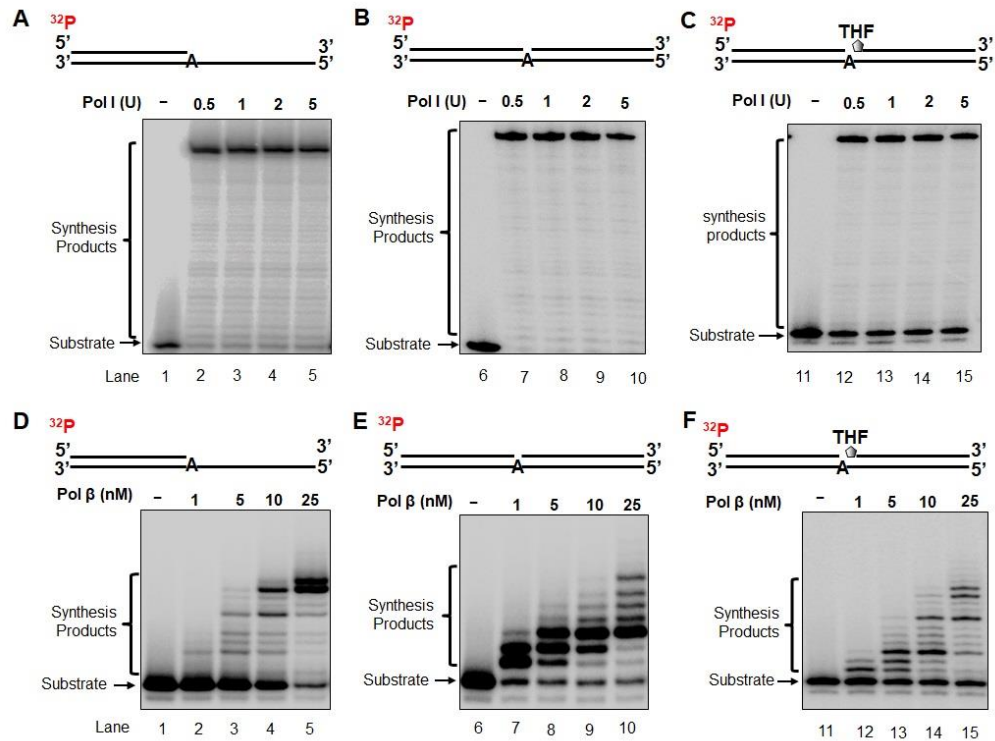
Figure 21. Extension of an incorporated AmdUTP **20** into a duplex DNA by pol I (A-C) and pol β (D-E) during DNA leading and lagging strand synthesis and BER. DNA synthesis by pol I on the open template (**A**), one-nucleotide gap substrate (**B**), and one-nucleotide gap substrate with a 5'-THF (**C**). DNA synthesis by pol β on the open template (**D**), one-nucleotide gap substrate (**E**), and one-nucleotide gap substrate with a 5'-THF (**F**). Lanes 1, 6, and 11 represent substrate only. Lanes 2-5, 7-10, and 12-15 represent DNA synthesis products.

To further examine if AmdU residues incorporated by DNA polymerases can be ligated into duplex DNA during DNA replication and repair, we determined the formation of ligation products resulting from incorporation of AmdUTP in the presence of dATP, dGTP and dCTP with the one-nucleotide gap substrates without or with a THF residue that mimics a sugar residue. We found that with the one-nucleotide gap substrate, pol I ranging from 0.5-5 U efficiently incorporated AmdUTP and other nucleotides, and this allowed conversion of all of the substrates into the ligation products, i.e. ligated products by 10 nM

DNA ligase I (LIG I; Figure 22A, lanes 2-5). For the one-nucleotide gap substrate, incorporation of AmdUTP by pol β at 1 nM only resulted in a small amount of ligated products (Figure 22C, lane 2). With increasing concentrations of pol β from 5 nM to 25 nM, the amount of the ligated products significantly increased (Figure 22C, lanes 3-5) indicating that increased incorporation of AmdUTP **20** facilitated the production of ligated products.
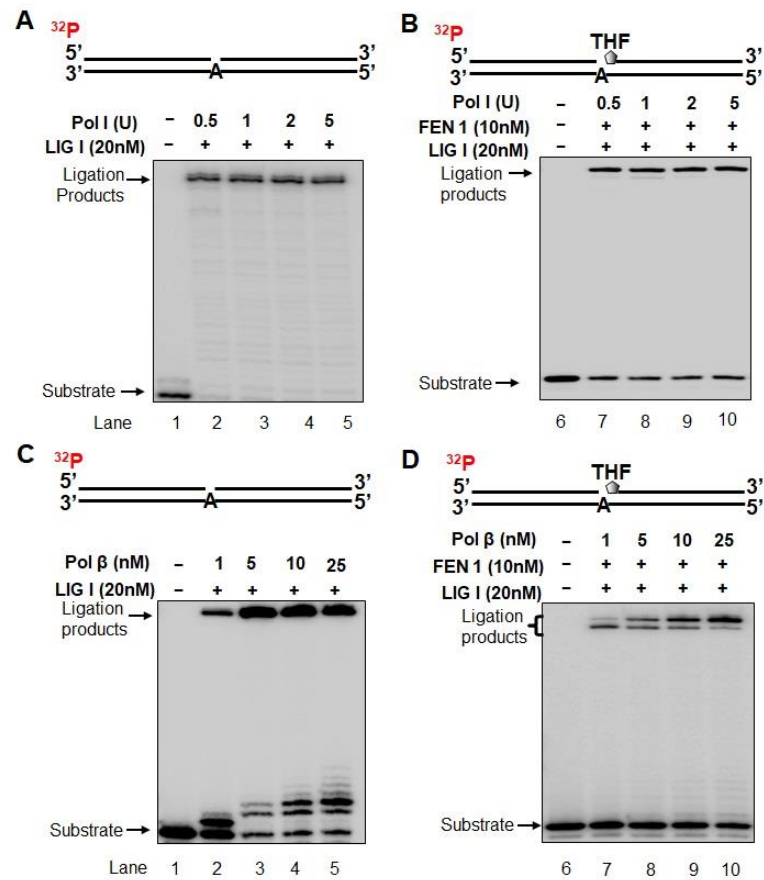
Figure 22. Ligation after incorporation of AmdUTP **20** into duplex DNA during lagging strand maturation and BER.
Measurement of ligation products, i.e. DNA lagging strand maturation products resulting from incorporation of AmdUTP by pol I (A) and pol β (C) on the one-nucleotide gap substrate. Lanes 1 represents substrate only. Lanes 2-5 represent the ligation products resulting from incorporation of AmdU. Measurement of repaired products resulting from BER mediated by incorporation of AmdUTP by pol I (B) and pol β (D) on the one-nucleotide gap substrate with a 5'-THF at the downstream primer. Lane 6 represents substrate only. Lanes 7-10 represent repaired products resulting from incorporation of AmdUTP.

To determine if AmdUTP **20** incorporated by pol I and pol β can be also ligated into a dsDNA during DNA BER, we further determined the incorporation of **20** during BER with the one-nucleotide gap substrate with a 5'-phosphorylated THF residue in the presence of 10 nM LIG I and 10 nM flap endonuclease 1 (FEN1). We found that similar to its incorporation of AmdUTP with the one-nucleotide gap substrate, pol I (0.5, 1, 2, and 5 U) performed strong DNA synthesis activity leading to the production of the full-length repair products (Figure 22B, lanes 7-10). The results indicate that AmdUTP can be efficiently incorporated into duplex DNA by Pol I during BER. On the other hand, incorporation of AmdUTP by pol β (1, 5, 10, and 25 nM) also resulted in the repaired products (Figure 22D, lanes 7-10). However, the repaired products resulting from pol β contain the repair products with the full-length or with the size that is one-nucleotide shorter than the full-length. With increasing concentrations of pol β, the amount of the full-length repaired products was significantly increased, whereas that of the short repair products was significantly decreased (Figure 22D, compare lanes 8-10 with lane 7). The result suggests that inefficient incorporation of AmdUTP **20** by a low concentration of pol β resulted in a gap during BER. This subsequently allowed the template to loop out leading to ligation and production of the short repaired product during BER.

Our results further indicate that AmdUTP **20** can be efficiently incorporated into dsDNA by DNA replication and repair polymerases during DNA replication and repair. This is consistent with a recent finding showing that AmdU were efficiently incorporated into newly synthesized DNA in human cancer cells.[40] Our results further demonstrated that the incorporation of AmdU in cancer cells is mediated by DNA replication and repair polymerases.

The incorporation of a AmdCTP **74** by pol β during DNA leading and lagging strand synthesis, and BER was also examined with an open template, one-nucleotide gap substrate, and one-nucleotide gap-THF substrate, respectively (Figure 23; see section 4.2 for the DNA fragments sequences and other details). The results showed that pol β at 1-25 nM efficiently inserted a AmdCTP in all three substrates to basepair with a template G (Figure 23A, lanes 2-5; 23B, lanes 6-10; 23C, lanes 12-15). Compared with the incorporation of an AmdUTP by pol β (Figure 20), 1 nM pol β incorporated a significant amount of an AmdCTP into the open template substrate (Figure 23A, lane 2), whereas the same concentration of pol β failed to incorporate an AmdUTP (Figure 20D, lane 3). Also, pol β at 10 nM incorporated an AmdUTP on the substrate with significantly reduced amount (Figure 20D, lane 6) compared with its incorporation with AmdCTP (Figure 23A, lane 4). Similarly, for the one-nucleotide gap substrate with or without a 5'-THF pol β at 1 nM, 5 nM, and 10 nM, incorporated an AmdUTP **20** with a reduced amount (Figure 20E, lanes 8-12 and Figure 20F, lanes 14-17) compared with its incorporation of an AmdCTP **74** at the same concentrations (Figure 23B, lanes 7-10 and Figure 23C, lanes 12-15).
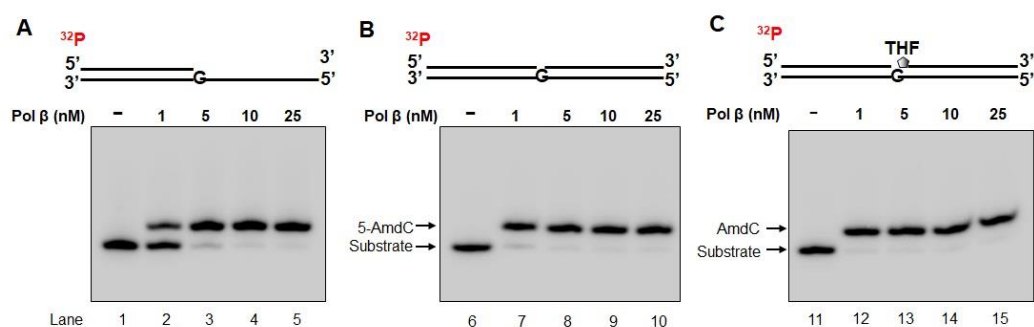
Figure 23. Incorporation of AmdCTP into duplex DNA by pol β.
Incorporation of a AmdCTP by pol β on the open template (A), one-nucleotide gap substrates (B), and one-nucleotide gap-THF substrates. Lanes 1, 6, and 11 represent substrate only. Lanes 2-5, 7-10, and 12-15 illustrate the products resulting from incorporation of a AmdCTP by pol β.

3.1.4. One-electron formation of aminyl radicals from 5-azidomethyl and 5-azidovinyl pyrimidine nucleosides and their subsequent reactions

The combination of ESR spectral studies and theoretical calculations provide evidences of radiation-produced electron-mediated formation of π-type aminyl radical (RNH•) and of its conversion to the σ-type iminyl radical (R=N•) in samples of AmdU **18** (Figure 24), AmdC **42** (Figure 25), AvdU **21** (Figure 26) and AvdC **43** in glassy systems (7.5 M LiCl/D$_2$O).

3.1.4.1. Formation of π-type RNH• and its bimolecular conversion to the σ-type R=N• in AmdU and AmdC

The ESR spectra of AmdU **18** after radiation-produced prehydrated one-electron attachment at 77 K and stepwise annealing as well as simulated spectra are shown in Figure 24. Spectra in Figure 24A presents the ESR spectrum (blue) of the radicals formed by radiation (absorbed dose = 500 Gy at 77 K) -produced prehydrated electron attachment to **18** (2.2 mg/mL) in supercooled homogeneous glassy (7.5 M LiCl/D$_2$O) solutions at 77 K.

Figure 24A has a total hyperfine splitting of ca. 178.5 G. Center of this spectrum does not show the reported doublet[126-128] due to U•$^-$. Wings of this spectrum show line components due to axially symmetric anisotropic nitrogen hyperfine coupling due to a single nitrogen. Sum of two isotropic β-proton couplings of ca. 93.5 G is assigned to the central doublet. The HFCCs at Figure 24A are nearly-identical to the reported HFCCs values for T(C5')-ND• generated from 5'-azido-5'-deoxythymidine (5'-AZT),[42] thus Figure 24A is assigned to the π-type U-(5-CH$_2$)-ND• generated from AmdU **18** (Scheme 20). The simulated spectrum (red) superimposed in Figure 24A nicely matches the line components due to nitrogen hyperfine couplings at the wings, the sharp outer peak of the doublet, and

qualitatively the broad line components at the center of the blue spectrum. Detailed analysis of HFCC will be published elsewhere.[129]
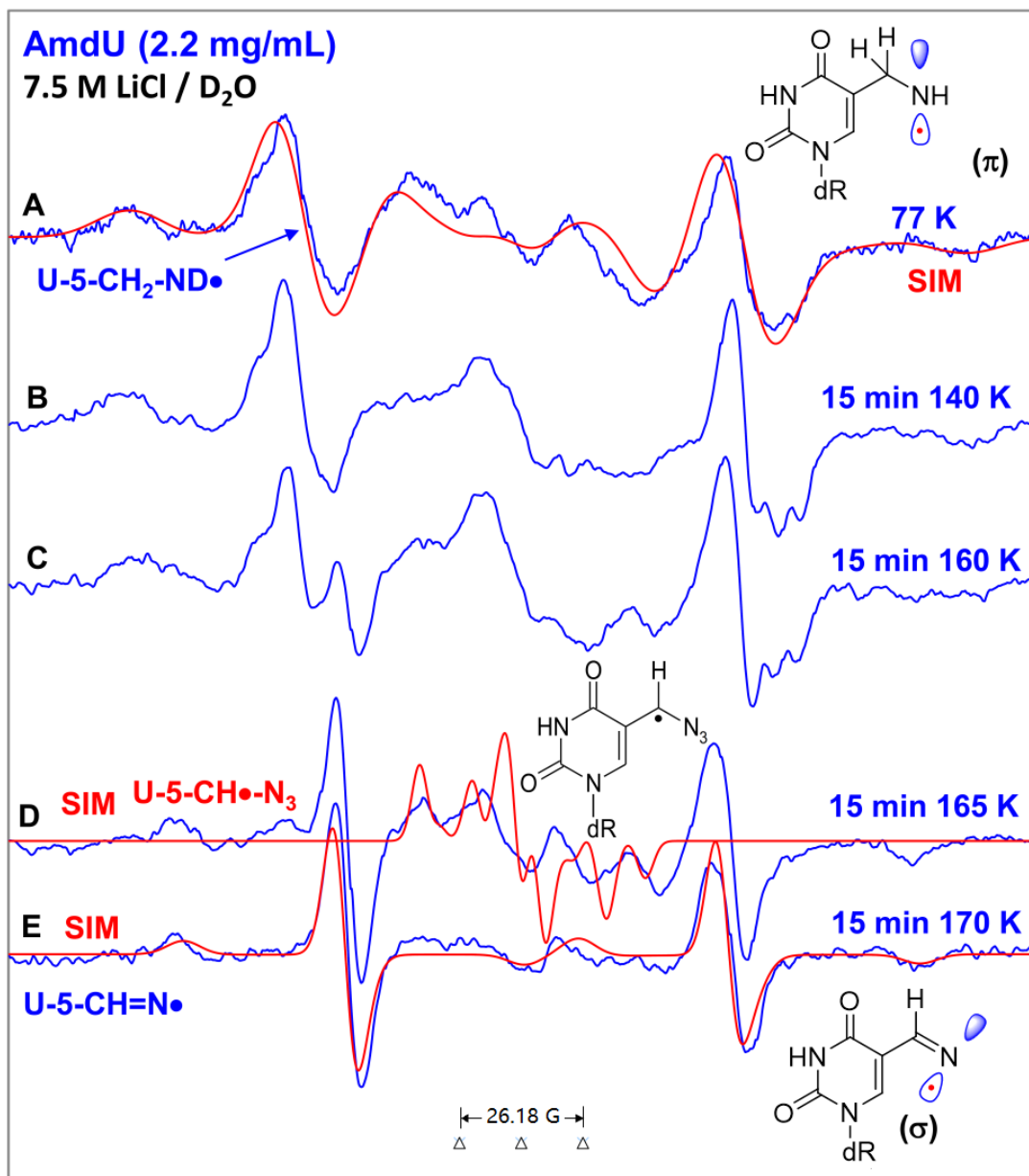
Figure 24. ESR spectra of AmdU **18** after radiation-produced prehydrated one-electron attachment at 77 K and stepwise annealing as well as simulated spectra
(A) ESR spectrum (blue) after radiation-produced prehydrated one-electron addition to AmdU **18** at 77 K in 7.5 M LiCl/D$_2$O. Spectra (B) to (E) were obtained via stepwise annealing of the sample for 15 min at 140, 160, 165, and 170 K. All spectra were recorded at 77 K. The red spectra in (A), (D) and in (E) are the simulated spectra. The radiation produced background Cl$_2$•$^-$ spectrum has been subtracted from spectra A and B for clarity.
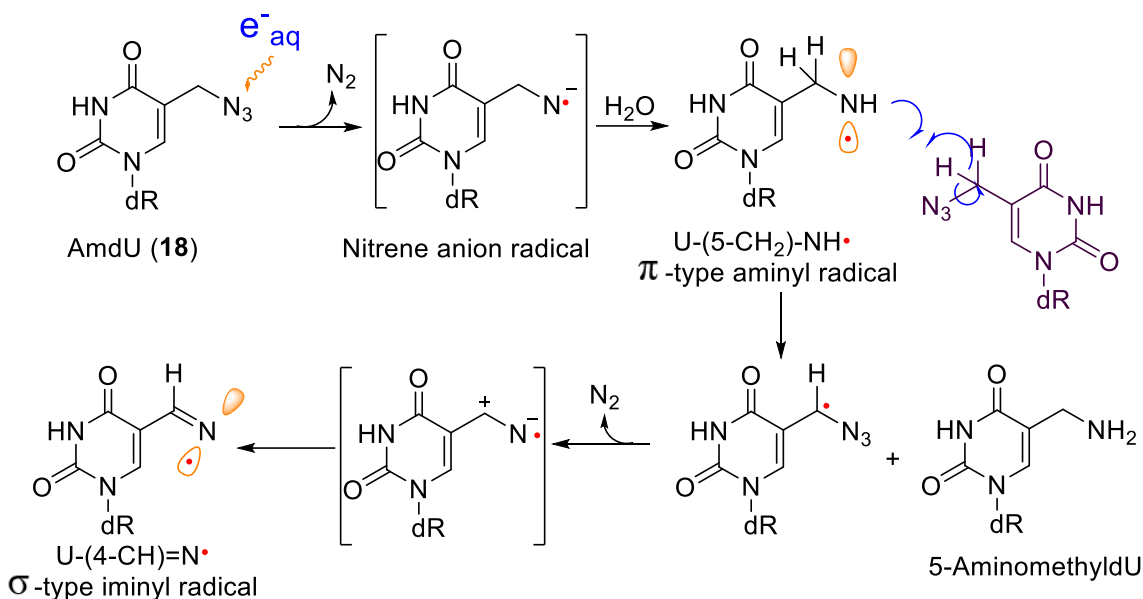
Scheme 20. Formation of π-type aminyl radical from AmdU **18** and its bimolecular conversion to the σ-type iminyl radical

After subsequent annealing of AmdU sample at 140 K in the dark for 15 min, spectrum was recorded at 77 K and is shown in Figure 24B. Upon stepwise warming, new line components are gradually developed at the center of these spectra. The line components are due to a C-centered α-azidoalkyl radical U-(5-CH•)-N_3 formed via a bimolecular H-atom abstraction by U-(5-CH_2)-ND• from a proximate AmdU **18** (Scheme 20). After subsequent stepwise annealing for 15 min in the dark at 160 K, 165 K, and 170 K, spectra have been recorded at 77 K and are shown in blue color in (C) to (E). Although line components due to the U-(5-CH•)-N_3 are present at the center of spectrum in (C), these line components become prominent with good resolution at the center of the blue spectrum in (D) but are not observed at the center of the blue spectrum in (E).

The calculated HFCCs of the C-centered radicals (U-(5-CH•)-N_3 using B3LYP/6-31G** method are found to be very similar to the HFCCs of the blue spectrum at Figure 24D. The simulated (red) spectrum of the U-(5-CH•)-N_3 superimposed on the

center of blue spectrum in Figure 23D well matches the blue spectrum. See Ref[129] for the theoretical calculation details. The π-type U-(5-CH_2)-ND• from **18** undergoing bimolecular H-atom abstraction (Scheme 20) was studied employing samples of 5'-azido-2'5'-dideoxyuridine **79** with different concentrations (0.5 mg/mL and 5 mg/mL), which is also detailed in Ref[129].

The broad central doublet of 82 G found in the blue spectrum in Figure 24E is due to one β-H of the methylene group that is attached to the C5 of the uracil base. In addition, anisotropic N HFCCs are very similar to those of $H_2C=N$•.[130] The simulated spectrum superimposed in (E) matched nicely with the blue spectrum. Therefore, the blue spectrum in (E) was assigned to the σ-type iminyl radical, U-(5-CH)=N•.

These results show that conversion of π-type U-(5-CH_2)-ND• to σ-type U(C5-H)=N• was bimolecular involving an α-azidoalkyl radical as intermediate (Scheme 20). α-Azidoalkyl radicals are known to undergo facile conversion to the σ-iminyl radicals.[131-133]

ESR spectra of AmdC **42** after radiation-produced prehydrated one-electron attachment at 77 K and stepwise annealing as well as simulated spectra are shown in Figure 25. It is noted that AmdC **42** also shows the formation of C-(5-CH_2)-ND• at 77 K along with its subsequent conversion to the σ-type iminyl radical, C-(5-CH)=N• in the temperature range (77 to 160 K) accompanied with decrease of total hyperfine splitting that is similar to U-(5-CH)=N• (Figure 25).
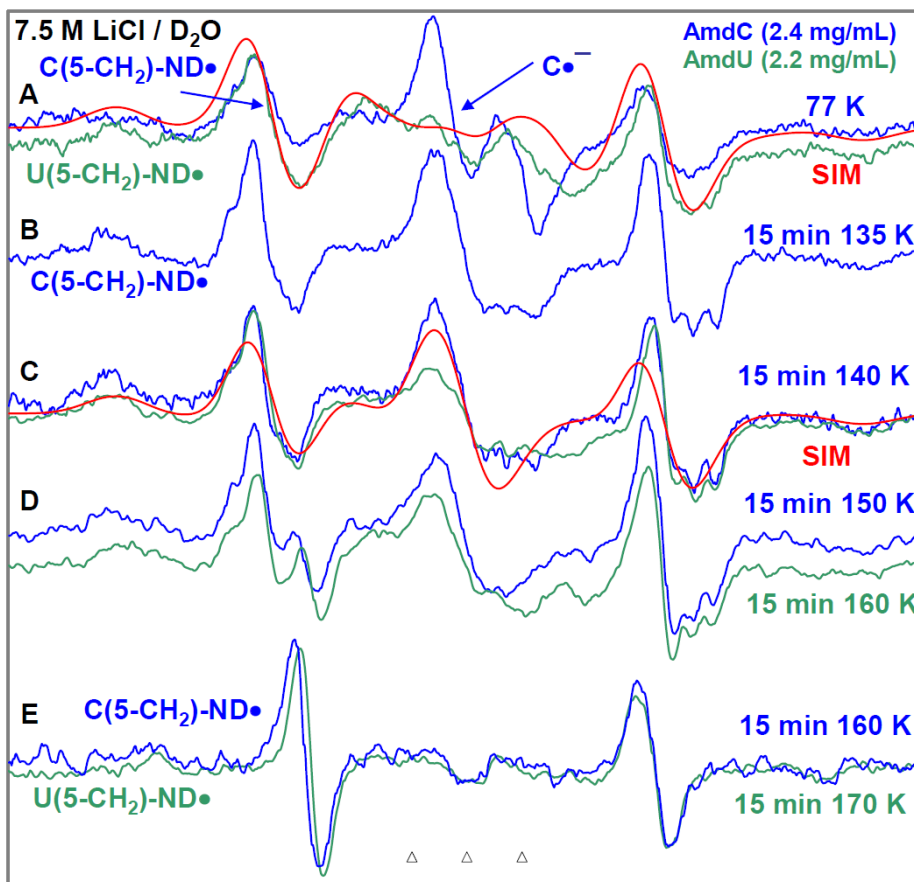
Figure 25. ESR spectra of AmdC after radiation-produced prehydrated one-electron attachment at 77 K and stepwise annealing as well as simulated spectra
Spectra (A-D) were obtained from AmdC **42** (2.4 mg/mL) by subtraction of 250 G $Cl_2\bullet^-$ spectrum from the individual experimentally recorded spectrum. (A) ESR spectrum (blue) after radiation-produced prehydrated one-electron addition to AmdC at 77 K in 7.5 M $LiCl/D_2O$. Spectra (B, blue) to (E, blue) were obtained from the same sample of **7** via stepwise annealing of the sample for 15 min at 134, 140, 150 and at 160 K. All spectra were recorded at 77 K. All spectra were recorded at 77 K. The experimental spectra from AmdU **18** (2.2 mg/mL, sea-green) are superimposed in (A), (C), (D), and (E) for comparison. The red spectra in (A) and in (E) are the simulated spectra.

3.1.4.2. Formation of π-type aminyl radical (RNH•) and its unimolecular conversion to the σ-type iminyl radical (R=N•) in AvdU and AvdC

The 77 K ESR spectrum (black) of the radicals formed by radiation (absorbed dose = 500 Gy at 77 K)-produced prehydrated electron attachment to AvdU **21** (1 mg/mL) in supercooled homogeneous glassy (7.5 M $LiCl/D_2O$) solutions is shown in Figure 26A. This spectrum shows line components due to D-atoms, and due to axially symmetric anisotropic

nitrogen HFCCs due to a single nitrogen. Furthermore, it also showed line components due to two anisotropic protons of the =CH$_2$ in AvdU **21** (or AvdC **43**). Therefore, the (A) was assigned to the π-type aminyl radical, U-(5-C=CH$_2$)-ND•. The ESR spectrum in (A) establishes that formation of U-(5-C=CH$_2$)-ND• from **21** (Scheme 21) happens following the same pathway shown in Scheme 20. The simulated a spectrum (red) superimposed in Figure 26(A) nicely matches the line components of the black spectrum and supports the assignment of the black spectrum to the π-type aminyl radical, U-(5-C=CH$_2$)-ND•.
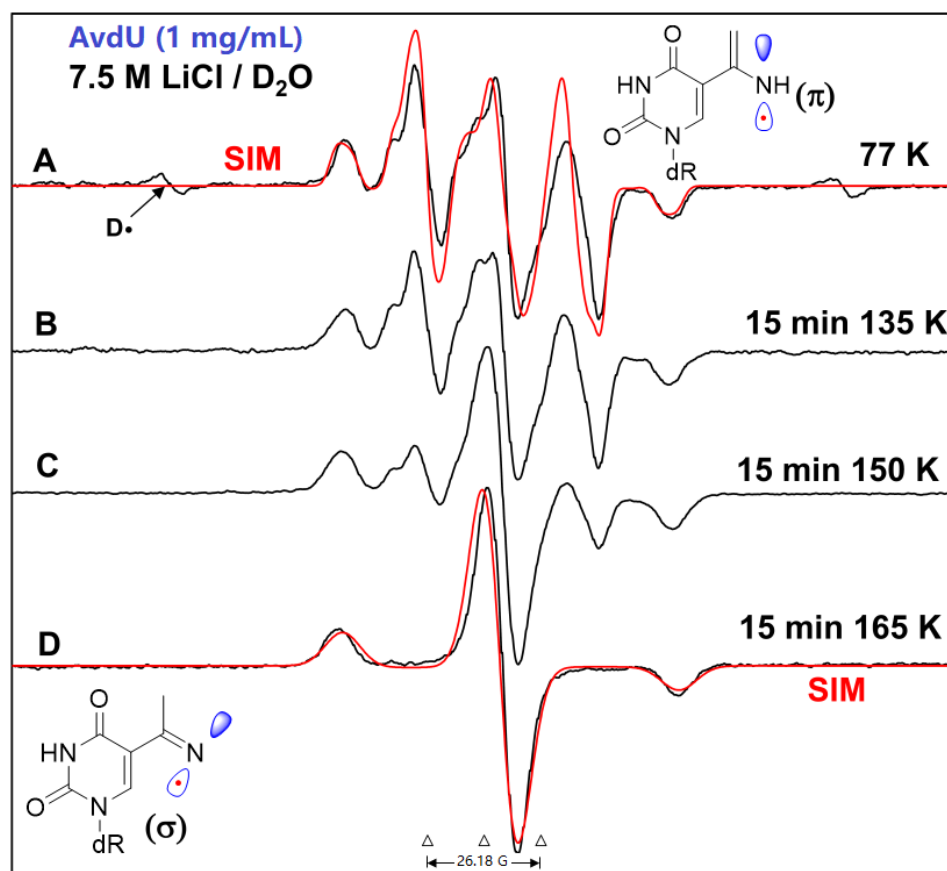
Figure 26. ESR spectra of AvdU **21** after radiation-produced prehydrated one-electron attachment at 77 K and stepwise annealing as well as simulated spectra
(A) ESR spectrum (black) after radiation-produced prehydrated one-electron addition to AvdU at 77 K in 7.5 M LiCl/D$_2$O. Spectra (B) to (D) were obtained via stepwise annealing of the sample for 15 min at 135, 150 and 165 K. All spectra were recorded at 77 K. The red spectra in (A) and (D) are the simulated spectra. The background Cl$_2$•$^-$ spectrum has been subtracted from spectra A and B for clarity.
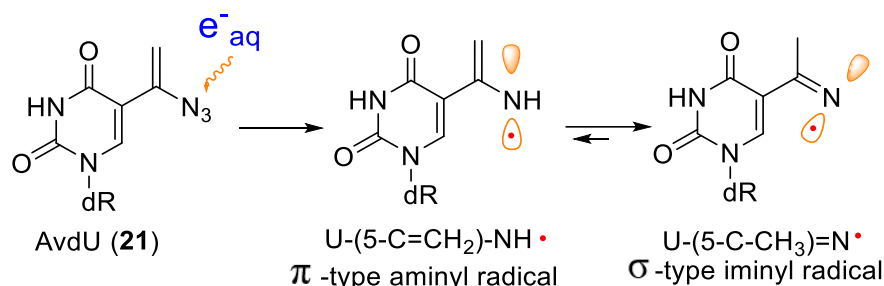
Scheme 21. Tautomerization of the π-type aminyl radical generated from AvdU **21** to the σ-type iminyl radical

ESR spectra (black) obtained upon progressively annealing the AvdU sample for 15 min in the dark at 135 K, at 150 K and at 165 K, are shown in Figure 26B-D. Comparison of the black spectrum in (D) with the black spectra in (A)-(C) shows that upon progressive annealing, height of the singlet at the center increases; concomitantly, height of the line components due to the two anisotropic -CH_2 protons decreases and eventually disappears upon annealing at 165 K. The black spectrum in (D) is only due to axially symmetric anisotropic nitrogen HFCCs. We assign this spectrum to the σ-type iminyl radical, U-(5-C-CH_3)=N•. The simulated a spectrum (red) superimposed on the experimental spectrum in Figure 26D nicely matches the line components of the black spectrum and supports the assignment of the black spectrum to the σ-type iminyl radical, U-(5-C-CH_3)=N•. Note that the axially symmetric anisotropic nitrogen HFCCs and the *g*-values of U-(5-C-CH_3)=N• are found to be identical to the reported values of σ-type iminyl radicals from one-electron oxidized 1-methylcytosine and its derivatives.[130]

Thus, our ESR spectral studies show that the radiation-produced electron mediated U-(5-C=CH_2)-ND• undergoes a facile tautomerization to U-(5-C-CH_3)=N• (Scheme 21). Nearly identical spectra were obtained from matched samples of **21** and **43**. Therefore, we conclude that, a facile tautomerization of the radiation-produced electron-mediated π-type

aminyl radical, C-(5-C=CH$_2$)-ND•, to thermodynamically more stable σ-type iminyl radical, C-(5-C-CH$_2$D)=N•, also occurs in **43**.

Increasing the concentration (1 to 5 mg/mL) of AvdU **21** in the solution appeared to have no effect on the extent of facile conversion from π-type RNH• to σ-type iminyl radical from the spectra recorded under the same microwave power, modulation, and gain. From these results, we conclude that the facile tautomerization from RNH• to iminyl radical observed in the samples of **21** and **43** occurs via very rapid intramolecular H-atom transfer from the aminyl group to the double bonded CH$_2$ group in the π-type RNH•. The rapid H-atom transfer process that is involved in the tautomerization, is, most possibly, the proton-coupled electron transfer process.

3.1.4.3. Summary and implication of aminyl radical and its resulting iminyl radicals

In contrast to the ESR spectral results obtained using samples of 3′-AZT **22**, 5'-azido-5'-deoxythymidine, 2′,3′-AZddG, and of azidopentoses,[42,73] that show the evidence of electron-induced π-type aminyl radical-mediated H-atom abstraction are not observed in the samples of AmdU, AmdC, AvdU, and AvdC. Rather, the π-type aminyl radicals, in AmdU, AmdC, AvdU, and AvdC undergo facile conversion to the σ-type iminyl radical. For AmdU and AmdC, the π-type RNH• to σ-type iminyl radical conversion is found to be bimolecular involving an α-azidoalkyl radical, while the corresponding conversion, observed for AvdU and AvdC is unimolecular (*i.e.,* tautomerization).

Owing to the high free radical scavenger concentrations in cells,[9,16] the bimolecular conversion of the π-type RNH• to σ-type iminyl radical from AmdU **18** and AmdC **42** (Scheme 20) should not take place as it has been observed in case of 5'-azido-5'-deoxythymidine. However, the facile unimolecular tautomerization of the π-type RNH• to

σ-type iminyl radical from AvdU **21** and AvdC **43** (Scheme 21) should occur. Further, the reactivity of the σ-type iminyl radical from AvdU **21** and AvdC **43** would be lower than the iminyl radicals obtained from **18** and **42** owing to the positive inductive effect of its methyl group (Figure 26 and Scheme 21). Therefore, it is expected that the π-type RNH•from AmdU **18** and AmdC **42** should augment the radiation damage more effectively than the σ-type iminyl radical from AvdU **21** and AvdC **43**. Tests of this hypothesis are reported in section 3.1.5.

3.1.5. Radiosensitizing effect of 5-azidomethyl and 5-azidovinyl pyrimidine nucleosides in aerobic and hypoxic cells

The radiation response of cells in the presence of 100 μM C5 azido-modified pyrimidine nucleosides in vitro was examined in both aerobic and hypoxic EMT6 cells. For the tests in aerobic cells, the cultures were treated with 100 μM azido compounds or vehicles for 48 h. For the test in hypoxic cells, hypoxic condition was applied for 4 h after the 44 h aerobic incubation with 100 μM azido compounds or vehicles. For the radiosensitizing effect tests, cells were irradiated with 7.5 Gy X-ray during the final few minutes of the 48 h aerobic incubation (aerobic cells) or of the 4 h hypoxic incubation (hypoxic cells). More experimental details are provided in section 4.4. The results are shown in Figure 27 and Table 4.
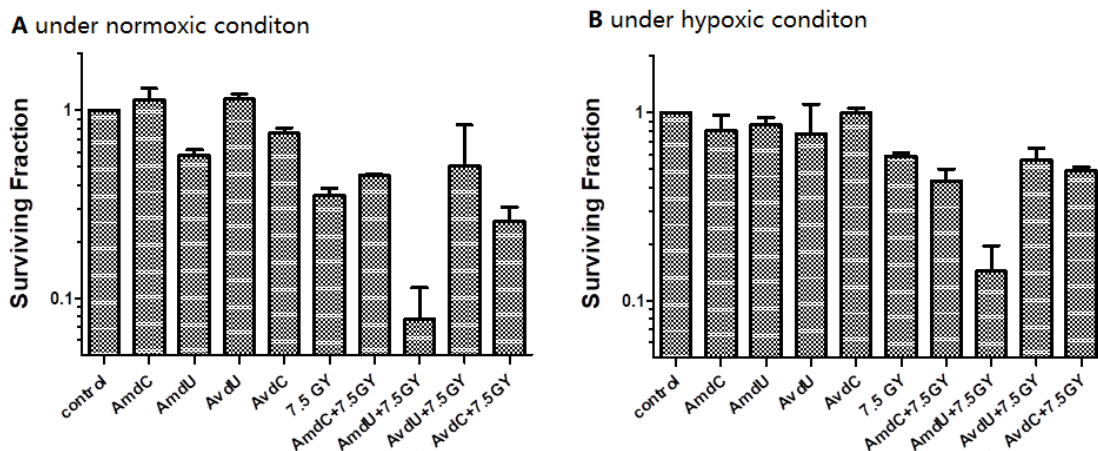
Figure 27. Radiosensitizing effect of 5-azidomethyl and 5-azidovinyl pyrimidine nucleosides at 100 μM concentration on EMT6 cells (A) normoxic, (B) hypoxic conditions

AmdU **18** showed radiosensitizing effect under both normoxic and hypoxic environment with sensitization enhancement ratio (SER) at 7.5 Gy X-ray ($SER_{SF7.5}$) of 4.57 and 4.10, respectively (Figure 27, Table 4). These results showed that one electron-induced aminyl radicals in AmdU **18** augment radiation damage to cells. In hypoxic microenvironment, RNH• formed from electron addition to AmdU **18** can be involved in the H-atom abstraction reactions that might cause DNA-strand breaks and/or crosslink formation[9,42,73] leading to lesions that can induce apoptosis of cancer cells.[16,19,134-136] On the other hand, in the aerobic cells, the aminyl radical generated from AmdU **18** can react with oxygen to generate aminylperoxyl radical RNHOO• and eventually lead to aminoxyl (nitroxyl) radicals RNHO•,[137] which also can lead to DNA damage.[138,139] Other azido nucleoside tested showed lower radiosensitizing effect with $SER_{SF7.5}$ index of 1.35 for AmdC **42** under hypoxic cells and 1.37 for AvdC **43** under aerobic cells.

Reasons for the difference in radiosensitization shown between AmdU **18** and AmdC **42** is unclear. Possible reasons include differences in drug uptake into cells, metabolic phosphorylation, and/or reactivity of the aminyl radical generated at the uracil and cytosine

59

base. The higher radiosensitizing effect of AmdU **18** than that of AvdU **21** and AvdC **43**

can be explained by the higher reactivity of π-type RNH• from AmdU **18** than that of the

σ-type iminyl radical from AvdU **21** and AvdC **43**. The optimization of the radiosensitizing

effect could involve increasing uptake of these azido-nucleosides into cancerous cells by

designing more lipophilic prodrugs and/or skipping metabolic 5'-phosphorylation in cells

by synthesizing their ProTides.

Table 4. Radiosensitizing effect of azidomethyl and azidovinyl pyrimidine nucleosides at 100 μM concentration in aerobic and hypoxic EMT6 cells

	Aerobic Conditions[a]									
X-Ray	0 Gy					7.5 Gy				
Cmpd	**Control**	**AmdC**	**AmdU**	**AvdU**	**AvdC**	**Vehicle**	**AmdC**	**AmdU**	**AvdU**	**AvdC**
SF	1	1.135	0.577	1.145	0.753	0.352	0.449	0.077	0.502	0.256
DER[c]	1	0.88	1.73	0.87	1.33	-	-	-	-	-
SER$_{SF7.5}$[d]	-	-	-	-	-	1	0.78	4.57	0.70	1.37
	Hypoxic Conditions[b]									
X-Ray	0 Gy					7.5 Gy				
Cmpd	**Control**	**AmdC**	**AmdU**	**AvdU**	**AvdC**	**Vehicle**	**AmdC**	**AmdU**	**AvdU**	**AvdC**
SF	1	0.800	0.857	0.769	0.995	0.587	0.434	0.143	0.561	0.492
DER[c]	1	1.25	1.17	1.30	1.00	-	-	-	-	-
SER$_{SF7.5}$[d]	-	-	-	-	-	1	1.35	4.10	1.05	1.19

[a] Drugs or vehicles were added to the cultures for 48 h treatment under normoxic condition, followed by 0 or 7.5 Gy X-ray irradiation. [b] Drugs or vehicles were added to the cultures for 44 h treatment under normoxic condtion and then for 4 h under hypoxic condition, followed by 0 or 7.5 Gy X-ray. [c] DER (drug enhancement ratio) was defined as the ratio of survival fractions (SF) of vehicle and SF of azido compounds. [d] SER$_{SF7.5}$ (sensitization enhancement ratio) was defined as the ratio of survival fractions at 7.5 Gy (SF$_{7.5}$) of vehicle and SF$_{7.5}$ of azido compounds.

3.2. The 2-azido-2'-deoxyinosine as precursor to study elusive guanine-based aminyl radical

3.2.1. Synthesis of 2-azido-2'-deoxyinosine

The 2-azido-2'-deoxyinosine (2-N$_3$dI, **44**) was synthesized from 2'-deoxyguanosine

(**dG**) as shown in Scheme 23. Acetyl protection of **dG** with acetic anhydride at 75 °C for

4 h provided 3',5'-di-*O*-acetyl-2'-deoxyguanosine **80** in 81% yield. The attempts to convert

2-amino from 2'-deoxyguanosine (dG) directly to 2-azido via diazotransfer and diazotization were not successful (Scheme 22), which led to the requirement of protection of O^6 with p-nitrophenethyl alcohol (NPEOH). The O^6-NPE protection required absolute anhydrous reaction condition and thus all the starting materials were dried along with P_2O_5 in a drying pistol (40 °C) for 12 hours and the solvent 1,4-dioxane was distillated with CaH_2 and then collected into a dried flask filled with Ar and activated 3 A molecular sieves. The O^6-NPE protection of **80** with p-nitrophenethyl alcohol via Mitsunobu reaction in the presence of triphenyl phosphite (Ph_3P), diisopropyl azodicarboxylate (DIAD), and activated molecular sieves powder at room temperature overnight yielded 3',5'-di-O-acetyl-O^6-(p-nitrophenethyl)-2'-deoxyguanosine **81** in 72% yield. Activated powder molecular sieves are required for the reaction to happen and to give good yield under humid environment. **81** was easily converted to **82** in 74% yield by treatment with tert-butyl nitrite and trimethylsilyl azide ($TMSN_3$) in ACN at -20°C for 12 h then at 0 °C for 24 h. Treatment of **82** with 1,8-diazabicyclo[5.4.0]undec-7-ene (DBU) at room temperature for 3 h followed by treatment with NH_3/MeOH at room temperature overnight provided the final product 2-N_3dI **44** in 83% yield.
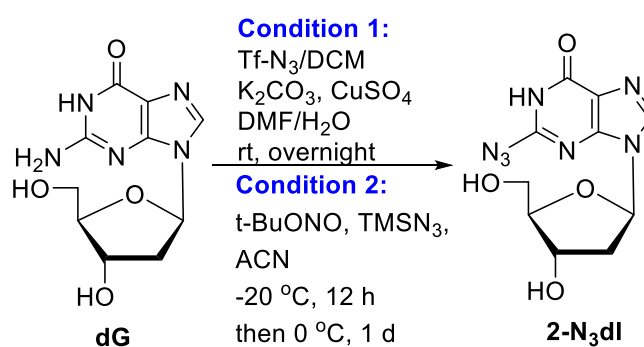
Scheme 22. Attempted one-step synthesis of 2-azido-2'-deoxyinosine
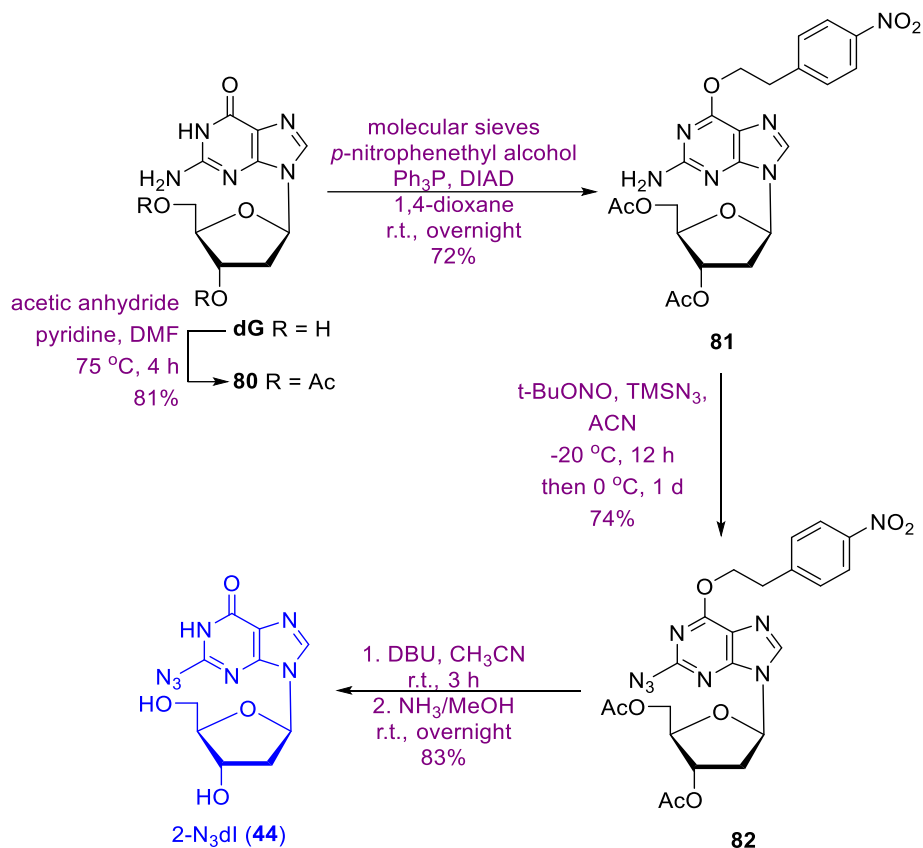
Scheme 23. Synthesis of 2-azido-2'-deoxyinosine

3.2.2. The formation of 2-aminyl radical from 2-azido-2'-deoxyinosine and subsequent radical transfers characterized using electron spin resonance

The ESR characterization of the formation of 2'-deoxyguanosin-N2-yl radical (dG(N2-H)•, **45**) on electron attachment to 2N₃dI **44** is under investigation. The N2-center radical **45** and its tautomers could be expected to be observed using ESR to offer direct evidence of electron-transfer process under γ-irradiation.

3.3. Design, synthesis, fluorescent properties, and cell imaging of 1*H*-1,2,3-triazol-4-yl analogues of C5 pyrimidine and C8 purine nucleosides

3.3.1. Synthesis of 5-(1*H*-1,2,3-triazol-4-yl) pyrimidine and 8-(1*H*-1,2,3-triazol-4-yl) purine nucleoside analogues

3.3.1.1. Method A catalyzed by Ag₂CO₃

As discussed in Section 3.1.2, during the synthesis of protected AvdC **65** (48%) from 3',5'-di-*O*-acetyl-5-ethynyl-2'-deoxycytidine **63a**[119,140] (Scheme 13) also the fluorescent 3',5'-di-*O*-acetyl-5-(1*H*-1,2,3-triazol-4-yl)-2'-deoxycytidine (diAc-5-TrzdC, **83**) was obtained in low yield (7%; Table 5, Entry 1; Method A). Also as was noted above in Section 3.1.2 the analogous hydroazidation of 3',5'-di-*O*-acetyl-5-ethynyl-2'-deoxyuridine **62**[110] produced protected AvdU **64** (55%) as the only product without formation of the corresponding triazole product **84** (Table 5, Entry 2; Method A).

Remarkably, contrary to the 5-ethynylpyrimidine nucleosides, hydroazidation of 8-ethynylpurine nucleosides produced triazole adducts as major products. Thus, hydroazidation of 8-ethynyl-2'-deoxyadenosine **85**[141] with TMSN₃ in the presence of Ag₂CO₃ produced 8-(1*H*-1,2,3-triazol-4-yl)-2'-deoxyadenosine (8-TrzdA, **46,** 50%) as the major product in addition to the vinylazide **89** (8-AvdA, 15%; Table 6, Entry 1; Method A). The estimated yield of 8-TrzdA **46** based on the TLC were approximately 70% (Table 6) but due to the strong binding of triazoles to the silica gel, the products after silica gel column chromatography were isolated in relatively low yields. Interestingly treatment of 3',5'-di-*O*-TBDMS-8-ethynyl-2'-deoxyadenosine **86**[141] by Method A provided 3',5'-di-*O*-TBDMS-8-(1*H*-1,2,3-triazol-4-yl)-2'-deoxyadenosine (diTBDMS-8-TrzdA, **88,** 30%; Table 6, Entry 2) as the only product without a trace of azidovinyl analogue **90**. The

treatment of 8-ethynyl-2'-deoxyguanosine **87**[142] by Method A also yielded 8-(1*H*-1,2,3-triazol-4-yl)-2'-deoxyguanosine (8-TrzdG, **47,** 52%; Entry 3) as the sole product.

Table 5. Synthesis of 5-(1*H*-1,2,3-triazol-4-yl) pyrimidine nucleoside analogues

63a X = NH$_2$, R = Ac
63b X = NH$_2$, R = H
62 X = OH, R = Ac
77 X = OH, R = H

83 X = NH$_2$, R = Ac
48 X = NH$_2$, R = H
84 X = OH, R = Ac
39 X = OH, R = H

65 X = NH$_2$, R = Ac
43 X = NH$_2$, R = H
64 X = OH, R = Ac
21 X = OH, R = H
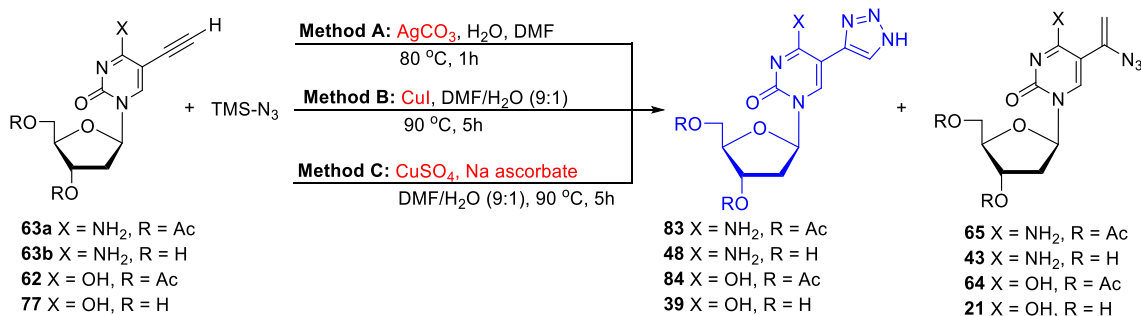
Entry	SM	Method	Trz	Yield^a [%]	azide	Yield^a [%]
1	**63a**	A	**83**	7	**65**	48
2	**62**	A	**84**	0	**64**	55
3	**63a**	B	**83**	32 (50)	**65**	0
4	**63b**	B	**48**	10 (20)	**43**	0
5	**62**	B	**84**	55 (85)	**64**	0
6	**77**	B	**39**	50 (85)	**3d**	0
7	**77**	B^b	**39**	42 (75)	**3d**	0
8	**63a**	C	**83**	65 (80)	**65**	0
9	**63b**	C	**48**	51 (85)	**43**	0
10	**62**	C	**84**	81 (95)	**64**	0
11	**77**	C	**39**	52 (90)	**3d**	0

^{a} Isolated yields; In parenthesis are estimated yields based on TLC; ^{b} Modified Method B: CuI, 2 eq. H$_2$O, DMF, 90 ^{o}C, 5h.

Since 5-triazolylpyrimidine and 8-triazolylpurine nucleosides show good fluorescent properties (section 3.3.4), it was significant to optimize reaction conditions to synthesize the triazolyl analogues of the four natural bases (*i.e.* dU, dC, dA, and dG) of DNA. To optimize the conditions to increase the percent yield of the triazoles and to be applicable for all four nucleosides, several strategies have been designed and performed.

Table 6. Synthesis of 8-(1H-1,2,3-triazol-4-yl) purine nucleoside analogues

Method A: $AgCO_3$, H_2O, DMF, 80 °C, 1h
Method B: CuI, DMF/H_2O (9:1), 90 °C, 5h
Method C: $CuSO_4$, Na ascorbate, DMF/H_2O (9:1), 90 °C, 5h

85 X = NH_2, Y = R = H
86 X = NH_2, Y = H, R = TBDMS
87 X = OH, Y = NH_2, R = H

46 X = NH_2, Y = R = H
88 X = NH_2, Y = H, R = TBDMS
47 X = OH, Y = NH_2, R = H

89 X = NH_2, Y = R = H
90 X = NH_2, Y = H, R = TBDMS
91 X = OH, Y = NH_2, R = H
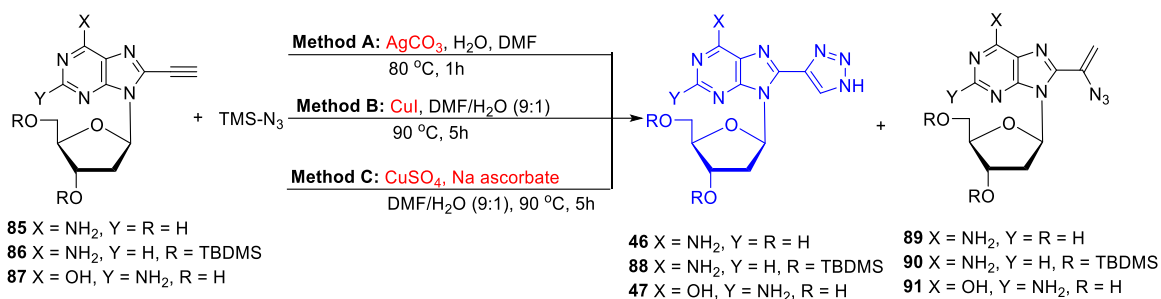
Entry	4	Method	5	Yield[b] [%]	6	Yield[b] [%]
1	85	A	46	50 (70)	89	15 (25)
2	86	A	88	30 (75)	90	0
3	87	A[a]	47	52 (90)	91	0
4	85	B	46	17 (60)	89	0
5	86	B	88	27 (70)	90	0
6	87	B	47	31 (65)	91	0
7	85	C	46	51 (85)	89	0
8	86	C	88	58 (85)	90	0
9	87	C	47	52 (80)	91	0

[a] Modified Method A: Ag_2CO_3, H_2O, DMF, 80 °C, 4h.

Alkynes bearing electron-withdrawing groups are better substrates for the direct addition to in-situ generated hydrazoic acid.[102,143] Thus, to increase the yield for the preparation of the unsubstituted 5-triazol-4-yl pyrimidine nucleosides, insertion of electron-withdrawing group to the pyrimidine bases was considered. Initially, the electron-deficiency of the pyrimidine nucleosides were attempted to be increased by preparing Boc-protected analogues (Scheme 24 and Scheme 25). Thus, di-N^4,N^4-Boc-3',5'-di-O-acetyl-5-ethynyl-2'-deoxycytidine (**92**, 70%) and N^4-Boc-3',5'-di-O-acetyl-5-ethynyl-2'-deoxycytidine (**93**, 10%) were synthesized by the treatment of 3',5'-di-O-acetyl-5-ethynyl-2'-deoxycytidine **63a** with (Boc)$_2$O as shown in Scheme 24. Similarly, N^3-Boc-3',5'-di-O-acetyl-5-ethynyl-2'-deoxyuridine (**94**, 52%) was prepared from 3',5'-di-O-acetyl-5-

ethyl-2'-deoxyuridine (**62**, Scheme 25). Unfortunately, hydroazidation of the Boc-protected pyrimidine nucleosides **92-94** by Method A resulted in unstable fluorescent products which were proved by NMR not to be the expected triazoles. The structures need to be further identified. The electron-withdrawing modification on pyrimidine bases did change the electron density that further led to different products rather than triazoles.
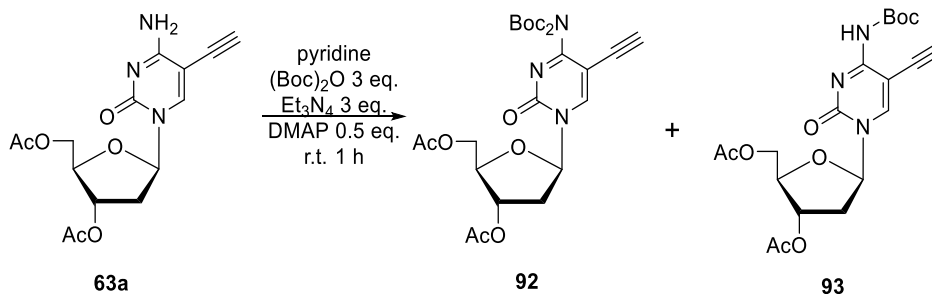
Scheme 24. Synthesis of 4-*N*-Boc protected 3',5'-di-*O*-acetyl-5-ethynyl-2'-deoxycytidine derivatives **92** and **93**
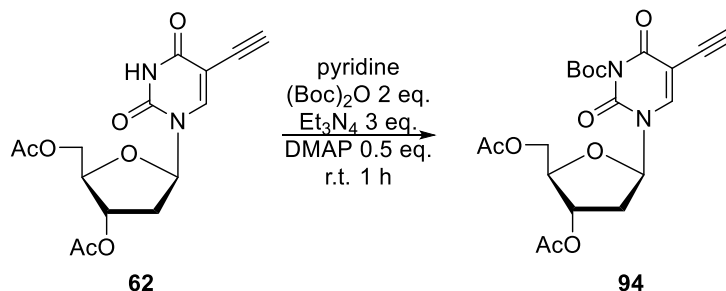
Scheme 25. Synthesis of 3-*N*-Boc-3',5'-di-*O*-acetyl-5-ethynyl-2'-deoxyuridine **94**

3.3.1.2. Method B catalyzed by CuI

Cycloaddition of the 5-ethynyl nucleosides and TMSN$_3$ in the presences of CuI as a catalyst[102] was found to produce triazoles as the sole products without formation of the vinylazides (Table 5, Entries 3-7; Table 6, Entries, 4-6; Method B). Thus, treatment of protected 5-ethynyl-2'-deoxycytidine **63a** with TMSN$_3$ in the presence of CuI gave diAc-5-TrzdC **83** with increased yield (32%; Table 5, Entry 3; Method B). Analogous

treatment of the unprotected 5-ethynyl-2'-deoxycytidine **63b**[140] by Method B gave 5-(1*H*-1,2,3-triazol-4-yl)-2'-deoxycytidine (5-TrzdC, **48)** even though with low isolated yield (10%; Table 5, Entry 4). Treatment of the uracil counterparts **62** and **77** under analogous reaction conditions yielded 3',5'-*di-O*-acetyl-5-(1*H*-1,2,3-triazol-4-yl)-2'-deoxyuridine (diAc-5-TrzdU, **84,** 55%;Table 5, Entry 5) and 5-(1*H*-1,2,3-triazol-4-yl)-2'-deoxyuridine (5-TrzdU, **39**, 50%; Entry 6), respectively. In Method B, DMF/H_2O (9:1) was used as solvent, in which H_2O was required for the reaction to give good yield.[102] Treatment of **77** by modified Method B in the presence of 2 eq. of H_2O in DMF (Entry 7) gave **39** (42%) as sole product, which showed that stoichiometric amount of H_2O was efficient for the reaction. It is noteworthy that **84** and **39** were not accessible under Ag_2CO_3 conditions (Method A).

Treatment of the 8-ethynylpurine nucleoside analogues **85-87** with $TMSN_3$ by Method B also yielded their corresponding 8-(1*H*-1,2,3-triazol-4-yl)-2'-deoxypurine nucleosides **46** (17%), **88** (27%), and **47** (31%; Table 6, Entry 4-6). However, the isolated yields were lower than that of reactions using Method A with Ag_2CO_3 as catalyst. There were more unwanted by-products below the triazole products on TLC, which meanwhile troubled the purification. After purification by regular column chromatography, further purification by HPLC (C18; A: 100% ACN, B: 5% ACN/H_2O; 0% A → 15% A in 30 min, flow rate = 2 mL/min) was required to obtain pure triazoles.

The explanation of substantial differences of reactions with various substrates and different catalysts (Ag_2CO_3 and Cu (I)) are still unclear.

3.3.1.3. Method C catalyzed by CuSO$_4$/sodium ascorbate

The relatively low yields of **83** and **48** from Method B using CuI as catalyst was due to the oxidation of Cu (I) to Cu (II) during the reaction, which was indicated by the color change of the reaction mixture from brown to dark green. To avoid the loss of catalytic ability of Cu (I), Method C employing in situ generation of Cu (I) from CuSO$_4$/sodium ascorbate was proved to be a better strategy for the synthesis of triazolyl nucleosides (Table 5, Entry 8-11; Table 6, Entries 7-9; Method C). The reaction mixtures stayed brown during the 5-hours reaction, which indicated the invariable catalytic activity of the in-situ generated Cu(I). Thus, the treatment of **63a** with TMSN$_3$ in the presence of CuSO$_4$/sodium ascorbate gave **83**, which had a better yield (Table 5, 65%; Entry 8) than that of reaction using CuI as catalyst (32%; Table 5, Entry 3). Compared to the Entry 4, the synthesis of 5-TrzdC **48** using CuSO$_4$/sodium ascorbate provided a much better yield of 51% (Entry 9). It is worth noting that the estimated yield based on the TLC was 85%. The hydroazidation of **62** by Method C gave **84** with quantitative conversion yield (Entry 10). When **77** was treated with TMSN$_3$ by Method C, similar yield of 5-TrzdU **39** (52%; Entry 11) was obtained compared to Entry 6 using Method with CuI as catalyst.

The treatment of the 8-ethynylpurine nucleoside analogues **85**-**87** with TMSN$_3$ by Method C gave their corresponding 8-(1H-1,2,3-triazol-4-yl)-2'-deoxypurine nucleosides **46** (51%; Table 6, Entry 7), **88** (58%; Entry 8), and **47** (52%; Entry 9), which were obviously much better than that given by Method B using CuI as catalyst. The unwanted by-products below the triazole products on TLC were much less.

The substrate scope of Method C for the synthesis of N-unsubstituted triazoles would be broad rather than just ethynyl nucleosides. Three presentative p-substituted

phenylacetylene, *i.e.* 4-ethynylanisole **95a** (CH$_3$O-, EDG), phenylacetylene **95b** (H-, neutral), and 4-ethynyl-α,α,α-trifluorotoluene **95c** (F$_3$C-, EWG) were chosen and applied to this CuSO$_4$/sodium ascorbate catalyzed procedure, and thus affording the corresponding triaozles in good yields (63-83%, 96a-96c, Table 7). It is noteworthy that phenylacetylene modified with electron-withdrawing group at the *p*-position promotes the formation of triazole, which matched the proposal reported.[102,144]

Table 7. Synthesis of *p*-substituted phenyl triazoles via cycloaddition catalyzed by CuSO$_4$/sodium ascorbate (Method C)

95a, 96a R = CH$_3$O
95b, 96b R = H
95c, 96c R= CF$_3$
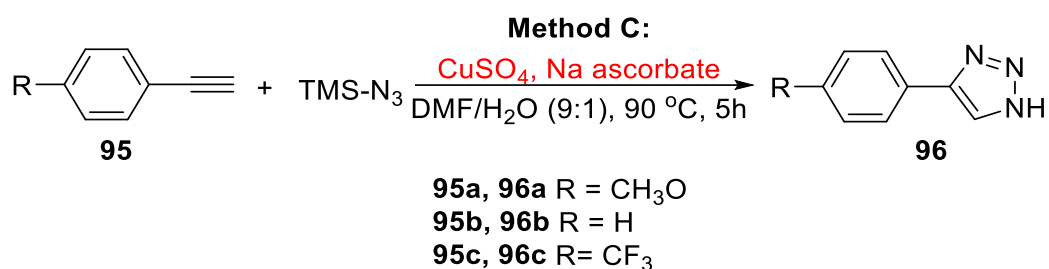
Entry	**95**	Method	**96**	Yield[b] [%]
1	**95a**	C	**96a**	63 (80)
2	**95b**	C	**96b**	73 (90)
3	**95c**	C	**96c**	83 (95)

In summary, the fluorescent sugar-protected/unprotected *N*-unsubstituted triazolyl analogues of the four natural bases of DNA can be readily prepared with good yields from the treatment of their corresponding 5- or 8-ethynyl-2'-deoxynucleosides with TMSN$_3$ in the presence of CuSO$_4$/sodium ascorbate as catalyst. Reactions catalyzed by CuI can also give triazole adducts as major products but suffered from the relatively low yield because of the loss of catalytic activities of Cu (I) to Cu (II) after oxidation. The synthesis of 8-(1*H*-1,2,3-triazol-4-yl)-2'-deoxyguanosine using Ag$_2$CO$_3$ as catalyst gave comparable yield and easier purification.

3.3.1.4. Reaction mechanism study

A tentative reaction mechanism to give the triazoles as sole products might involve first formation of vinylazide followed by 1,5-electrocyclization and tautomerization. However, attempts to validate this mechanism were performed by treatment of AvdU **21** under Method C and treatment of 8-AvdA **89** under Method A (Scheme 26) and were proved that vinyl azide did not undergo cyclization to 1,2,3-triazoles. Thus, the mechanism involving a [3+2] cycloaddition of the alkyne with in-situ generated HN_3 seems more probable (Scheme 27). The terminal alkyne substrate **97** reacts with Cu (I) or Ag (I) and forms metal activated alkyne **98**, which further reacts with hydrazoic acid **99** in-situ generated from $TMSN_3$ and H_2O to produce intermediate **100**. Protonation of **100** yields the final product *N*-unsubstituted 1,2,3-triazol-4-yl nucleosides **101** and releases Cu (I) or Ag (I) as catalyst.
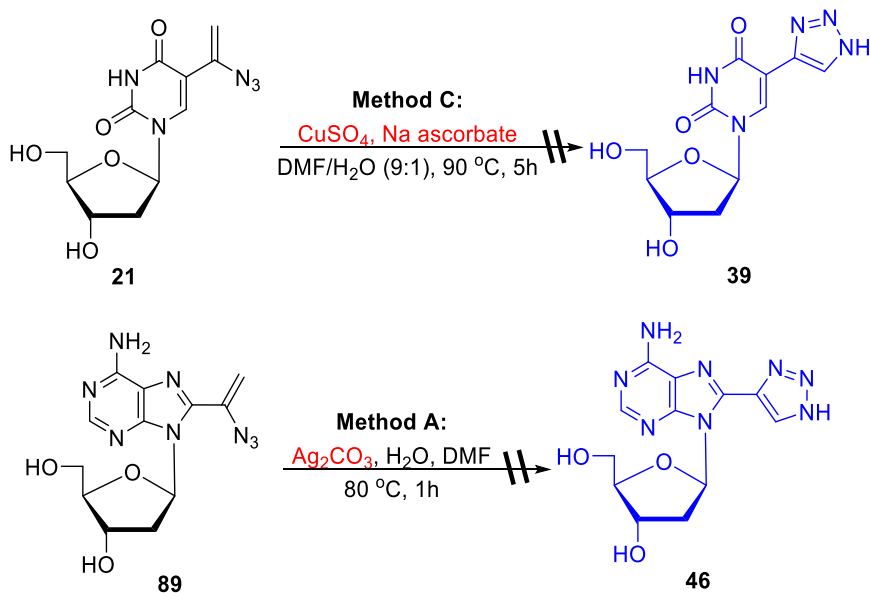
Scheme 26. Attempted conversion of vinylazides to triazoles

70
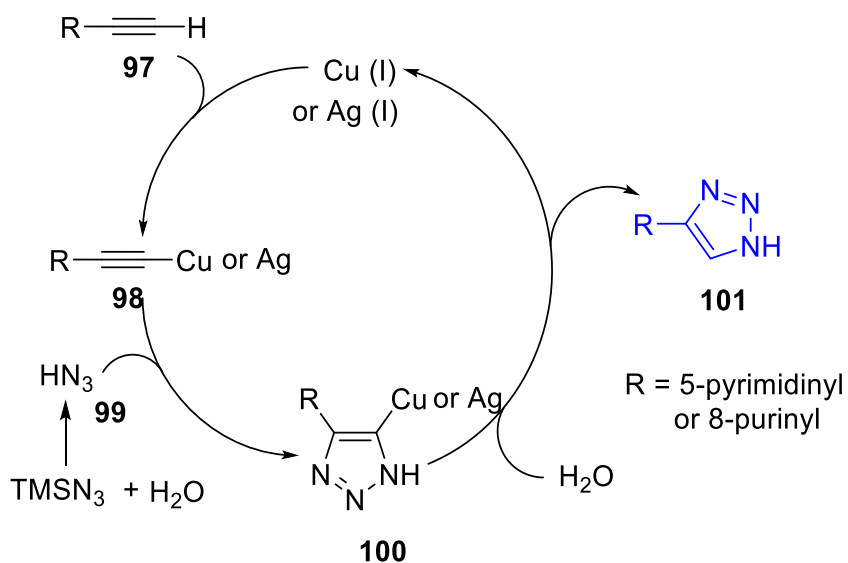
Scheme 27. Mechanism for the formation of *N*-unsubstituted 1,2,3-triazoles

3.3.2. Stabilities of *N*-unsubstituted triazolyl nucleosides

The metabolic phosphorylation by kinase in cells and the following incorporation of modified nucleosides into DNA usually requires incubation of the cells with the compounds for more than one hour.[145,146] Typically, the incubation time is one or two days or even longer. For animal test, the whole process may need several days. As a result, the biological applications demand the compounds be stable under physiological conditions. The chemical stabilities of 8-TrzdA **46**, 8-TrzdG **47**, 5-TrzdC **48**, and 5-TrzdU **39** were evaluated in D_2O/DMSO-d_6 (500 µL/50 µL) by monitoring the decomposition using ^{1}H NMR. The samples were kept in a 37 ^{o}C oil bath in the dark (covered with aluminum foil). The ^{1}H NMR spectra were recorded at 0 h, 20h, and 48 h. The ^{1}H NMR spectra of 8-TrzdA was shown in Figure 28A and the fraction remaining of the four compounds over the time was shown in Figure 28B. The results showed that 8-TrzdA **46**, 8-TrzdG **47**, 5-TrzdC **48**, and 5-TrzdU **39** were very stable and exhibited no detectable decomposition in aqueous solution after 48 h at 37 ^{o}C.

71
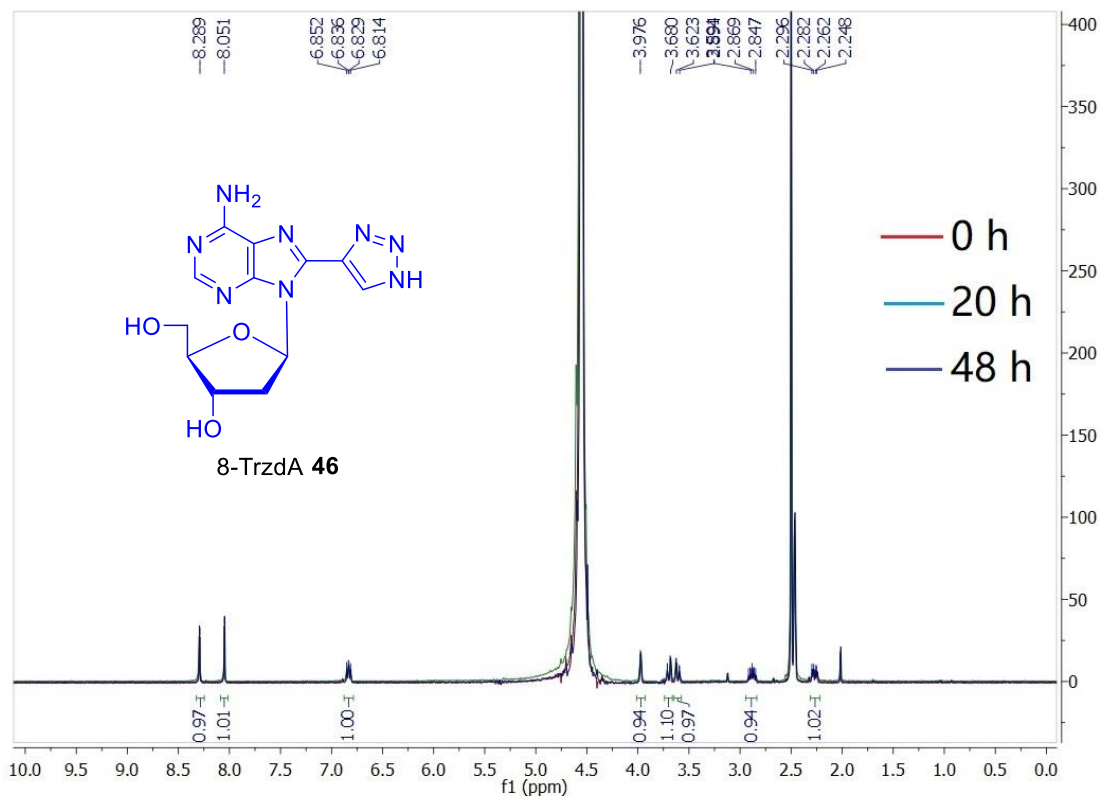
Figure 28. Stability of triazolyl nucleosides at 37 °C in aqueous solution

(A) ^{1}H NMR of 8-TrzdA in D$_2$O solution (10% DMSO) incubated at 37 ºC for 0 h, 20 h, and 48 h. (B) Fraction remaining of 8-TrzdA, 8-TrzdG, 5-TrzdU, and 5-TrzdC in D$_2$O solution (10% DMSO) incubated at 37 ºC vs. time

3.3.3. Inhibition of cell proliferation

For effective metabolic labeling, the cytotoxicity of the labeling probe is an important consideration.[146] Moreover, I was also interested in the potential application in anticancer of this group of novel nucleosides. Thus, 8-TrzdA **46**, 8-TrzdG **47**, 5-TrzdC **48**, and 5-TrzdU **39** were examined for their antiproliferative activity in HEL, HeLa, Vero, and MDCK cells. The results showed that all the compounds exhibited no cytotoxicity with $CC_{50} > 100\ \mu M$.

3.3.4. Fluorescent properties of triazolyl nucleosides

The normalized fluorescence emission, absorption, and excitation spectra for the four 1*H*-1,2,3-triazol-4-yl nucleosides in methanol were shown in Figure 29. Their photophysical data are summarized in Table 8. As expected, 8-TrzdA **46** with the C4 of triazolyl attaching to the C8 of adenine exhibits the high quantum yield (Φ_F) of 44%. 8-TrzdA **46** emits at 300-480 nm with the maximum emission at 355 nm. The diTBDMS-protected 8-TrzdA analogue **88** exhibits matching fluorescent properties with a Φ_F of 48%, which is reasonable since protection at sugar moiety does not change to the conjugated system and thus no difference would be expected. Similarly, the emission of 8-TrzdG **47** starts at 300 nm but extends to 540 nm and the maximum emission is at 364 nm. Compared to the Φ_F of 8-TrzdA **46**, the Φ_F of 8-TrzdG **88** is a little bit smaller as 9%.
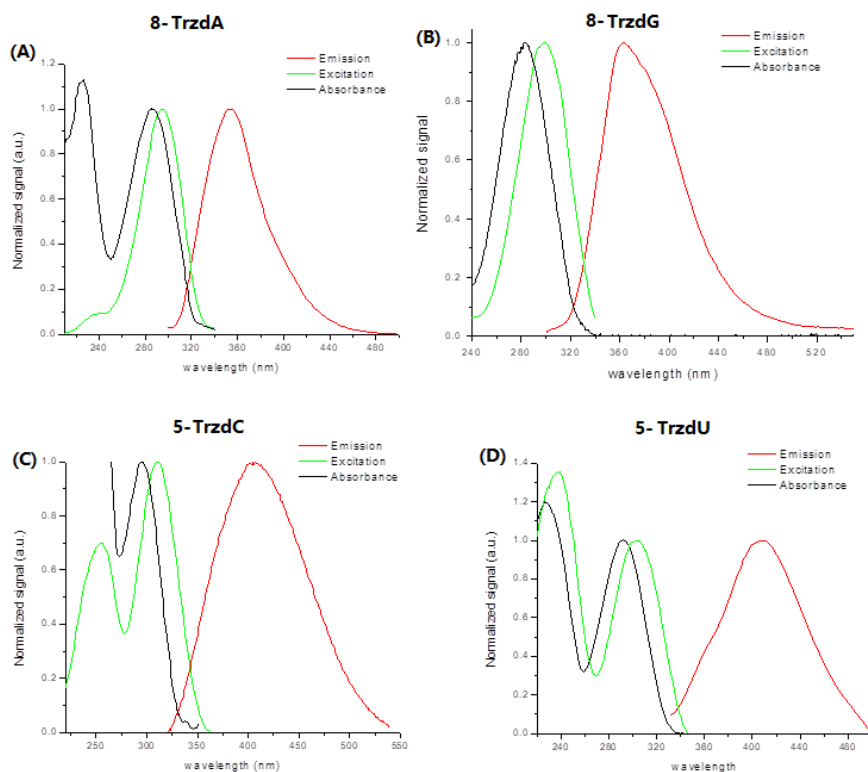
Figure 29. Normalized fluorescence emission, absorption, and excitation spectra for (A) 8-TrzdA, (B) 8-TrzdG, (C) 5-TrzdC, and (D) 5-TrzdU in MeOH

Table 8. Photophysical data for 8-TrzdA (**46**), 8-TrzdG (**47**), 5-TrzdC (**48**), 5-TrzdU (**39**), and their analogues

Comp'd	83	48	84	39	46	88	47
ε_{max} (M^{-1} cm^{-1})	4150	18750	10700	12400	17950	14100	14800
λ_{max} (abs) (nm)	293	295	291	291	287	285	283
λ_{max} (exc) (nm)	259	311	239	238	295	232	299
λ_{max} (exc) (nm)	312	254	294	302	235	292	-
λ_{max} (emi) (nm)	421	407	400	408	355	355	364
Stokes shift (nm)	128	112	109	117	68	70	81
Φ_F	0.02	0.02	0.003	0.004	0.44	0.48	0.09
τ_1 (ns)	0.46	0.10	0.05	0.14	0.69	1.01	0.61
τ_2 (ns)	4.48	4.35	1.59	1.06	2.07	2.82	3.22
$\tau_{average}$ (ns)	4.20	3.72	0.82	0.805	1.55	2.22	2.47
f_1 (%)	0.07	0.15	0.50	0.27	0.37	0.33	0.28
f_2 (%)	0.93	0.85	0.50	0.73	0.63	0.67	0.71

In contrast, the 5-pyrimidine analogues 5-TrzdU **39** and 5-TrzdC **48** showed a large Stokes shift of ~110 nm with the maximum emission approximately at 408 nm and much lower quantum yields. 5-TrzdC **48** emits at 320-550 nm ($\Phi_F = 2\%$), while 5-TrzdU **39** emits at 320-500 nm ($\Phi_F = 0.3\%$). Even though the quantum yield of 5-TrzdU is relatively low, it is still good enough to show bright fluorescence in solution and in cells (see cell imaging results in section 3.3.5). Similarly, the acetyl-protection at sugar doesn't alter the fluorescent properties of the triazolyl pyrimidine nucleosides.

All triazoles showed biphasic fluorescence decay. The four unprotected triazoles present a fast lifetime of 0.1-4.4 ns (Table 8). 5-TrzdC **48** shows the longest lifetime of 4.35 ns and longest average life time of 3.7 ns. 8-TrzdA (63%), 8-TrzdG (71%), 5-TrzdC (85%), and 5-TrzdU (73%) showed the larger contribution of the long lifetime (τ_2).

The application of these fluorescent nucleosides with the minimalistic modification at heterocyclic bases to cell imaging and DNA modifications will be discussed below.

3.3.5. Cell imaging

Primary mouse astrocytes were treated with vehicle (0.05% DMSO) or 10, 100, 1000 uM of triazoles (with 0.05% DMSO) for 24 hours. The live cells were imaged using FV10i Confocal Laser Scanning Microscope from Olympus. The selected cell images were shown in Figure 30. In the negative controls, background fluorescence was indistinguishable in cells (Figure 30A). Due to the relatively high λ (exc) of the excitation filter at 405 nm while the λ_{max} (exc) of those triazoles were at around 290-310 nm, the fluorescence was somewhat weak in Figure 30B-E. Nevertheless, we could still observe clear blue fluorescence from the triazoles in the cytosol of live cells rather than in the nucleus, which match our previous result on live cell imaging using in-situ generated fluorescent triazoles in cells.[51]
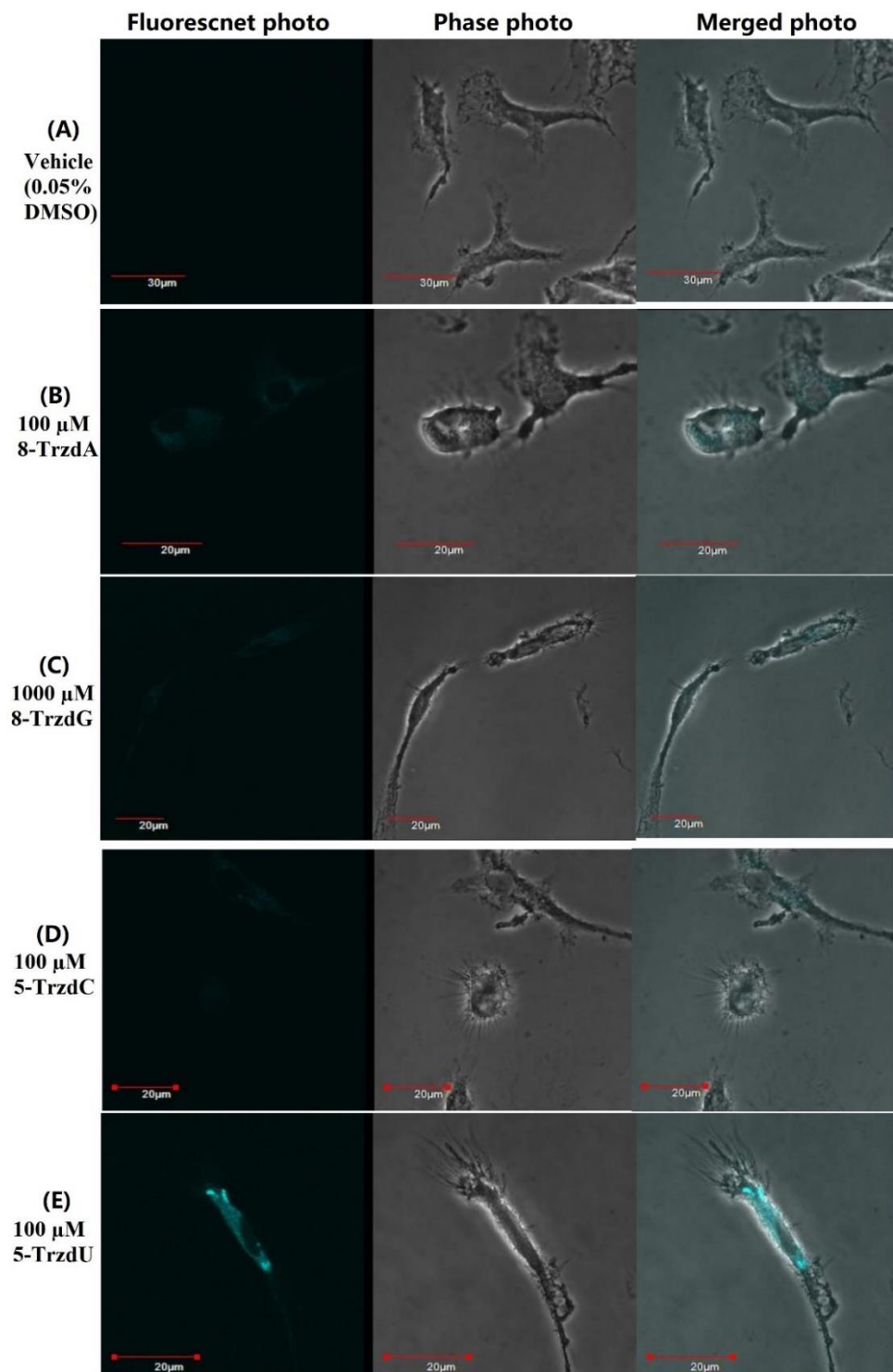
Figure 30. Fluorescence microscopy images and phase photos of primary mouse astrocytes cells treated with 8-TrzdA, 8-TrzdG, 5-TrzdC, and 5-TrzdU

To further prove that the fluorescent triazoles showed fluorescence in the cytosol, 3T3-L1 mouse pre-adipocytes (Zen-bio #SP-L1-F) transfected with pMX-puro-GFP were employed to show clearly the edge of cells and to localize the cell nucleus with its green fluorescence. 3T3-L1 mouse pre-adipocytes transfected with pMX-puro-GFP were treated with the vehicle (0.05% DMSO), 200 uM of 8-TrzdA, or 200 uM of 5-TrzdU (with 0.05% DMSO) for 24 hours. Fixed cells were mounted with ProLong™ Gold Antifade Mountant (Thermo Fisher Scientific) and observed under the Olympus FV 1200 confocal microscope (Ex/Em = 473/519 nm for imaging of GFP; Ex/Em = 405/461 nm for triazoles). Figure 31 showed clearly the cells and the nucleus. In the negative controls, background fluorescence was indistinguishable in cells incubated without any triazoles. The fluorescent 8-TrzdA (Figure 31B) and 5-TrzdU (Figure 31C) were localized at cytosol.
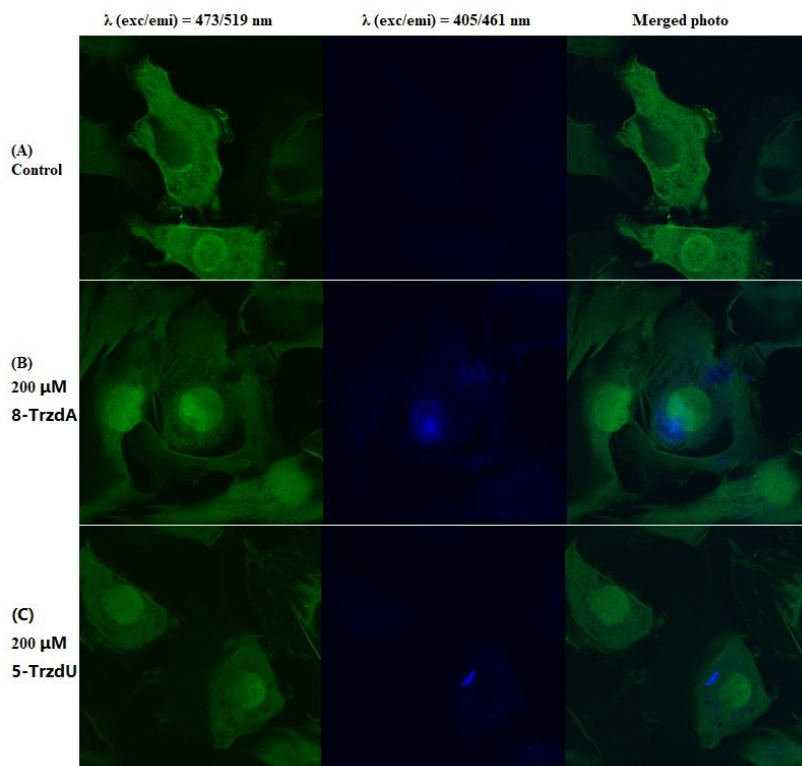
Figure 31. Fluorescence microscopy images of fixed pMX-puro-GFP transfected 3T3-L1 mouse pre-adipocytes treated with 8-TrzdA and 5-TrzdU

The reasons why the fluorescent stain was only found in cell cytosol rather than in the nucleus is still unclear. The possible reasons may be a) The triazolyl nucleosides are not substrates for polymerases, b) the triazoles are sensitive to the microenvironment and the fluorescence is quenched after being incorporated into duplex DNA.

3.3.6. Polymerase-catalyzed incorporation of 8-TrzdA into DNA and fluorescent sensitivities to varied microenvironments

3.3.6.1. Synthesis of TrzdATP

The 8-TrzdATP **102** was synthesized following the triphosphorylation reported in section 3.1.3. The reaction of 8-TrzdA **46** with POCl$_3$ in the presence of proton sponge followed by addition of TBAPP **73** and then TBA yielded 8-TrzdATP (**102**, 30%, Scheme 28) after DEAE-Sephadex purification. The phosphates were characterized by ^{1}H (Figure 32A), ^{13}C, ^{31}P NMR (Figure 32B) as well as HR-MS (details at experimental section 4.1.4).
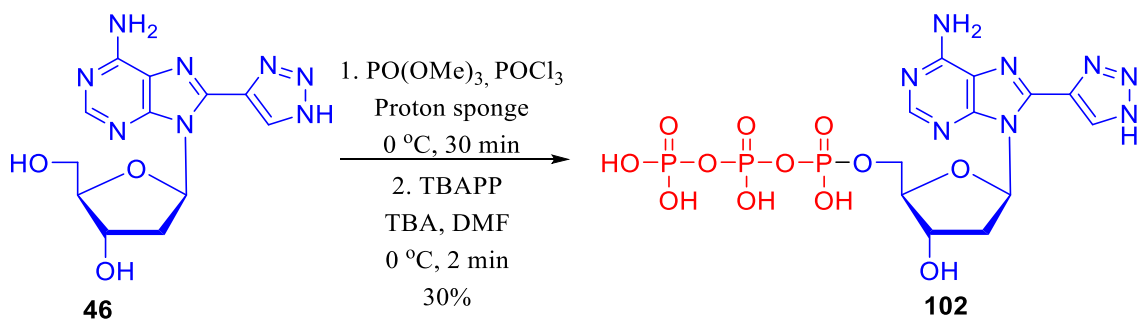
Scheme 28. Synthesis of TrzdATP
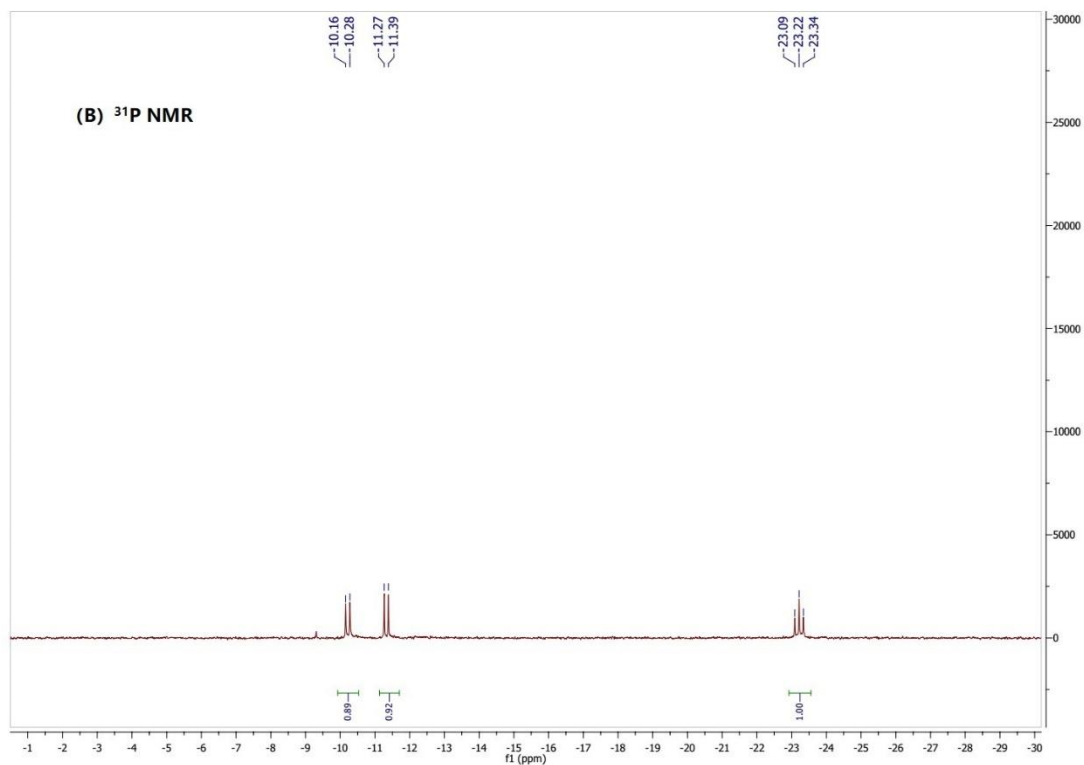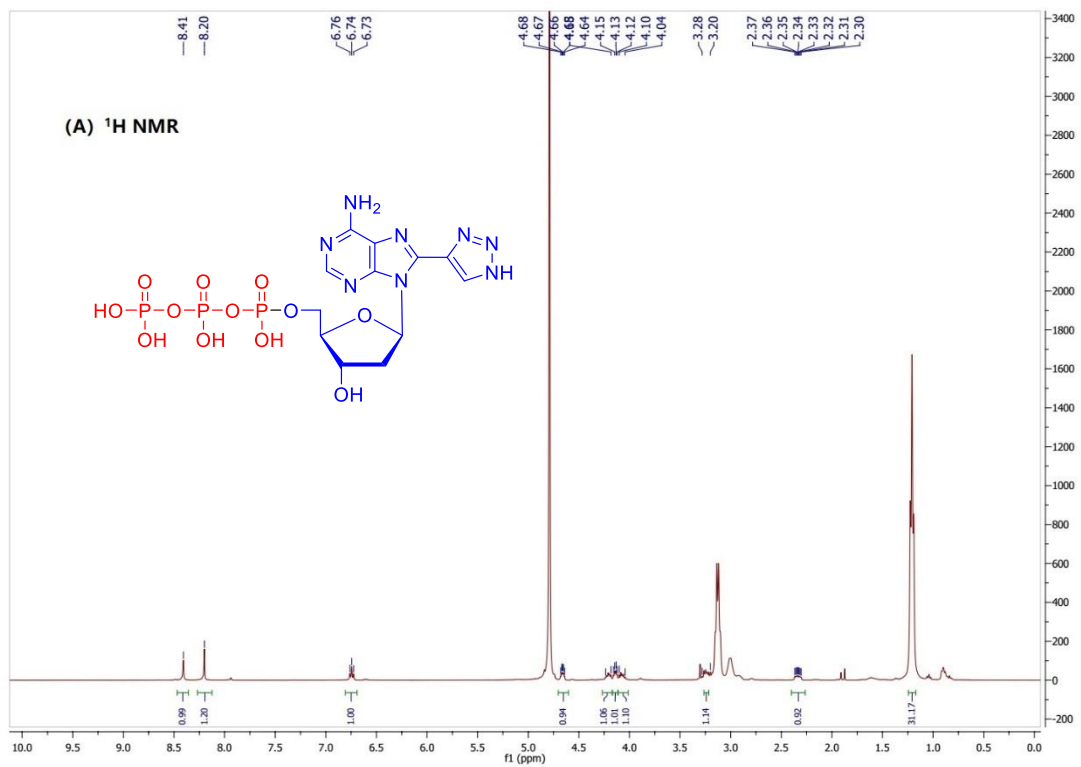
Figure 32. ^{1}H (A) and ^{31}P (B) NMR of 8-TrzdATP

3.3.6.2. Enzymatic incorporation of 8-TrzdATP into DNA

To determine the reasons leading to fluorescent stain localization to the cell cytosol rather than in the nucleus, 8-TrzdATP **102** was prepared to investigate if it could be substrate for polymerases and also to test the changes of fluorescent properties of the triazoles before and after being incorporated into duplex DNA (Figure 33).
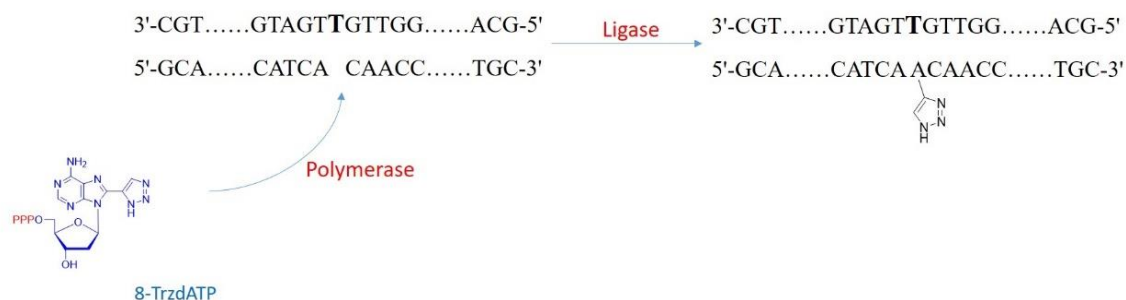
Figure 33. Proposed incorporation of 8-TrzdATP into DNA

3.4. Antiviral and cytostatic evaluation of 5-(1-halo-2-sulfonylvinyl) and 5-(2-furyl) uracil nucleosides

The work on section 3.4 as well as experimental section 4.1.5, 4.7 and 4.8 was published as an original paper at Arch Pharm/Wiley (Z. Wen, S. H. Suzol, J. Peng, Y. Liang, R. Snoeck, G. Andrei, S. Liekens, S. F. Wnuk, *Archiv der Pharmazie* **2017**, *350*, e1700023-n/a).[147]

3.4.1. Chemistry

Tetrabutylammonium fluoride (TBAF)-mediated direct C-H arylation of 5-iodouracil nucleosides (**103** or **105**) with furan yielded 5-(fur-2-yl)-2'-deoxyuridine **106** (73%)[111] or 2',3',5'-tri-*O*-acetyl-5-(fur-2-yl)uridine **107** (67%, Scheme 29). Treatment of 5-iodo-2'-deoxyuridine **103** with 2-heptylfuran gave 2'-deoxy-5-(5-heptylfur-2-yl)uridine **108** (61%) as a single isomer. Analogous cross-coupling of the protected 2'-deoxyuridine **104** or

uridine **105** with 2-heptylfuran provided regioselectively acetyl protected 5-(5-heptylfur-2-yl) derivatives **109** (60%) and **110** (55%). Deacetylation of **110** with methanolic ammonia afforded 5-(5-heptylfur-2-yl)uridine (**111**; 81%). Esterification of **106** with undecanoic anhydride yielded 5'-*O*-undecanoyl- and 3',5'-di-*O*-undecanoyl-5-(fur-2-yl)-2'-deoxyuridine **112** and **113**. Analogously **108** was converted to 5-(5-heptylfur-2-yl) esters **114** and **115**.

103 R= R^1 = X = H
104 R = R^1 = Ac, X = H
105 R = R^1 = Ac, X = OAc

106 R = R^1 = X = Y = H
107 R = R^1 = Ac, X = OAc, Y = H
108 R = R^1 = X = H, Y = C$_7$H$_{15}$
109 R = R^1 = Ac, X = H, Y = C$_7$H$_{15}$
110 R = R^1 = Ac, X = OAc, Y = C$_7$H$_{15}$
111 R = R^1 = H, X = OH, Y = C$_7$H$_{15}$

NH$_3$/MeOH
0 °C, 12 h

112 R = C$_{10}$H$_{21}$CO, R^1 = Y = H
113 R = R^1 = C$_{10}$H$_{21}$CO, Y = H
114 R= C$_{10}$H$_{21}$CO, R^1 = H, Y = C$_7$H$_{15}$
115 R= R^1 = C$_{10}$H$_{21}$CO, Y = C$_7$H$_{15}$

TBAF, Pd$_2$(dba)$_3$, DMF
100 °C, 1 h

(C$_{10}$H$_{21}$CO)$_2$O
DMAP, DMF, r.t.
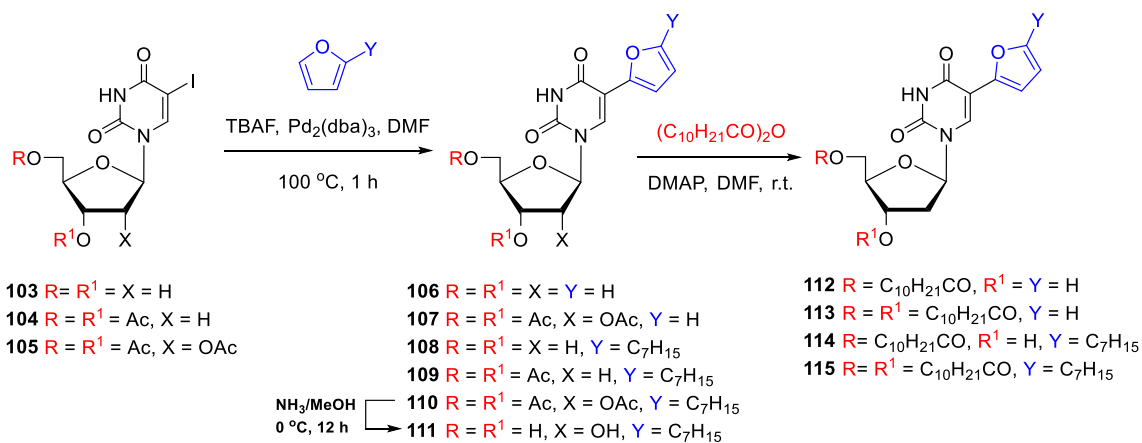
Scheme 29. Synthesis of 5-(fur-2-yl)- or 5-(5-heptylfur-2-yl)uracil nucleosides by direct C-H arylation

For the synthesis of 5'-monoesters of the 5-furyl substituted uridines (e.g., **119** and **120**), I have developed a three-step protocol starting from 2',3'-*O*-isopropylideneuridine **116** (Scheme 30). Thus, treatment of **116** with undecanoic acid in the presence of DCC gave 2',3'-*O*-isopropylidene-5'-*O*-undecanoyluridine (**117**) in 90% yield. Iodination of **117** with ICl in CH$_2$Cl$_2$ yielded 5'-*O*-undecanoyl-5-iodouridine (**118**). Direct C-H cross-coupling of **118** with furan or 2-heptylfuran in the presence of TBAF[111] gave 5'-*O*-undecanoyl-5-(fur-2-yl)uridine (**119**, 63%) or 5'-*O*-undecanoyl-5-(5-heptylfur-2-yl)uridine (**120**, 44%), respectively.
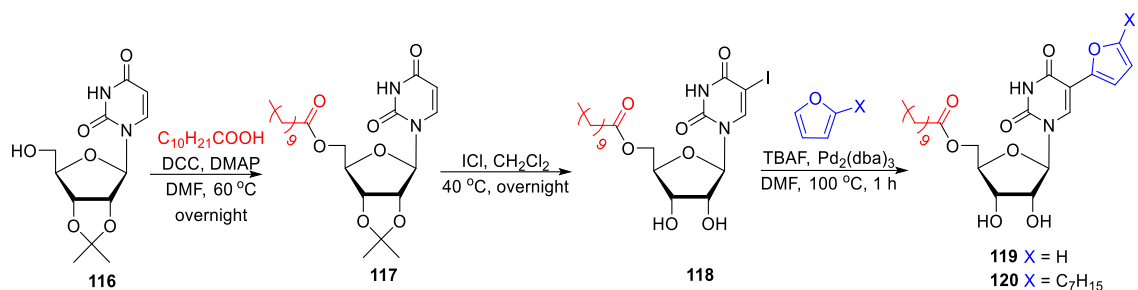
Scheme 30. Synthesis of 5-(fur-2-yl)- or 5-(5-heptylfur-2-yl)uridine and their 5'-esters

The 5-vinyl sulfone analogues: (*E*)-5-(1-bromo-2-tosylvinyl)-2'-deoxyuridine (**121**), (*E*)-3',5'-di-*O*-acetyl-5-(1-chloro-2-tosylvinyl)-2'-deoxyuridine (**122**), (*E*)-5-(1-chloro-2-tosylvinyl)uridine (**123**), (*E*)-5-(1-bromo-2-tosylvinyl)uridine (**124**), (*E*)-1-(*β*-D-arabinofuranosyl)-5-(1-chloro-2-tosylvinyl)uracil (**125**), (*E*)-5-(1-propylthio-2-tosylvinyl)-2'-deoxyuridine (**126**), and (*E*)-5-(1-propylthio-2-tosylvinyl)uridine (**127**) were prepared as reported.[110] The 5-heteroarene analogues: 3',5'-di-*O*-acetyl-5-(fur-2-yl)-2'-deoxyuridine (**128**), 5-(fur-2-yl)uridine (**129**), 1-(*β*-D-arabinofuranosyl)-5-(fur-2-yl)uracil (**130**), 1-(2,3,5-tri-*O*-acetyl-*β*-D-arabinofuranosyl)-5-(fur-2-yl)uracil (**131**), 5-(thiophen-2-yl)uridine (**132**), and 5-(5-methylthiophen-2-yl)uridine (**133**) were prepared as reported[111] (Figure 34).
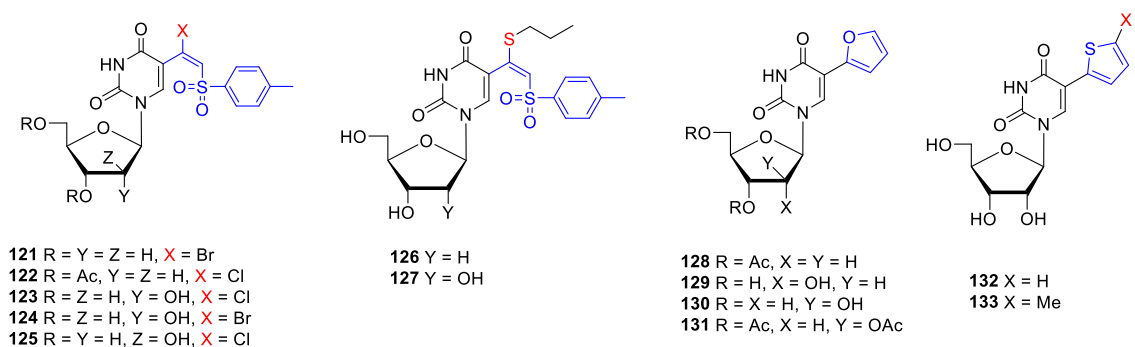
Figure 34. Structures of 5-(1-substituted-2-tosylvinyl) **121**-**127** and 5-(2-heteroaryl) **128**-**133** uracil nucleosides tested

82

3.4.2. Inhibition of cell proliferation

The C5 substituted pyrimidine nucleosides (**106**-**115**, **119**-**133**) were first examined for their antiproliferative activity in murine leukemia (L1210), human leukemia (CEM) and human cervical carcinoma (HeLa) cells. From the (β-halo)vinyl sulfones tested (**121-125**), only the acetyl protected 2'-deoxyuridine (β-chloro)vinyl sulfone **122** inhibited the growth of these cell lines in the lower μM range (Table 9). From the 5-(fur-2-yl) analogues tested (**106-115**, **119**, **120**, **128-131**), the 2'-deoxy-5-(5-heptylfur-2-yl)uridine **108** inhibited the growth of CEM cell lines in the μM range.

Table 9. Inhibitory effects of 5-(1-substituted-2-tosylvinyl) and 5-(2-heteroaryl)uracil nucleosides on the proliferation of murine leukemia cells (L1210), human T-lymphocyte cells (CEM), and human cervix carcinoma cells (HeLa)

Compound	IC_{50}^{a} (μM)		
	L1210	CEM	HeLa
106	> 100	> 100	32 ± 1
107	> 100	80 ± 8	> 100
108	48 ± 6	16 ± 4	> 100
109	65 ± 10	36 ± 3	> 100
110	88 ± 17	53 ± 1	> 100
111	95 ± 8	42 ± 2	> 100
114	> 100	93 ± 4	> 100
115	> 100	78 ± 16	> 100
119	43 ± 8	70 ± 2	64 ± 5
122	5.6 ± 4.7	11 ± 10	23 ± 8
125	> 100	> 100	> 100
127	> 100	> 100	93 ± 14
129	> 100	60 ± 27	83 ± 25
130	> 100	> 100	> 100
131	40 ± 10	63 ± 3	> 100
132	> 100	86 ± 6	> 100
133	> 100	> 100	> 100

[a] 50% inhibitory concentration.

83

3.4.3. Antiviral activity

The antiviral activity of all compounds was tested against a broad range of DNA and RNA viruses and the human immunodeficiency (HIV) virus. Some of the compounds proved active against herpesviruses though they were less potent than the reference anti-herpesvirus drugs (Table 10). The 5-(5-heptylfur-2-yl) (**108**) and 3',5'-Di-*O*-acetyl-5-(5-heptylfur-2-yl) **(109)** derivatives inhibited the replication of human cytomegalovirus (HCMV) and varicella-zoster virus (VZV) bearing a wild-type thymidine kinase (TK$^+$) with 50% effective concentrations (EC$_{50}$'s) in the range of 10-20 µM. Compound **108** was equally active against TK$^+$ and TK-deficient (TK$^-$) VZV strains while compound **109** failed to inhibit a TK$^-$ VZV mutant virus. Neither compound **108** nor **109** were able to decrease herpes simplex virus 1 (HSV-1) and 2 (HSV-2) induced cytopathic effect. In contrast, the 5-(fur-2-yl)uracil nucleoside **106** emerged among the compounds synthesized as the most potent inhibitor of the HSV-1 TK$^+$ strain Kos with an EC$_{50}$ of 4 µM. Compound **106** was less active against HCMV, HSV-2 and the VZV TK$^+$ Oka strain than against HSV-1 while it lacked activity against TK$^-$ HSV-1 and VZV. The spectrum of activity of compound **130** only included HSV-1 and VZV TK$^+$ strains. The (β-chloro)vinyl sulfone **122** showed an EC$_{50}$ of 4 µM for the Oka strain (VZV TK$^+$) and marginal activity against HCMV. Except for compound **108** that displayed antiviral activity against parainfluenza virus (Table 11), none of the compounds showed activity against the other tested viruses.

Table 10. Anti-herpesvirus activity of 5-(1-substituted-2-tosylvinyl) and 5-(2-heteroaryl)uracil nucleosides in HEL (human embryonic lung) fibroblasts

Compound	Cytotoxicity (μM)	EC$_{50}$ (μM)[a]						
	MCC[b]	HSV-1 (KOS)	HSV-2 (G)	HSV-1 TK⁻ (KOS ACV^r)	HCMV (AD-169)	HCMV (Davis)	VZV TK⁺ (Oka)	VZV TK⁻ (07-1)
106	>100	4 ± 0	47 ± 37	>100	45	20	32	>100
108	100	>100	>100	>100	10	20	13 ± 2	12 ± 5
109	100	>100	>100	>100	10 ± 2	12 ± 4	20	>20
122	100	>100	>100	>100	>20	20	4	>20
130	>100	14 ± 8	>100	>100	>100	>100	25	>100
Acyclovir	>440	0.4 ± 0.1	0.3 ± 0.1	110 ± 104	ND	ND	0.7 ± 0.1	44 ± 7
Brivudin	>300	0.04 ± 0	188 ± 88	27 ± 32	ND	ND	0.02 ± 0.01	29 ± 10
Ganciclovir	>350	0.06 ± 0.04	0.07 ± 0.03	4.4 ± 3.4	7.9 ± 2.4	4.3 ± 3.6	ND	ND
Cidofovir	>350	2.7 ± 1.0	1.5 ± 0.7	1.4 ± 0.9	0.9 ± 0.6	0.8 ± 0.6	ND	ND

[a] Required to reduce virus-induced cytopathogenicity by 50%.
[b] Minimum cytotoxic concentration (MCC) required to cause a microscopically detectable alteration of normal cell morphology.

Table 11. Activity of 5-(5-heptylfur-2-yl)-2'-deoxyuridine against Parainfluenza virus

Compound	Cytotoxicity (μM)	EC$_{50}$ (μM)[a]
	MCC[b]	Parainfluenza-3 virus
108	>100	14 ± 8

[a] Required to reduce virus-induced cytopathogenicity by 50%.
[b] Minimum cytotoxic concentration (MCC) required to cause a microscopically detectable alteration of normal cell morphology.

4. EXPERIMENTAL SECTION

4.1. Synthesis

4.1.1. General Procedure

^{1}H (400 MHz) and ^{13}C (100.6 MHz) NMR spectra were recorded in solutions of $CDCl_3$ unless otherwise noted. Reaction progress was monitored by TLC on Merck Kieselgel 60-F_{254} sheets with product detection by 254-nm light. Products were purified by column chromatography using Merck Kiselgel 60 (230-400 mesh) or by automated flash chromatography using a CombiFlash system. Reagent grade chemicals were used and solvents were dried by reflux and distillation from CaH_2 under N_2 unless otherwise specified. All reactions were carried out under the Argon atmosphere.

4.1.2. Synthesis of pyrimidine nucleosides with azidomethyl and azidovinyl modification at C5 position and their 5'-phosphates

5-Azidomethyl-2'-deoxyuridine 5'-monophosphate (AmdUMP, 19). Phosphoryl chloride (11.2 μL, 18.4 mg, 0.12 mmol) was added to a stirred solution of AmdU **18**[40] (28.3 mg, 0.1 mmol) and proton sponge (32 mg, 0.15 mmol) in trimethyl phosphate (1 mL) at 0 ºC. The resulting mixture was stirred at 0 ºC for 30 min and then quenched by adjusting the pH to 7.5 with 2 M TEAB buffer. The residue was dissolved in water (5 mL) and was extracted with EtOAc (3 x 5 mL). The water layer was evaporated and coevaporated with mixture of EtOH/H_2O (1:1, 5 mL). The residue was column chromatographed (DEAE–Sephadex®, TEAB 0.1 M → 0.4 M) and the appropriate fractions were evaporated in vacuum and coevaporate 5 times with mixture of EtOH/H_2O (1:1, 10 mL) to remove excess of TEAB salt to give AmdU monophosphate triethylammonium salt **19**. (25.5 mg, 70.4%): ^{1}H NMR (D_2O) δ 2.36-2.39 (m, 2H, H2',2''), 3.99-4.08 (m, 2H, H5',5''), 4.16-4.20 (m, 1H,

H4'), 4.18 (s, 2H, CH$_2$), 4.55-4.59 (m, 1H, H3'), 6.31 (t, J = 6.4 Hz, 1H, H1'), 8.09 (s, 1H, H6); ^{31}P NMR (D$_2$O) δ 1.16 (s); ^{13}C NMR (D$_2$O) δ 39.1, 47.0, 64.6, 71.0, 85.6, 85.8, 109.6, 141.0, 151.5, 165.2; HRMS calcd for C$_{10}$H$_{14}$N$_5$O$_8$P [M-H]$^-$ 362.05072, found 362.05042.

5-Azidomethyl-2'-deoxyuridine 5'-triphosphate (AmdUTP, 20). Phosphoryl chloride (11.2 μL, 18.4 mg, 0.12 mmol) was added to a stirred solution of AmdU **18**[40] (28.3 mg, 0.1 mmol) and proton sponge (32 mg, 0.15 mmol) in trimethyl phosphate (1 mL) at 0 °C. The resulting mixture was stirred at 0 °C for 30 min. 0.5 M tributylammomium pyrophosphate solution in DMF (1 mL, 0.5 mmol) and then tributylamine (71.2 μL, 55.6 mg, 0.3 mmol) were added to the reaction mixture and stirred at 0 °C for 2 min. The reaction was quenched by adjusting the pH to 7.5 with 2 M TEAB buffer. The residue was dissolved in water (5 mL) and was extracted with EtOAc (3 x 5 mL). The water layer was evaporated and coevaporated with mixture of EtOH/H$_2$O (1:1, 5 mL). The residue was column chromatographed (DEAE–Sephadex®, TEAB 0.1 M → 0.6 M) and the appropriate fractions were evaporated in vacuum and coevaporate 5 times with mixture of EtOH/H$_2$O (1:1, 10 mL) to give AmdU triphosphate triethylammonium salt **20**. (39.5 mg, 75.6%). ^{1}H NMR (D$_2$O) δ 2.37-2.41 (m, 2H, H2',2"), 4.20 (s, 2H, CH$_2$), 4.20-4.29 (m, 3H, H4',5',5"), 4.64-4.67 (m, 1H, H3'), 6.32 (t, J = 6.0, 1H, H1'), 8.06 (s, 1H, H6); ^{31}P NMR (D$_2$O) δ -23.25 (t, J = 19.7, 1P, β), -11.64 (d, J = 19.8, 1P, α), -10.80 (d, J = 19.8, 1P, γ); ^{13}C NMR (D$_2$O) δ 38.9, 47.1, 65.4, 70.8, 85.5, 85.8, 109.7, 141.0, 151.5, 165.2; HRMS calcd for C$_{10}$H$_{16}$N$_5$O$_{14}$P$_3$ [M-H]$^-$ 521.98338, found 521.98262.

5-(1-Azidovinyl)-2'-deoxyuridine (AvdU, 21). Procedure A. *Step a*: Ag$_2$CO$_3$ (5.5 mg, 0.02 mmol) was added to a solution of **62**[110] (67.3 mg, 0.2 mmol), TMSN$_3$ (52.5 μL, 46 mg, 0.4 mmol), and H$_2$O (7 μL, 7 mg, 0.4 mmol) in DMF (2 mL). The resulting mixture

was stirred at 80 °C for 1 hour. After cooling to ambient temperature, the volatiles were evaporated under the reduced pressure and the residue was column chromatographed (hexane/EtOAc 50:50) to give **64** (39 mg, 52%): ^{1}H NMR δ 2.07 (s, 6H, Ac), 2.33-2.46 (m, 2H, H2',2''), 4.24-4.29 (m, 3H, H4', 5',5''), 5.06 (s, 1H, =CH$_2$), 5.19-5.21 (m, 1H, H3'), 6.00 (s, 1H, =CH$_2$), 6.14 (t, J = 6.4 Hz, 1H, H1'), 7.83 (s, 1H, H6), 11.73 (s, 1H, NH); ^{13}C NMR δ 20.37, 20.81, 36.71, 63.75, 74.19, 81.84, 85.36, 101.58, 107.30, 136.87, 138.33, 149.26, 160.88, 170.09, 170.17. *Step b*: Methanolic ammonia (4 mL) was added to **64** (38.9 mg, 0.1 mmol) in 2 mL MeOH and the resulting mixture was stirred at 0 °C → r.t for 12 hours. Volatiles were evaporated and the residue was column chromatographed (EtOAc/MeOH 95:5) gave AvdU **21** (27.4 mg, 90%): UV (MeOH) λ$_{max}$ 227, 248 (sh), 286 nm (ε 10650, 7600, 8700), λ$_{min}$ 204, 264 nm (ε 4050, 7200); ^{1}H NMR (DMSO-d6) δ 2.09-2.19 (m, 2H, H2' & 2''), 3.54-3.64 (m, 2H, H5' & 5''), 3.82 (q, J = 3.1, 1H, H4'), 4.23-4.27 (m, 1H, H3'), 5.00 (d, J = 0.7 Hz, 1H, =CH$_2$), 5.11 (t, J = 4.5 Hz, 1H, 5'-OH), 5.28 (d, J = 4.2 Hz, 3'-OH), 5.91 (d, J = 0.8 Hz, 1H, =CH$_2$), 6.16 (t, J = 6.4 Hz, 1H, H1'), 8.26 (s, 1H, H6), 11.60 (s, 1H, NH); ^{13}C NMR (DMSO-d6) δ 40.2, 61.0, 70.3, 84.8, 87.6, 101.3, 107.1, 137.3, 139.4, 149.4, 161.0; HRMS calcd for C$_{11}$H$_{13}$N$_5$O$_5$Na [M+Na]$^+$ 318.0809, found 318.0784.

5-Azidomethyl-2'-deoxycytidine (AmdC, 42). *Step a:* TIPBS-Cl (59 mg, 0.2 mmol) was added to a stirring solution of **54**[40] (67 mg, 0.13 mmol), DMAP (2 mg, 0.016 mmol), and triethylamine (27 µL, 19.7 mg, 0.2 mmol) in CH$_2$Cl$_2$ (1.5 mL) at ambient temperature. After 1 h, the residue was partitioned between CH$_2$Cl$_2$ and H$_2$O. The organic layer was washed with NaHCO$_3$/H$_2$O and brine. Then 2.5 mL THF and 4 mL of aq. NH$_3$ was added into the reaction residue and stirred at rt overnight. The volatiles were evaporated and the residue was partitioned between EtOAc and saturated brine and was column

chromatographed (CHCl₃/MeOH, 0:100 → 85:15) to give **55** (57.4 mg, 86%) of sufficient purity to be used in next step: ^{1}H NMR (DMSO-d_6) δ 0.07 (s, 6H, 2 x CH₃), 0.08 (s, 6H, 2 x CH₃), 0.87 (s, 9H, 3 x CH₃), 0.88 (s, 9H, 3 x CH₃), 2.00-2.07 (m, 1H, H2'), 2.15 (ddd, J = 13.6, 6.5, 3.4 Hz, 1H, H2''), 3.71-3.72 (m, 2H, H5',5''), 3.82 (q, J = 4.2 Hz, H4'), 4.22 (s, 2H, CH₂N₃), 4.32-4.35 (m, 1H, H3'), 6.14 (t, J = 6.8 Hz, H1'), 7.13 (s, 1H, NH), 7.54 (s, 1H, NH), 7.70 (s, 1H, H6); ^{13}C NMR (DMSO-d_6) δ -5.5, -5.0, -4.8, 17.6, 17.9, 25.6, 25.7, 40.0, 47.3, 62.8, 72.2, 84.8, 86.9, 100.0, 141.4, 154.4, 164.0 Step b: 1 M TBAF/THF (330 uL, 0.33 mmol) was added to a stirring solution of **55** (57.4 mg, 0.11 mmol) in THF (5 mL). After 4 h, volatiles were evaporated and the residue was column chromatographed (CHCl₃/MeOH, 100:0→85:15) and further purified by HPLC (C18; A: 100% ACN, B: 5% ACN/H₂O; 0% A → 5% A in 30 min, flow rate = 2 mL/min) to give **42** (27.3 mg, 88%): UV (MeOH) λ_{max} 206, 276 nm (ε 18 000, 6300), λ_{min} 256 nm (ε 4800); ^{1}H NMR (DMSO-d_6) δ 1.91-1.98 (m, 1H, H2'), 2.14 (ddd, J = 13.4, 5.9, 3.5 Hz, H2''), 3.52-3.62 (m, 2H, H5',5''), 3.78 (q, J = 4.0 Hz, 1H, H4'), 4.19-4.23 (m, 1H, H3'), 4.23 (s, 2H, CH₂N₃), 5.01 (t, J = 4.8 Hz, 1H, 5'-OH), 5.22 (d, J = 4.0 Hz, 1H, 3'-OH), 6.12 (t, J = 6.1, 1H, H1'), 7.12 (s, 1H, NH), 7.49 (s, 1H, NH), 7.97 (s, 1H, H6); ^{13}C NMR (DMSO-d_6) δ 40.4, 47.4, 61.3, 70.2, 85.0, 87.3, 99.9, 142.0, 154.6, 164.0; HRMS calcd for $C_{10}H_{14}N_6O_4Na$ [M+Na]$^+$ 305.0969, found 305.0969.

5-(1-Azidovinyl)-2'-deoxycytidine (AvdC, 43). **Method A**. *Step a:* Treatment of **63a**[119] (297 mg, 0.88 mmol) with TMSN₃ by procedure A, *step a,* (column chromatography; CHCl₃/MeOH, 100:0 → 90:10) gave 3',5'-di-*O*-acetyl-5-(1-azidovinyl)-2'-deoxycytidine **65** (169 mg, 51%): ^{1}H NMR δ 2.03 (s, 3H, Ac), 2.06 (s, 3H, Ac), 2.32-2.42 (m, 2H, H2',2''), 4.19-4.28 (m, 3H, H4',5',5''), 5.06 (d, J = 1.5 Hz, 1H, =CH₂), (d, J = 1.4 Hz, 1H, =CH₂),

5.16-5.18 (m, 1H, H3'), 6.15 (t, J = 6.5 Hz, 1H, H1'), 7.05 (s, 1H, NH), 7.64 (s, 1H, NH), 7.69 (s, 1H, H6). *Step b*: Treatment of **65** (160 mg, 0.42 mmol) with methanolic ammonia by Procedure A, s*tep b,* (HPLC, C18; A: 100% ACN, B: 5% ACN/H_2O; 0% A → 5% A in 50 min, flow rate = 2 mL/min; R_t = 15.6 min) gave AvdC **43** (59 mg, 48%): UV (MeOH) λ_{max} 213, 244 (sh), 283 nm (sh) (ε 18500, 10800, 5350); ^{1}H NMR (DMSO-d6) δ 1.98-2.00 (m, 1H, H2'), 2.16 (s, J = 3.8, 1H, H2''), 3.52-3.63 (m, 2H, H5' & 5''), 3.79 (q, J = 3.3, 1H, H4'), 4.20-4.23 (m, 1H, H3'), 5.00 (d, J = 1.7 Hz, 1H, =CH_2), 5.05 (d, J = 1.7 Hz, 1H, =CH_2), 5.06 (s, 1 H, 5'-OH), 5.22 (s, 1H, 3'-OH), 6.11 (t, J = 7.1 Hz, 1H, H1'), 6.93 (s, 1H, NH), 7.52 (s, 1H, NH), 8.05 (s, 1H, H6); ^{13}C NMR (DMSO-d6) δ 40.7, 60.9, 70.0, 85.2, 87.4, 101.8, 103.5, 139.2, 141.5, 154.1, 162.4; HRMS calcd for $C_{11}H_{14}N_6O_4Na$ [M+Na]$^+$ 317.0969, found 317.0976.

Method B. Treatment of 5-ethynyl-2'-deoxycytidine **63b**[120] (40 mg, 0.16 mmol) with TMS-N_3 by procedure A *step a* (column chromatography; CHCl$_3$/MeOH, 95:5 → 85:15) gave **43** (16 mg, 34%).

Method C. TIPBSCl (68 mg, 0.22 mmol) was added to a stirring solution of **64** (56.7 mg, 0.15 mmol), DMAP (2.3 mg, 0.018 mmol), and TEA (32 μL, 22.8 mg, 0.22 mmol) in CH_2Cl_2 (1.5 mL) at ambient temperature. After 1 h, the residue was partitioned between CH_2Cl_2 and H_2O. The organic layer was washed with NaHCO$_3$/H_2O and brine. Then 3 mL THF and 4.5 mL of aq. NH$_3$ was added into the reaction residue and stirred at rt overnight. The volatiles were evaporated and the residue was column chromatographed (CHCl$_3$/MeOH, 100:0 → 85:15) to give **43** (28 mg, 63%).

3',5'-di-*O*-acetyl-5-azidomethyl-2'-deoxyuridine (diAcAmdU, 56). Into a solution of AmdU **18**[40] (85 mg, 0.3 mmol) and 4-dimehtylaminopyridine (3.7 mg, 0.03 mmol) in 3

mL acetonitrile was added triethylamine (209 µL, 151.8 mg, 1.5 mmol). The resulting mixture was stirred for 5 min. Acetic anhydride (85 µL, 91.9 mg, 0.9 mmol) was added and the reaction mixture was stirred at room temperature for 1 h. The volatiles were evaporated and the residue was dissolved in EtOAc and was extracted with $NaHCO_3$ aqueous solution. The organic layer was collected and dried over Na_2SO_4. The volatiles were evaporated under the reduced pressure and the residue was column chromatographed (hexane/EtOAc 70:30 → 40:60) to give **56** (71.3 mg, 65%): ^{1}H NMR δ 2.11-2.20 (m, 1H, H2'), 2.12 (s, 3H, CH_3), 2.14 (s, 3H, CH_3), 2.53 (ddd, J = 14.2, 5.3, 1.7 Hz, 1H, H2"), 4.13 (d, J = 5.2 Hz, 1H, CH_2N_3), 4.24 (d, J = 3.9 Hz, 1H, CH_2N_3), 4.27-4.33 (m, 2H, H4',5'), 4.42 (dd, J = 12.6, 5.3 Hz, 1H, H5"), 5.21-5.24 (m, 1H, H3'), 6.31 (dd, J = 9.3, 6.0 Hz, 1H, H1'), 7.56 (s, 1H, H6), 9.04 (s, 1H, NH). ^{13}C NMR δ 20.9, 21.1, 38.0, 47.3, 64.0, 74.3, 77.4, 82.7, 85.5, 110.5, 137.2, 149.9, 162.2, 170.5, 170.6.

5-(Dimethoxymethyl)-2'-deoxyuridine (58). The solution of thymidine **41** (72.7 mg, 0.3 mmol), $NaHCO_3$ (25.2 mg, 0.3 mmol), and $Na_2S_2O_8$ (213 mg, 0.9 mmol) in H_2O/MeCN (2:3, 4 mL) was degassed for 15 min. Tosyl azide (69 µL, 88.8 mg, 0.45 mmol) was added into the resulting mixture and then the reaction was stirred under 80 °C for 1 h. After the reaction, the temperature was lower down to room temperature and 0.5 mL aqueous solution $Na_2S_2O_3$ (268mg, 1.08 mmol) and NaI (45 mg, 0.3 mmol) was added to quench the excess $Na_2S_2O_8$. The volatiles were evaporated and the residue was column chromatographed ($CHCl_3$/MeOH, 100:0→85:15) and further purified by HPLC (C18; A: 100% ACN, B: 5% ACN/H_2O; 0% A → 5% A in 60 min, flow rate = 2 mL/min) to give **58** (58.1 mg, 64%): ^{1}H NMR (DMSO-d_6) δ 2.02-2.09 (m, 1H, H2'), 2.14 (ddd, J = 13.3, 6.1, 3.4 Hz, H2"), 3.22 (s, 3H, CH_3), 3.24 (s, 3H, CH_3), 3.52-3.58 (m, 2H, H5',5"), 3.80 (q,

J = 3.3 Hz, 1H, H4'), 4.20-4.25 (m, 1H, H3'), 4.97 (t, J = 4.7 Hz, 1H, 5'-OH), 5.17 (s, 1H, CH), 5.25 (d, J = 4.2 Hz, 1H, 3'-OH), 6.16 (t, J = 6.9, 1H, H1'), 7.92 (s, 1H, H6), 11.39 (s, 1H, NH).

5'-DMT-5-azidomethyl-2'-deoxyuridine (5'-DMTAmdU, 59). AmdU **18**[40] (337 mg, 1.19 mmol) and 4,4'-dimethoxytrityl chloride (484 mg, 1.43 mmol) were dissolved in 6 mL of pyridine. The resulting solution was stirred at rt for 2 h. The volatiles were removed. The residue was dissolved in EtOAc and washed with $NaHCO_3$ solution followed by saturated NaCl solution and was column chromatographed (hexane/EtOAc/ triethylamine, 70:30:2 → 80:20:2) to give compound 5'-DMT-5-azidomethyl-2'-deoxyuridine **59** (501.8 mg, 72%): ^{1}H NMR (CD_2Cl_2) δ 2.28-2.33 (m, 1H, H2'), 2.41 (ddd, J = 13.9, 6.2, 3.9 Hz, 1H, H2''), 3.36-3.40 (m, 3H, CH_2,H5',5''), 3.59 (d, J = 15.0, 1H, CH_2), 3.79 (s, 6H, 2xOCH_3), 4.04 (q, J = 3.3, 1H, H4'), 4.60 (quin, J = 3.3, 1H, H3'), 6.32 (dd, J = 7.7, 6.2 Hz, 1H, H1'), 6.84-6.88 (m, 4H, Ph), 7.26-7.34 (m, 7H, Ph), 7.39-7.41 (m, 2H, Ph), 7.75 (s, 1H, H6); ^{13}C NMR (CD_2Cl_2) δ 41.6, 47.4, 55.8, 64.0, 72.7, 85.6, 86.8, 87.6, 110.2, 113.9, 127,8, 128.6, 128.7, 130.7, 135.6, 136.1, 139.5, 145.1, 150,5, 159,5; HRMS calcd for $C_{31}H_{31}N_5O_7Na$ [M+Na]$^+$ 608.2116, found 608.2127.

3'-CEP-5'-DMT-5-azidomethyl-2'-deoxyuridine (3'-CEP-5'-DMTAmdU, 60). 2-Cyanoethyl *N,N*-diisopropylchlorophosphoramidite (54 µL, 56.8 mg, 0.24 mmol) was added to a solution of 5'-DMT-5-azidomethyl-2'-deoxyuridine **59** (117 mg, 0.2 mmol) and DIPEA (52 µL, 38.8 mg, 0.3 mmol) in DCM (2 mL). The resulting solution was stirred at rt for 10 min. The residue was diluted with CH_2Cl_2 and washed with saturated $NaHCO_3$ solution followed by brine solution and the organic layer was dried with anhydrous Na_2SO_4. The solvent was removed with high vacuum evaporator under ice/acetone bath (-10 ºC).

The residue was column chromatographed (hexane/EtOAc/triethylamine, 50:50:2 →
40:60:2) to give compound 3'-CEP-5'-DMT-5-azidomethyl-2'-deoxyuridine **60** (118 mg,
75%): ^{1}H NMR (CD$_2$Cl$_2$) δ 1.17 (d, J = 2.2 Hz, 6H, 2xCH$_3$), 1.19 (d, J = 2.0 Hz, 6H,
2xCH$_3$), 2.31-2.38(m, 1H, H2'), 2.46 (t, J = 6.4 Hz, 2H, CH$_2$CN), 2.46-2.54 (m, 1H, H2''),
3.32 (d, J = 13.4, 1H, CH$_2$N$_3$), 3.37 (dd, , J = 10.6, 3.1 Hz, 1H, H5'), 3.46 (dd, , J = 10.6,
2.8 Hz, 1H, H5''), 3.57 (d, J = 13.4 , 1H, CH$_2$N$_3$), 3.55-3.71 (m, 4H, OCH$_2$, 2xCH), 3.79
(s, 6H, OCH$_3$), 4.19 (q, J = 2.6, 1H, H4'), 4.70 (ddd, J = 13.6, 6.4, 3.1 Hz, 1H, H3'), 6.33
(dd, J = 7.3, 6.3 Hz, 1H, H1'), 6.84-6.88 (m, 4H, ph), 7.27-7.35 (m, 7H, ph), 7.40-7.42 (m,
2H, ph), 7.81 (s, 1H, H6)); ^{31}P NMR (CD$_2$Cl$_2$) δ 148.85 (s); ^{13}C NMR (CD$_2$Cl$_2$) δ 24.9,
40.6, 47.4, 55.8, 59.0, 63.6, 73.8, 85.7, 86.4, 87.6, 110.2, 113.9, 118.2, 127.8, 128.6, 128.8,
130.8, 135.9, 136.0, 139.6, 145.0, 150.4, 159.5, 163.0; HRMS calcd for C$_{40}$H$_{48}$N$_7$O$_8$PNa
[M+Na]$^+$ 808.3194, found 808.3154.

**5-Formyl-2'-deoxyuridine (67) and 5-azirinyl-2'-deoxyuridine (68) from the UV
decomposition of AvdU 21.** The solution of AvdU **21** (16.3 mg, 0.055 mmol) in 5 mL
MeOH in a dark box was irradiated by a 254 nm UV lamp (UVG-11, 4 W, 0.16 Amps) for
1.5 h. , The volatiles were evaporated under the reduced pressure and the residue was
column chromatographed (CHCl$_3$/MeOH, 100:0 → 95:5) to give 5-formyl-2'-deoxyuridine
(**67**, 5.7 mg, 40.7%) and 5-azirinyl-2'-deoxyuridine (**68**, 5.1 mg, 34.7%). 5-Formyl-2'-
deoxyuridine (**67**) has ^{1}H NMR (DMSO-d6) δ 2.12-2.29 (m, 2H, H2',2''), 3.56-3.66 (m, 2H,
H5',5''), 3.86 (q, J = 3.2 Hz, 1H, H4'), 4.22-4.26 (m, 1H, H3'), 5.12 (t, J = 5.2 Hz, 1H, 5'-
OH), 5.28 (d, J = 4.4 Hz, 1H, 3'-OH), 6.09 (t, J = 6.4, 1H, H1'), 8.71 (s, 1H, H6), 9.76 (s,
1H, CHO), 11.75 (s, 1H, NH). ^{13}C NMR (DMSO-d6) δ 40.6, 60.7, 69.8, 85.9, 87.9, 110.7,
147.1, 149.5, 161.6, 186.1. 5-Azirinyl-2'-deoxyuridine (**68**) has ^{1}H NMR (DMSO-d6) δ

1.27 (d, J = 8.4 Hz, 1H, azirinyl), 1.31 (d, J = 8.4 Hz, 1H, azirinyl), 2.20-2.30 (m, 2H, H2',2"), 3.57-3.71 (m, 2H, H5',5"), 3.84 (q, J = 3.2 Hz, 1H, H4'), 4.27 (quin, J = 5.6 Hz, 1H, H3'), 5.21 (t, J = 4.8 Hz, 1H, 5'-OH), 5.29 (d, J = 4.4 Hz, 1H, 3'-OH), 6.12 (t, J = 6.0, 1H, H1'), 8.81 (s, 1H, H6), 11.82 (s, 1H, NH). ^{13}C NMR (DMSO-d6) δ 14.7, 40.6, 60.3, 69.2, 85.6, 87.7, 101.1, 148.3, 149.4, 158.0, 159.4.

5'-DMT-5-(1-azidovinyl)-2'-deoxyuridine (69). AvdU **21** (24.8 mg, 0.084 mmol) and 4,4'-dimethoxytrityl chloride (34 mg, 0.1 mmol) were dissolved in 0.5 mL of pyridine. The resulting solution was stirred at rt for 2 h. The volatiles were removed. The residue was dissolved in EtOAc and washed with NaHCO$_3$ solution followed by saturated NaCl solution and was column chromatographed (hexane/EtOAc/ triethylamine, 70:30:2) to give compound 5'-DMT-5-(1-azidovinyl)-2'-deoxyuridine **69** (30 mg, 60%): ^{1}H NMR (CD$_2$Cl$_2$) δ 2.23 (m, J = 13.7, 7.2, 6.4 Hz, 1H, H2'), 2.42 (ddd, J = 13.7, 6.4, 4.0 Hz, 1H, H2"), 3.33 (dd, J = 10.2, 4.0 Hz, 1H, H5'), 3.44 (dd, J = 10.4, 4.0 Hz, 1H, H5"), 3.78 (s, 6H, 2xOCH$_3$), 4.05 (q, J = 3.5 Hz, 1H, H4'), 4.43 (quin, J = 3.3 Hz, 1H, H3'), 4.92 (d, J = 2.0 Hz, 1H, CH$_2$), 6.10 (d, J = 1.8 Hz, 1H, CH$_2$), 6.28 (dd, J = 7.3, 6.0 Hz, 1H, H1'), 6.82-6.85 (m, 4H, Ph), 7.21-7.35 (m, 7H, Ph), 7.43-7.46 (m, 2H, Ph), 7.97 (s, 1H, H6); ^{13}C NMR (CD$_2$Cl$_2$) δ 41.3, 55.6, 63.9, 72.5, 85.8, 86.6, 87.1, 101.5, 108.8, 113.5, 127.3, 128.2, 128.4, 130.4, 136.0, 136.1, 137.0, 138.2, 145.0, 149.6, 159.2, 160.9, 171.2.

3'-CEP-5'-DMT-5-(1-azidovinyl)-2'-deoxyuridine (70) (not obtained after column due to the Staudinger reaction). 2-Cyanoethyl *N,N*-diisopropylchlorophosphoramidite (9 μL, 9.5 mg, 0.04 mmol) was added to a solution of 5'-DMT-5-(1-azidovinyl)-2'-deoxyuridine **69** (20 mg, 0.033 mmol) and DIPEA (9 μL, 6.5 mg, 0.05 mmol) in DCM (1 mL). The resulting solution was stirred at rt for 10 min. The residue was diluted with

CH$_2$Cl$_2$ and washed with saturated NaHCO$_3$ solution followed by brine solution and the organic layer was dried with anhydrous Na$_2$SO$_4$. The solvent was removed with high vacuum evaporator under ice/acetone bath (-10 ^{o}C). The residue was column chromatographed (hexane/EtOAc/triethylamine, 70:30:2) to give compound, which was characterized as non-**70**(16.4 mg, 63%). The NMR data of the isomer with higher R$_f$ of 0.71 after column are provided: ^{1}H NMR (CD$_2$Cl$_2$) δ 1.19-1.20 (m, 12H, 4xCH$_3$), 2.47-2.65 (m, 4H, CH$_2$CN, H2',2''), 3.30-3.46 (m, 2H, H5',5''), 3.39 (s, 6H, OCH$_3$), 3.95-4.04 (m, 4H, OCH$_2$, 2 x CH), 4.30-4.33 (m, 1H, H4'), 4.88 (d, J = 2.0 Hz, CH$_2$), 4.92-4.96 (m, 1H, H3'), 6.06 (d, J = 2.0 Hz, CH$_2$), 6.31(dd, J = 8.8, 5.6 Hz, 1H, H1'), 6.82-6.84 (m, 4H, ph), 7.21-7.36 (m, 7H, ph), 7.42-7.47 (m, 2H, ph), 8.02 (s, 1H, H6); ^{31}P NMR (CD$_2$Cl$_2$) δ 7.52 (s, major) 148.85 (s); Based on the ^{1}H and ^{31}P NMR, it was concluded that the phosphoramidite was oxidized to P (IV) through the Staudinger reaction.

5-Azidomethyl-2'-deoxycytidine triphosphate (AmdCTP, 74). POCl$_3$ (19 μL, 31.2 mg, 0.2 mmol) was added to a stirred solution of AmdC **42** (24 mg, 0.085 mmol) and proton sponge (54.6 mg, 0.255 mmol) in trimethyl phosphate (1 mL) at 0 ^{o}C. The resulting mixture was stirred at 0 ^{o}C for 30 min. 0.5 M tributylammomium pyrophosphate solution in DMF (1.275 mL, 0.5 mmol) and then tributylamine (90.9 μL, 70.9 mg, 0.38 mmol) were added to the reaction mixture and stirred at 0 ^{o}C for 2 min. The reaction was quenched by adjusting the pH to 7.5 with 2 M TEAB buffer. The residue was dissolved in water (5 mL) and was extracted with EtOAc (3 x 5 mL). The water layer was evaporated and coevaporated with mixture of EtOH/H$_2$O (1:1, 5 mL). The residue was column chromatographed (DEAE–Sephadex®, TEAB 0.1 M → 0.6 M) and the appropriate fractions were evaporated in vacuum and coevaporate 5 times with mixture of EtOH/H$_2$O

(1:1, 10 mL) to give AmdC triphosphate triethylammonium salt **74**. (10.2 mg, 23%). ^{1}H

NMR (D$_2$O) δ 2.36-2.43 (m, 1H, H2'), 2.49 (ddd, J = 14.4, 6.7, 4.4 Hz, 1H, H2''), 4.19-4.28

(m, 3H, H4',5',5''), 4.41 (d, J = 15.0, 1H, CH$_2$N$_3$), 4.48 (d, J = 14.6, 1H, CH$_2$N$_3$), 4.61-4.64

(m, 1H, H3'), 6.24 (t, J = 5.9, 1H, H1'), 8.33 (s, 1H, H6); ^{31}P NMR (D$_2$O) δ -23.41 (t, J =

19.7, 1P, β), -11.72 (d, J = 20.5, 1P, α), -10.93 (d, J = 20.0 Hz, 1P, γ); ^{13}C NMR (D$_2$O) δ

39.6, 47.4, 65.1, 70.3, 86.2, 86.9, 101.9, 144.6, 148.0, 158.3; HRMS calcd for

C$_{10}$H$_{16}$N$_5$O$_{14}$P$_3$ [M-H]$^-$ 520.99937, found 520.99934.

5-Acetyl-2'-deoxyuridine triphosphate (75). POCl$_3$ (22.4 μL, 36.8 mg, 0.24 mmol)

was added to a stirred solution of AvdU **21** (59 mg, 0.2 mmol) and proton sponge (64.3

mg, 0.3 mmol) in trimethyl phosphate (1.5 mL) at 0 °C. The resulting mixture was stirred

at 0 °C for 30 min. 0.5 M tributylammomium pyrophosphate solution in DMF (2 mL, 1

mmol) and then tributylamine (142.5 μL, 111.2 mg, 0.6 mmol) were added to the reaction

mixture and stirred at 0 °C for 2 min. The reaction was quenched by adjusting the pH to

7.5 with 2 M TEAB buffer. The residue was dissolved in water (5 mL) and was extracted

with EtOAc (3 x 5 mL). The water layer was evaporated and coevaporated with mixture of

EtOH/H$_2$O (1:1, 5 mL). The residue was column chromatographed (DEAE–Sephadex®,

TEAB 0.1 M → 0.6 M) and further purified by HPLC (C18; A: 20 mM TEAA buffer (pH

= 7.1, in ACN/H$_2$O = 1:1), B: 20 mM TEAA buffer (pH = 7.1, in H$_2$O); 0% A → 25% A

in 20 min, flow rate = 1 mL/min then stay with 25% A for 40 min). The appropriate

fractions were evaporated in vacuum and coevaporate 5 times with mixture of EtOH/H$_2$O

(1:1, 5 mL). to give 5-acetyl-2'-deoxyuridine triphosphate triethylammonium salt **75**[125]

(23.4 mg, 23%). ^{1}H NMR (D$_2$O) δ 2.40-2.53 (m, 5H, H2',2'', CH$_3$), 4.22-4.25 (m, 2H,

H5',5''), 4.28-4.30 (m, 1H, H4'), 4.64-4.67 (m, 1H, H3'), 6.25 (t, J = 6.0, 1H, H1'), 8.65 (s,

1H, H6); ^{31}P NMR (D$_2$O) δ -23.35 ("s", 1P, β), -11.64 ("s", 1P, α), -10.97 ("s", 1P, γ); ^{13}C NMR (D$_2$O) δ 28.7, 39.5, 65.5, 70.4, 86.4, 87.1, 112.3, 148.5, 150.5, 162.4, 197.8.

5-Ethynyl-2'-deoxyuridine triphosphate (78). POCl$_3$ (44.7 μL, 73.6 mg, 0.48 mmol) was added to a stirred solution of 5-ethynyl-2'-deoxyuridine **77**[110] (100 mg, 0.4 mmol) and proton sponge (128. 6 mg, 0.6 mmol) in trimethyl phosphate (3 mL) at 0 °C. The resulting mixture was stirred at 0 °C for 30 min. 0.5 M tributylammomium pyrophosphate solution in DMF (4 mL, 2 mmol) and then tributylamine (285 μL, 222.4 mg, 1.2 mmol) were added to the reaction mixture and stirred at 0 °C for 2 min. The reaction was quenched by adjusting the pH to 7.5 with 2 M TEAB buffer. The residue was dissolved in water (10 mL) and was extracted with EtOAc (3 x 10 mL). The water layer was evaporated and coevaporated with mixture of EtOH/H$_2$O (1:1, 5 mL). The residue was column chromatographed (DEAE–Sephadex®, TEAB 0.1 M → 0.6 M) and the appropriate fractions were evaporated in vacuum and coevaporate 5 times with mixture of EtOH/H$_2$O (1:1, 10 mL) to give 5-ethynyl-2'-deoxyuridine triphosphate triethylammonium salt **78** (104 mg, 53%). ^{1}H NMR (D$_2$O) δ 2.28-2.37 (m, 2H, H2',2''), 3.55 (s, 1H, CH), 4.09-4.16 (m, 3H, H4',5',5''), 4.53-4.56 (m, 1H, H3'), 6.20 (t, J = 6.8, 1H, H1'), 8.15 (s, 1H, H6); ^{31}P NMR (D$_2$O) δ -23.46 (t, J = 20.9, 1P, β), -11.68 (d, J = 19.9, 1P, α), -10.86 (d, J = 20.7, 1P, γ); ^{13}C NMR (D$_2$O) δ 38.8, 65.3, 70.6, 83.4, 85.6, 85.8, 98.7, 145.6, 150.5, 164.5.

4.1.3. Synthesis of 2-azido-2'-deoxyinosine

3',5'-di-*O*-acetyl-2'-deoxyguanosine (80). Acetyl anhydrite (1.5 mL, 1.65 g, 16.5 mmol) was added to a solution of 2'-deoxyguanosine (**dG**,1.3 g, 5 mmol) and pyridine (1.5 ml) in DMF (4 mL). The resulting mixture was stirred at 75 °C for 4h. After cooling to ambient temperature, the volatiles were evaporated under the reduced pressure and the

residue was column chromatographed (CHCl₃/MeOH, 100:0 → 85:15) to give **80**[148] (1.4 g, 81%): ^{1}H NMR (DMSO-d6) δ 2.04 (s, 3H, Ac), 2.08 (s, 3H, Ac), 2.42-2.48 (m, 1H, H2'), 2.88-2.95 (m, 1H, H2''), 4.16 (m, 3H, H4',5',5''), 5.28-5.29 (m, 1H, H3'), 6.13 (dd, J = 8.4, 5.6 Hz, 1H, H1'), 6.52 (s, 2H, NH₂), 7.92 (s, 1H, H8), 10.69 (s, 1H, NH).

3',5'-di-*O*-acetyl-O⁶-(*p*-nitrophenethyl)-2'-deoxyguanosine (81). 3',5'-di-O-acetyl-2'-deoxyguanosine **80** (703 mg, 2 mmol), PPh₃ (840 mg, 3.2 mmol), *p*-nitrophenethyl alcohol (500 mg, 3 mmol), and activated molecular sieves were dispersed in 40 mL 1,4-dioxane and stirred for 30 min. Then DIAD (630 μL, 646 mg, 3.2 mmol) was added to the mixture and stirred at room temperature overnight. Molecular sieves were filtrated and the volatiles were evaporated under reduced pressure. The solid residue was washed with Et₂O to remove triphenylphosphate and then column chromatographed (CHCl₃/MeOH, 100:0 → 95:5) to give **81**[148] (720 g, 72%): ^{1}H NMR (DMSO-d6) δ 2.02 (s, 3H, Ac), 2.08 (s, 3H, Ac), 2.43-2.47 (m, 1H, H2'), 2.97-3.04 (m, 1H, H2''), 3.25 (t, , J = 7.2 Hz, 2H, CH₂), 4.16-4.22 (m, 2H, 5',5''), 4.28 (t, J = 6.4 Hz, 1H, H4'), 4.67 (t, , J = 6.8 Hz, 2H, CH₂), 5.30-5.33 (m, 1H, H3'), 6.22 (dd, J = 7.6, 6.4 Hz, 1H, H1'), 6.53 (s, 2H, NH₂), 7.63 (d, J = 8.4 Hz, 2H, Ph), 8.07 (s, 1H, H8), 8.18 (d, J = 8.4 Hz, 2H, Ph).

3',5'-di-*O*-acetyl-2-azido-O⁶-(*p*-nitrophenethyl)-2'-deoxyinosine (82). 3',5'-di-*O*-acetyl-O⁶-(*p*-nitrophenethyl)-2'-deoxyguanosine **81** (200 mg, 0.4 mmol) was dissolved in 5 mL acetonitrile. The mixture was cooled down to -10 ᵒC (acetone/ice bath) and then tert-butyl nitrite (264 μL, 206 mg, 2 mmol) and trimethylsilyl azide (TMSN₃, 262 μL, 230 mg, 2 mmol) were added. The resulting mixture was kept in -20 ᵒC freezer and 12 h and then 4 ᵒC refrigerator for 24 h. The volatiles were evaporated under the reduced pressure and the residue was column chromatographed (CHCl₃/MeOH, 100:0 → 95:5) to give **82** (155.4 mg,

74%): ^{1}H NMR (DMSO-d6) δ 1.99 (s, 3H, Ac), 2.09 (s, 3H, Ac), 2.56 (ddd, J = 14.4, 6.4, 3.2 Hz, 1H, H2'), 3.04-3.11 (m, 1H, H2"), 3.29-3.30 (m, 2H, CH$_2$), 4.16-4.30 (m, 3H, H4',5',5"), 4.81 (t, , J = 6.8 Hz, 2H, CH$_2$), 5.38-5.41 (m, 1H, H3'), 6.35 (t, J = 6.4 Hz, 1H, H1'), 7.63 (d, J = 9.2 Hz, 2H, Ph), 8.18 (d, J = 8.0 Hz, 2H, Ph), 8.49 (s, 1H, H8).

2-azido-2'-deoxyinosine (2-N$_3$dI, 44). To a solution of **82** (79 mg, 0.15 mmol) in acetonitrile was added 1,8-diazabicyclo[5.4.0]undec-7-ene (DBU, 449 μL, 456 mg, 3 mmol). The resulting mixture was stirred at room temperature for 3 h. The volatiles were evaporated under the reduced pressure and dried under high vacuum. 2 mL MeOH was added to the reaction residue and cooled down to 0 °C (ice bath), followed by adding 3 mL NH$_3$/MeOH. The resulting mixture was stirred at 0 °C to room temperature overnight. The volatiles were evaporated under the reduced pressure and the residue was column chromatographed (CHCl$_3$/MeOH, 100:0 → 85:25) and further purified by HPLC (C18; A: 100% ACN, B: 100% H$_2$O; 0% A then 0% A → 5% A in 30 min, flow rate = 2 mL/min) to give **44**[149] (36.6 mg, 83%): ^{1}H NMR (DMSO-d6) δ 2.21 (ddd, J = 12.9, 6.3, 3.1 Hz, 1H, H2'), 2.68 (ddd, J = 13.7, 8.6, 6.3 Hz, 1H, H2"), 3.49-3.55 (m, 1H, H5'), 3.59-3.64 (m, 1H, H5"), 3.86 (q, J = 4.3 Hz, 1H, H4'), 4.37-4.40 (m, 1H, H3'), 5.24-5.29 (m, 2H, 3'OH,5'OH), 6.29 (dd, J = 7.8, 5.9 Hz, 1H, H1'), 8.03 (s, 1H, H8); ^{13}C NMR (DMSO-d6) δ 39.2, 48.6, 62.0, 71.1, 83.4, 87.8, 115.1, 137.6, 150.4, 152.2, 156.3. MS (ESI): m/z calcd for [C$_{10}$H$_{12}$N$_7$O$_4$]$^+$, 294.1; found 294.3.

4.1.4. Preparation of triazolyl nucleoside analogues

3',5'-*di-O*-acetyl-5-(1*H*-1,2,3-triazol-4-yl)-2'-deoxycytidine (diAc-5-TrzdC, 83)

Procedure A using Ag₂CO₃ as catalyst

Ag$_2$CO$_3$ (2.8 mg, 0.01 mmol) was added to a solution of **63a**[119] (33.5 mg, 0.1 mmol), azidotrimethylsilane (26.3 μL, 23 mg, 0.2 mmol), and H$_2$O (3.6 μL, 3.6 mg, 0.2 mmol) in DMF (1 mL). The resulting mixture was stirred at 80 °C for 1 hour. After cooling to ambient temperature, the volatiles were evaporated under the reduced pressure and the residue was column chromatographed (CHCl$_3$/MeOH, 100:0 → 90:10) to give **83** (2.6 mg, 7%)**:** UV (MeOH) λ_{max} 208, 238, 293 nm (ε 13050, 9400, 4150), λ_{min} 225, 271 nm (ε 8350, 3150); ^{1}H NMR (DMSO-d_6) δ 1.99 (s, 3H, CH$_3$), 2.08 (s, 3H, CH$_3$), 2.36 (ddd, J = 14.1, 5.8, 2.0 Hz, 1H, H2"), 2.47-2.44 (m, 1H, H2'), 4.23-4.20 (m, 1H, H4'), 4.35-4.26 (m, 2H, H5', 5"), 5.22-5.20 (m, 1H, H3'), 6.21 (dd, J = 7.6, 6.2 Hz, 1H, H1'), 7.67 (s, 1H, NH), 7.90 (s, 1H, NH), 8.07 (s, 1H, H6), 8.24 (s, 1H, CH), 15.28 (s, 1H, NH); ^{13}C NMR (DMSO-d_6) δ 20.5, 20.7 (Ac), 36.6 (C2'), 63.7 (C5'), 74.3 (C3'), 81.6 (C4'), 86.0 (C1'), 97.2 (C5), 126.9 (triazolyl), 139.8 (C6), 153.6 (C4), 162.4 (C2), 170.0, 170.2 (Ac); HRMS (ESI): m/z calcd for C$_{15}$H$_{19}$N$_6$O$_6$ [M+H]$^+$ 379.1361; found 379.1372.

Procedure B using CuI as catalyst

The stirred solution of **63a** (33.5 mg, 0.1 mmol) in 1 mL DMF/H$_2$O (9/1) was degassed with argon for 15 min. Azidotrimethylsilane (26.3 μL, 23 mg, 0.2 mmol) and CuI (1 mg, 0.005 mmol) were added to the solution, which was further degassed for another 5 min. The resulting mixture was stirred at 90°C for 5 h. After cooling to ambient temperature, the volatiles were evaporated and the residue was column chromatographed (CHCl$_3$/MeOH, 100:0 → 90:10) to give **83** (12.0 mg, 32%) with the spectroscopic data as described above.

Procedure C using CuSO₄/sodium ascorbate as catalyst

63a (33.5 mg, 0.1 mmol) and $CuSO_4 \cdot 5H_2O$ (2.5 mg, 0.01 mmol) were dissolved in 1 mL DMF/H_2O (9/1) at ambient temperature. The stirred solution was degassed with argon for 15 min. Azidotrimethylsilane (26.3 μL, 23 mg, 0.2 mmol) and sodium ascorbate (4 mg, 0.02 mmol) were added to the solution, which was further degassed for another 5 min. The resulting mixture was stirred at 90°C for 5 h. After cooling to ambient temperature, the volatiles were evaporated and the residue was column chromatographed ($CHCl_3$/MeOH, 100:0 → 90:10) to give **83** (24.6 mg, 65%) with the spectroscopic data as described above.

5-(1H-1,2,3-triazol-4-yl)-2'-deoxyuridine (5-TrzdU, 39). Treatment of **77**[110] (25.1 mg, 0.1 mmol) with CuI by Procedure B (column chromatography; $CHCl_3$/MeOH, 100:0 → 85:15) gave **39** (14.8 mg, 50%): UV (MeOH) λ_{max} 231, 292 nm (ε 12400, 11450), λ_{min} 259 nm (ε 3700); ^{1}H NMR (DMSO-d_6) δ 2.18 (dd, J = 6.3, 4.7 Hz, 2H, H2',2''), 3.63-3.55 (m, 2H, H5',5''), 3.84 (q, J = 3.4 Hz, 1H, H4'), 4.31-4.25 (m, 1H, H3'), 5.04 ("s", 1H, 3'-OH), 5.29 (d, J = 4.1 Hz, 1H, 5'-OH), 6.22 (t, J = 6.6 Hz, 1H, H1'), 8.14 (s, 1H, NH), 8.49 (s, 1H, H6), 11.68 (s, 1H, 3-NH), 15.10 (s, 1H, NH); ^{13}C NMR (DMSO-d_6) δ 39.7 (C2'), 61.3 (C5'), 70.5 (C3'), 84.7 (C1'), 87.6 (C4'), 136.4 (C6), 149.7 (C2), 161.3 (C4); HRMS (ESI): m/z calcd for $C_{11}H_{14}N_5O_5$ [M+H]$^+$ 296.0989; found 296.0983.

Treatment of **77** (25.1 mg, 0.1 mmol) with CuI by modified Procedure B with 2 equivalents of H_2O and DMF as solvent (column chromatography; $CHCl_3$/MeOH, 100:0 → 85:15) gave **39** (12.5 mg, 42%) with the spectroscopic data as described above.

Treatment of **77** (25.1 mg, 0.1 mmol) with CuSO₄/sodium ascorbate by Procedure C (column chromatography; CHCl₃/MeOH, 100:0 → 85:15) gave **39** (15.3 mg, 52%) with the spectroscopic data as described above.

8-(1H-1,2,3-triazol-4-yl)-2'-deoxyadenosine (8-TrzdA, 46). Treatment of **85**[141] (27.5 mg, 0.1 mmol) with Ag₂CO₃ by Procedure A (column chromatography; CHCl₃/MeOH, 100:0 → 85:15) gave **46** (15.4 mg, 50%): UV (MeOH) λ_{max} 203, 228, 287 nm (ε 15900, 16050, 17950), λ_{min} 213, 250 nm (ε 13800, 5100); ¹H NMR (DMSO-d_6) δ 2.20 (ddd, J = 12.9, 5.9, 1.7 Hz, 1H, H2"), 3.18-3.12 (m, 1H, H2'), 3.55-3.49 (m, 1H, H5"), 3.72-2.69 (m, 1H, H5'), 3.90 (q, J = 3.7 Hz, 1H, H4'), 4.51-4.46 (m, 1H, H3'), 5.27 (d, J = 3.7 Hz, 1H, 3'-OH), 5.80-5.77 (m, 1H, 5'-OH), 7.08 (t, J = 7.2 Hz, 1H, H1'), 7.48 (s, 2H, NH₂), 8.13 (s, 1H, H2), 8.42 (s, 1H, NH), 15.64 (s, 1H, NH); ¹³C NMR (DMSO-d_6) δ 38.1 (C2'), 62.4 (C5'), 71.5 (C3'), 85.9 (C1'), 88.4 (C4'), 119.4 (C5), 130.3 (triazolyl), 141.5 (C8), 149.8 (C4), 152.1 (C2), 156.2 (C6); HRMS (ESI): m/z calcd for $C_{12}H_{14}N_8O_3Na$ [M+Na]⁺ 341.1081; found 341.1062.

Treatment of **85** (27.5 mg, 0.1 mmol) with CuI by Procedure B (column chromatography; CHCl₃/MeOH, 100:0 → 85:15; HPLC: C18, A: 100% ACN, B: 5% ACN/H₂O; 0% A → 15% A in 30 min, flow rate = 2 mL/min) gave **46** (5.3 mg, 17%) with the spectroscopic data as described above.

Treatment of **85** (27.5 mg, 0.1 mmol) with CuSO₄/sodium ascorbate by Procedure C (column chromatography; CHCl₃/MeOH, 100:0 → 85:15; HPLC: C18, A: 100% ACN, B: 5% ACN/H₂O; 0% A → 15% A in 30 min, flow rate = 2 mL/min) gave **46** (16.2 mg, 51%) with the spectroscopic data as described above.

8-(1*H*-1,2,3-triazol-4-yl)-2'-deoxyguanosine (8-TrzdG, 47). Treatment of **87**[142] (29.1 mg, 0.1 mmol) with Ag_2CO_3 by Procedure A (column chromatography; $CHCl_3$/MeOH, 100:0 → 80:20) gave **47** (17.4 mg, 52%): UV (MeOH) λ_{max} 205, 283 nm (ε 14450, 14800); λ_{min} 238 (ε 2600); ^{1}H NMR (DMSO-d_6) δ 2.13-2.07 (m, 1H, H2"), 3.19-3.12 (m, 1H, H2'), 3.50 (dd, J = 11.7, 5.3 Hz, 1H, H5"), 3.65 (dd, J = 11.8, 4.8 Hz, 1H, H5'), 3.81-3.78 (m, 1H, H4'), 4.44-4.38 (m, 1H, H3'), 5.05 ("s", 1H, 5'-OH), 5.18 (d, J = 3.7 Hz, 1H, 3'-OH), 6.43 (s, 2H, NH$_2$), 8.34 (t, J = 7.8 Hz, 1H, H1'), 10.83 (s, 1H, NH), 15.42 (s, 1H, NH); ^{13}C NMR (DMSO-d_6) δ 37.4 (C2'), 62.3 (C5'), 71.4 (C3'), 84.8 (C1'), 88.0 (C4'), 117.6 (C5), 128.8 (triazolyl), 151.9 (C4), 153.1 (C2), 154.0 (C6), 156.5 (C8); HRMS (ESI): m/z calcd for $C_{12}H_{15}N_8O_4$ [M+H]$^+$, 335.1211; found 335.1214.

Treatment of **87** (29.1 mg, 0.1 mmol) with CuI by Procedure B (column chromatography; $CHCl_3$/MeOH, 100:0 → 80:20; HPLC: C18, A: 100% ACN, B: 5% ACN/H_2O; 0% A → 15% A in 30 min, flow rate = 2 mL/min) gave **47** (10.2 mg, 31%) with the spectroscopic data as described above.

Treatment of **87** (29.1 mg, 0.1 mmol) with $CuSO_4$/sodium ascorbate by Procedure C (column chromatography; $CHCl_3$/MeOH, 100:0 → 80:20; HPLC: C18, A: 100% ACN, B: 5% ACN/H_2O; 0% A → 15% A in 30 min, flow rate = 2 mL/min) gave **47** (26.0 mg, 52%) with the spectroscopic data as described above.

5-(1*H*-1,2,3-triazol-4-yl)-2'-deoxycytidine (5-TrzdC, 48). Treatment of **63b**[120] (25.1 mg, 0.1 mmol) with CuI by Procedure B (column chromatography; $CHCl_3$/MeOH, 100:0 → 80:20) gave **48** (2.9 mg, 10%): UV (MeOH) λ_{max} 207, 238, 296 nm (ε 18750, 13900, 5 500), λ_{min} 224, 273 nm (ε 11900, 3500); ^{1}H NMR (DMSO-d_6) δ 2.14-2.08 (m, 1H, H2"),

2.21 (ddd, J = 13.2, 6.1, 4.7 Hz, 1H, H2'), 3.66-3.59 (m, 1H, H5''), 3.75-3.68 (m, 1H, H5'), 3.82 (q, J = 3.3 Hz, 1H, H4'), 4.30-4.24 (m, 1H, H3'), 7.68 (s, 1H, 3'-OH), 5.29 (s, 1H, 5'-OH), 6.18 (t, J = 6.1 Hz, 1H, H1'), 7.68 (s, 1H, NH), 7.80 (s, 1H, NH), 8.07 (s, 1H, NH), 8.60 (s, 1H, H6), 15.18 (s, 1H, NH), ^{13}C NMR (DMSO-d_6) δ 40.9 (C2'), 60.6 (C5'), 69.5 (C3'), 85.4 (C1'), 87.3 (C4'), 96.4 (C5), 128.0 (triazolyl), 140.1 (C6), 153.7 (C4), 162.2 (C2); HRMS (ESI): m/z calcd for $C_{11}H_{15}N_6O_4$ [M+H]$^+$ 295.1149; found 295.1160.

Treatment of **63b** (25.1 mg, 0.1 mmol) with CuSO$_4$/sodium ascorbate by Procedure C (column chromatography; CHCl$_3$/MeOH, 100:0 → 80:20) gave **48** (15.0 mg, 51%) with the spectroscopic data as described above.

3',5'-*di*-*O*-acetyl-5-(1*H*-1,2,3-triazol-4-yl)-2'-deoxyuridine (diAc-5-TrzdU, 84). Treatment of **62**[110] (33.6 mg, 0.1 mmol) with CuI by Procedure B (column chromatography; CHCl$_3$/MeOH, 100:0 → 92:8) gave **84** (20.8 mg, 55%): UV (MeOH) λ$_{max}$ 231, 293 nm (ε 10700, 9600), λmin 258 nm (ε 2900); ^{1}H NMR (DMSO-d_6) δ 2.08 (s, 3H, CH$_3$), 2.13 (s, 3H, CH$_3$), 2.46-2.36 (m, 2H, H2',2''), 4.26-4.22 (m, 2H, H5', 5''), 4.31-4.27 (m, 1H, H4'), 5.26-5.21 (m, 1H, H3'), 6.25 (t, J = 6.3 Hz, 1H, H1'), 8.18 (s, 1H, NH), 8.31 (s, 1H, H6), 11.82 (s, 1H, 3-NH), 15.19 (s, 1H, NH); ^{13}C NMR (DMSO-d_6) δ 20.7, 20.8 (Ac), 36.7 (C2'), 63.8 (C5'), 74.2 (C3'), 81.7 (C4'), 84.9 (C1'), 105.5 (C5), 135.8 (C6), 149.6 (C2), 161.2 (C4), 170.1, 170.4 (Ac); HRMS (ESI): m/z calcd for $[C_{15}H_{18}N_5O_7]^+$, 380.1201; found 380.1208.

Treatment of **62** (33.6 mg, 0.1 mmol) with CuSO$_4$/sodium ascorbate by Procedure C (column chromatography; CHCl$_3$/MeOH, 100:0 → 92:8) gave **84** (30.6 mg, 81 %) with the spectroscopic data as described above.

3',5'-diTBDMS-8-(1H-1,2,3-triazol-4-yl)-2'-deoxyadenosine (diTBDMS-8-TrzdA, 88). Treatment of **86**[141] (50.4 mg, 0.1 mmol) with Ag_2CO_3 by Procedure A (column chromatography; hexane/EtOAc 50:50 → 0:100) gave **88** (16.4 mg, 30%): UV (MeOH) λ_{max} 225, 285 nm (ε 17 500, 14 100), λ_{min} 247 nm (ε 3 900); ^{1}H NMR (DMSO-d_6) δ -0.08 (s, 3H, CH_3), -0.02 (s, 3H, CH_3), 0.170 (s, 3H, CH_3), 0.173 (s, 3H, CH_3), 0.80 (s, 9H, 3 x CH_3), 0.94 (s, 9H, 3 x CH_3), 2.28-2.35 (m, 1H, H2'), 3.73 (dd, J = 11.3, 5.4 Hz, 1H, H5'), 3.83-3.90 (m, 1H, H2''), 3.96 (dd, J = 11.3, 5.9 Hz, 1H, H5''), 4.05 ("q", J = 4.9, 1H, H4'), 5.05 (q, J = 5.9 Hz, 1H, H3'), 6.72 (t, J = 6.9 Hz, 1H, H1'), 8.37 (s, 1H, H2), 8.53 (s, 1H, Htrz); ^{13}C NMR (DMSO-d_6) δ -5.4 (CH_3), -5.3 (CH_3), -4.6 (CH_3), -4.4 (CH_3), 18.2 (CH_3), 18.5 (CH_3), 25.98 (CH_3), 26.01 (CH_3), 37.2 (C2'), 62.9 (C5'), 72.5 (C3'), 85.3 (C1'), 87.8 (C4'), 119.7 (C5), 133.1(Htrz), 143.8 (C8), 151.0 (C4), 152.8 (C2), 155.4 (C6); HRMS calcd for $C_{24}H_{43}N_8O_3Si_2$ [M+H]$^+$ 547.2991, found 547.3004.

Treatment of **86** (50.4 mg, 0.1 mmol) with CuI by Procedure B (column chromatography; hexane/EtOAc 50:50 → 0:100) gave **88** (14.8 mg, 27%) with the spectroscopic data as described above.

Treatment of **86** (50.4 mg, 0.1 mmol) with $CuSO_4$/sodium ascorbate by Procedure C (column chromatography; hexane/EtOAc 50:50 → 0:100) gave **88** (31.7 mg, 58%) with the spectroscopic data as described above.

8-(1H-1,2,3-triazol-4-yl)-2'-deoxyadenosine 5'-triphosphate (8-TrzdATP, 102). Phosphoryl chloride (28 μL, 46 mg, 0.3 mmol) was added to a stirred solution of 8-TrzdA **46** (48 mg, 0.15 mmol) and proton sponge (80 mg, 0.375 mmol) in trimethyl phosphate (2 mL) at 0 °C. The resulting mixture was stirred at 0 °C for 30 min. 0.5 M tributylammomium pyrophosphate solution in DMF (1.5 mL, 0.75 mmol) and then

tributylamine (106.8 μL, 83.4 mg, 0.45 mmol) were added to the reaction mixture and stirred at 0 °C for 2 min. The reaction was quenched by adjusting the pH to 7.5 with 2 M TEAB buffer. The residue was dissolved in water (5 mL) and was extracted with EtOAc (3 x 5 mL). The water layer was evaporated and coevaporated with mixture of $EtOH/H_2O$ (1:1, 5 mL). The residue was column chromatographed (DEAE–Sephadex®, TEAB 0.1 M → 0.6 M) and the appropriate fractions were evaporated in vacuum and coevaporate 5 times with mixture of $EtOH/H_2O$ (1:1, 10 mL) to give 8-TrzdATP triethylammonium salt **102**. (33.4 mg, 30%). ^{1}H NMR (D_2O) δ 2.33 (ddd, J = 13.4, 6.5, 3.9, 1H, H2'), 3.22-3.26 (m, 1H, H2''), 4.04-4.10 (m, 1H, H5'), 4.14 (q, J = 5.2 Hz, 1H, H4'), 4.18-4.24 (m, 1H, H5''), 4.66 (quin, J = 3.9 Hz, 1H, H3'), 6.74 (t, J = 7.8, 1H, H1'), 8.20 (s, 1H, H2), 8.41 (s, 1H, Trz); ^{31}P NMR (D_2O) δ -23.22 (t, J = 21.0, 1P, β), -11.34 (d, J = 21.0, 1P, α), -10.22 (d, J = 21.0, 1P, γ); ^{13}C NMR (D_2O) δ 36.2, 65.2, 70.6, 84.3, 84.8, 118.6, 128.8, 136.1, 143.0, 149.9, 152.6, 155.0; HRMS calcd for $C_{12}H_{16}N_8O_{12}P_3$ [M-H]$^-$ 557.0106, found 557.0091.

4.1.5. Synthesis of 5-(1-halo-2-sulfonylvinyl) and 5-(2-furyl) uracil nucleoside analogues

2',3',5'-Tri-*O*-acetyl-5-(fur-2-yl)uridine (107). Procedure B. Furan (0.7 mL, 680 mg, 10 mmol) and TBAF (1 M/THF, 3.5 mL, 3.5 mmol) were added to a stirred solution of **105**[150] (248 mg, 0.5 mmol) in DMF (5 mL) containing tris(dibenzylideneacetone)dipalladium (22.9 mg, 0.025 mmol) at ambient temerature. The resulting suspension was stirred for 1 h at 100°C. The volatiles were evaporated under reduced pressure and the residue was dissolved in EtOAc and washed with saturated $NaHCO_3/H_2O$ and brine and the organic layer was dried over anhydrous Na_2SO_4. The residue was column chromatographed ($CHCl_3$/MeOH, 95:5) to give **107** (146 mg, 67%):

¹H NMR δ 2.10 (s, 3H, CH₃), 2.15 (s, 3H, CH₃), 2.22 (s, 3H, CH₃), 4.38-4.40 (m, 3H, H4',5',5''), 5.38-5.42 (m, 2H, H2',3'), 6.24-6.28 (m, 1H, H1'), 6.47 (dd, J = 3.3, 1.8 Hz, 1H, furan), 7.09 (d, J = 3.4, 1H, furan), 7.33 (d, J = 1.4, 1H, furan), 7.91 (s, 1H, H6), 9.20 (s, 1H, NH); ¹³C NMR δ 20.5, 20.7, 20.8, 64.6, 70.9, 73.0, 80.6, 86.8, 108.4, 110.2, 112.3, 132.5, 141.3, 145.6, 149.6, 157.8, 169.77, 169.83, 170.4; HRMS calcd for $C_{19}H_{21}N_2O_{10}$ [M+H]⁺ 437.1191, found 437.1178.

5-(5-Heptylfur-2-yl)-2'-deoxyuridine (108). Treatment of 5-iodo-2'-deoxyuridine **103**[111] (53 mg, 0.15 mmol) with 2-heptylfuran (0.29 mL, 249 mg, 1.5 mmol) as described by Procedure B (column chromatography; hexane/EtOAc, 20:80) gave **108** (35 mg, 61%): UV (MeOH) λ_{max} 256, 326 nm (ε 14 250, 11 300), λ_{min} 287 nm (ε 4000); ¹H NMR (DMSO-d_6) δ 0.86 (t, J =6.7 Hz, 3H, CH₃), 1.24-1.31 (m, 8H, 4 x CH₂), 1.60 (quin, J = 6.7 Hz, 2H, heptyl), 2.17 ("dd", J = 6.6, 4.9 Hz, 2H, H2',2''), 2.60 (t, J = 7.4 Hz, 2H, CH₂), 3.60-3.62 (m, 2H, H5',5''), 3.83 (q, J = 3.3 Hz, 1H, H4'), 4.29 (quin, J = 4.2, 1H, H3'), 5.05 (t, J = 5.0 Hz, 1H, 5'-OH), 5.28 (d, J = 4.1 Hz, 1H, 3'-OH), 6.11 (d, J = 3.1 Hz, 1H, furan), 6.21 (t, J = 6.6 Hz, 1H, H1'), 6.72 (d, J = 3.1 Hz, 1H, furan), 8.27 (s, 1H, H6), 11.58 (s, 1H, NH); ¹³C NMR δ 14.2, 22.1, 27.0, 28.6, 31.1, 39.4, 60.8, 70.3, 84.5, 87.4, 105.7, 106.8, 108.6, 133.6, 144.5, 149.6, 154.8, 160.0; HRMS calcd for $C_{20}H_{29}N_2O_6$ [M+H]⁺ 393.2020, found 393.2023.

3',5'-Di-*O*-acetyl-5-(5-heptylfur-2-yl)-2'-deoxyuridine (109). Treatment of **104**[118] (150 mg, 0.34 mmol) with 2-heptylfuran (0.6 mL, 565 mg, 3.4 mmol) as described by Procedure B (column chromatography; hexane/EtOAc, 80:20 → 60:40) gave **109** (86 mg, 60%): ¹H NMR δ 0.87 (t, J = 7.1 Hz, 3H, CH₃), 1.22-1.37 (m, 8H, 4 x CH₂), 1.61 (q, J = 7.4 Hz, 2H, CH₂), 2.11 (s, 3H, CH₃), 2.12 (s, 3H, CH₃), 2.25 ("ddd", J = 16.6, 8.7, 2.2 Hz,

1H, H2'), 2.50-2.57 (m, 1H, H2"), 2.59 (t, J = 7.5 Hz, 2H, CH$_2$), 4.30-4.34 (m, 1H, H4'),

4.38-4.42 (m, 2H, H5',5"), 5.28 ("dt", J = 6.4, 1.6 Hz, 1H, H3'), 6.05 (d, J = 3.3 Hz, 1H,

furan), 6.40 (dd, J = 8.6, 5.5 Hz, 1H, H1'), 6.98 (d, J = 3.3 Hz, 1H, furan), 7.85 (s, 1H, H6),

9.30 (s, 1H, NH); ^{13}C NMR δ 14.2 (CH$_3$), 20.9, 21.1 (Ac), 22.8, 28.1, 28.2, 29.2, 29.3, 31.9

(CH$_2$), 38.1(C2'), 61.2 (C5'), 74.7 (C3'), 82.7 (C4'), 85.7 (C1'), 107.4 (furan), 108.2 (C5),

111.0 (furan), 131.3 (C6), 143.8, 149.4 (furan), 156.2 (C2), 159.9 (C4), 170.3, 170.5 (Ac);

HRMS calcd for C$_{24}$H$_{32}$N$_2$NaO$_8$ [M+Na]$^+$ 499.2056, found 499.2078.

2',3',5'-Tri-*O*-acetyl-5-(5-heptylfur-2-yl)uridine (110). Treatment of 2',3',5'-tri-*O*-

acetyl-5- iodouridine **105** (400 mg, 0.8 mmol) with 2-heptylfurane (1.5 mL, 665 mg, 4.0

mmol) by Procedure B (column chromatography; hexane/EtOAc, 50:50) gave **110** (236

mg, 55%): ^{1}H NMR δ 0.88 (t, J = 6.7 Hz, 3H, CH$_3$), 1.25-1.34 (m, 8H, 4 x CH$_2$), 1.62 (quin,

J = 7.8 Hz, 2H, CH$_2$), 2.10 (s, 3H, Ac), 2.15 (s, 3H, Ac), 2.18 (s, 3H, Ac), 2.59 (t, J = 7.8

Hz, 2H, CH$_2$), 4.38-4.40 (m, 3H, H4',5',5"), 5.40-5.44 (m, 2H, H2',3'), 6.05 (d, J = 3.6 Hz,

1H, furan), 6.21 (d, J = 5.5 Hz, 1H, H1'), 6.99 (d, J = 3.3 Hz, 1H, furan), 7.75 (s, 1H, H6),

9.03 (s, 1H, NH); ^{13}C NMR δ 14.0 (CH$_3$), 20.4, 20.6, 20.8 (Ac), 22.6, 28.0, 28.1, 29.0, 29.2,

31.7 (CH$_2$), 63.4 (C5'), 70.8 (C3'), 72.7 (C2'), 80.4 (C4'), 87.0 (C1'), 107.3 (furan), 108.5

(C5), 111.2 (furan), 131.2 (C6), 143.5, 149.4 (furan), 156.1 (C2), 160.0 (C4), 169.7, 169.7,

170.1 (Ac); HRMS calcd for C$_{26}$H$_{35}$N$_2$O$_{10}$ [M+H]$^+$ 535.2286, found 535.2288.

5-(5-Heptylfur-2-yl)uridine (111). Methanolic ammonia (6.4 mL) was added to **110**

(100 mg, 0.19 mmol) in 1.6 mL MeOH and the resulting mixture was stirred at 0 ^{o}C → rt

for 12 hours. Volatiles were evaporated and the residue was column chromatographed

(EtOAc/MeOH, 95:5) to give **111** (62 mg, 81%): UV (MeOH) λ$_{max}$ 254, 326 nm (ε 13 600,

10 950), λ$_{min}$ 287 nm (ε 3850); ^{1}H NMR (DMSO-d_6) δ 0.86 (t, J = 6.6 Hz, 3H, CH$_3$), 1.24-

1.31 (m, 8H, 4 x CH$_2$), 1.60 (quin, J = 6.9, 2H, CH$_2$), 2.60 (t, J = 7.3 Hz, 2H, CH$_2$), 3.60 (ddd, J = 12.0, 4.8, 3.1 Hz, 1H, H5'), 3.68 (ddd, J = 12.0, 4.8, 2.9 Hz, 1H, H5"), 3.89-3.91 (m, 1H, H4'), 4.02 (q, J = 4.8 Hz, 1H, H3'), 4.10 (q, J = 5.0 Hz, 1H, H2'), 5.11 (d, J = 5.2 Hz, 1H, 3'-OH), 5.15 (t, J = 4.8 Hz, 1H, 5'-OH), 5.44 (d, J = 5.6 Hz, 1H, 2'-OH), 5.86 (d, J = 4.8 Hz, 1H, H1'), 6.11 (d, J = 3.1 Hz, 1H, furan), 6.73 (d, J = 3.1 Hz, 1H, furan), 8.36 (s, 1H, H6), 11.60 (s, 1H, NH). ^{13}C NMR (DMSO-d_6) δ 13.9, 22.0, 27.2, 27.3, 28.3, 28.5, 31.2 (heptyl), 60.6 (C5'), 69.9 (C3'), 74.0 (C2'), 84.9 (C1'), 88.3 (C4'), 105.9 (C5), 106.7 (furan), 108.7 (furan), 133.9 (C6), 144.5 (furan), 149.6 (furan), 154.7 (C2), 160.1 (C4); HRMS calcd for C$_{20}$H$_{29}$N$_2$O$_7$ [M+H]$^+$ 409.1969, found 409.1982.

5'-*O*-Undecanoyl-5-(fur-2-yl)-2'-deoxyuridine (112). Treatment of **106**[111] (25 mg, 0.08 mmol) with undecanoic anhydride by Procedure A (column chromatography; hexane/EtOAc, 100:0 → 70:30) gave **112** (18 mg, 52%) and **113** (5 mg, 10%) in addition to unchanged **106** (~15%; TLC). Compound **112** had: ^{1}H NMR δ 0.88 (t, J = 7.1 Hz, 3H, CH$_3$), 1.22-1.40 (m, 14H, 7 x CH$_2$), 1.60 ("quin", J = 7.3 Hz, 2H, CH$_2$), 2.10-2.17 (m, 1H, H2'), 2.35 (t, J = 7.6 Hz, 2H, CH$_2$), 2.50 (ddd, J =13.7, 6.3, 3.9 Hz, 1H, H2"), 3.05 (br s, 1H, 3'-OH), 4.15 (q, J = 3.9, 1H, H4'), 4.25 (dd, J = 12.1, 3.3 Hz, 1H, H5'), 4.36-4.42 (m, 2H, H3',5"), 6.26 (t, J = 6.3 Hz, 1H, H1'), 6.60 (dd, J = 3.3, 1.8 Hz, 1H, furan), 7.05 (d, J = 3.5 Hz, 1H, furan), 7.38 (d, J = 1.2 Hz, 1H, furan), 8.25 (s, 1H, H6), 8.38 (s, 1H, NH); HRMS calcd for C$_{24}$H$_{34}$N$_2$NaO$_7$ [M+Na]$^+$ 485.2264; found 485.2271.

3',5'-Di-*O*-undecanoyl-5-(fur-2-yl)-2'-deoxyuridine (113). Treatment of **106**[111] (25 mg, 0.08 mmol) with undecanoic anhydride (84 mg, 0.24 mmol) by Procedure A (6 h) gave **113** (38.5 mg, 77%): ^{1}H NMR δ 0.82-0.91 (m, 6H, 2 x CH$_3$), 1.20-1.40 (m, 28H, 14 x CH$_2$), 1.60-1.68 (m, 4H, 2 x CH$_2$), 2.24 (ddd, J = 14.6, 8.6, 6.5 Hz, 1H, H2'), 2.33-2.40 (m, 4H,

2 x CH$_2$), 2.54 (ddd, J = 14.1, 5.6, 1.3 Hz, 1H, H2"), 4.30 ("q", J = 2.7 Hz, 1H, H4'), 4.36 (dd, J = 12.2, 2.8 Hz, 1H, H5'), 4.45 (dd, J =11.8, 3.5 Hz, 1H, H5"), 5.27 ("dt", J = 6.4, 1.6 Hz, 1H, H3'), 6.40 (dd, J = 8.8, 6.1 Hz, 1H, H1'), 6.47 (dd, J = 3.3, 1.8 Hz, 1H, furan), 7.05 (d, J = 3.4 Hz, 1H, furan), 7.33 (d, J = 1.6 Hz, 1H, furan), 8.00 (s, 1H, H6), 8.95 (s, 1H, NH); ^{13}C NMR δ 14.5, 23.0, 25.1, 25.2, 29.3, 29.4, 29.6, 29.7, 29.9, 32.3, 34.1, 34.3, 34.5, 39.0 (C2'), 64.0 (C5'), 74.6 (C3'), 83.2 (C4'), 86.0 (C1'), 108.0 (C5), 110.0 (furan), 112.5 (furan), 133.0 (C6), 142.0 (furan), 146.0 (furan), 149.5 (C2), 160.2 (C4), 173.2, 173.4 (C=O); HRMS calcd for C$_{35}$H$_{54}$N$_2$NaO$_8$ [M+Na]$^+$ 653.3778, found 653.3778.

5'-*O*-Undecanoyl-5-(5-heptylfur-2-yl)-2'-deoxyuridine (114). Treatment of **108** (25 mg, 0.064 mmol) with undecanoic anhydride by Procedure A (hexane/EtOAc, 100:0 → 80:20) gave **114** [17 mg, 48%; TLC (CHCl$_3$/MeOH, 95:5), R$_f$ = 0.50), **115** (4.7 mg, 10%; R$_f$ = 0.90) and unchanged **108** (~15%, TLC; R$_f$ = 0.10). Compound **114** had: ^{1}H NMR δ 0.85-0.90 (m, 6H, 2 x CH$_3$), 1.28-1.31 (m, 22H, 11 x CH$_2$), 1.54-1.64 (m, 4H, 2 x CH$_2$), 2.13-2.16 (m, 1H, H2'), 2.27-2.32 (m, 2H, CH$_2$), 2.46 (ddd, J =13.9, 6.4, 4.3 Hz, 1H, H2"), 2.56 (t, J = 7.4 Hz, 2H, CH$_2$), 2.98 (s, 1H, 3'-OH), 4.19 (q, J = 3.5, 1H, H4'), 4.28 (dd, J = 12.3, 3.4 Hz, 1H, H5'), 4.33-4.41 (m, 2H, H3',5"), 6.05 (d, J = 3.2 Hz, 1H-furan), 6.28 (t, J = 6.4 Hz, 1H, H1'), 6.90 (d, J = 3.2 Hz, 1H-furan), 8.10 (s, 1H, H6), 8.44 (s,1H, NH); ^{13}C NMR δ 14.2, 22.9 (CH$_3$), 24.9, 28.1, 28.2, 29.2, 29.2, 29.3, 29.4, 29.5, 29.6, 29.7, 31.9, 32.1, 34.2, 34.3, 34.4 (CH$_2$), 40.7 (C2'), 63.6 (C5'), 71.8 (C3'), 84.4 (C4'), 85.5 (C1'), 108.2 (C5), 110.6 (furan), 113.0 (furan), 129.0 (furan), 133.0 (C6), 149 (C2), 156.0 (furan), 159.6 (C4), 174.0 (C=O); HRMS calcd for C$_{31}$H$_{48}$N$_2$NaO$_7$ [M+Na]$^+$ 583.3359, found 583.3375.

Note: Also isolated from column chromatography was a product (2 mg, 5%; TLC, $R_f = 0.55$) whose structure was tentatively assigned as 3'-*O*-undecanoyl-5-(5-heptylfur-2-yl)-2'-deoxyuridine [^{1}H NMR δ 5.39 ("dt", $J = 8.1$, 1.6 Hz, 1H, H3').

3',5'-Di-*O*-undecanoyl-5-(5-heptylfur-2-yl)-2'-deoxyuridine (115). Treatment of **108** (25 mg, 0.064 mmol) with undecanoic anhydride (65 mg, 0.19 mmol) by Procedure A (6 h) gave **115** (36 mg, 80%). Compound **115** had: ^{1}H NMR δ 0.83-0.92 (m, 9H, 3 x CH$_3$), 1.22-1.38 (m, 36H, 18 x CH$_2$), 1.55-1.70 (m, 6H, 3 x CH$_2$), 2.25 (ddd, $J = 14.7$, 8.5, 6.6 Hz, 1H, H2'), 2.30-2.40 (m, 4H, 2 x CH$_2$), 2.53-2.57 (m, 1H, H2"), 2.60 (t, $J = 7.6$ Hz, 2H, CH$_2$), 4.31 (q, $J = 3.0$ 1H, H4'), 4.38 (dd, $J = 12.2$, 2.8 Hz, 1H, H5'), 4.42 (dd, $J = 11.3$, 3.8 Hz, 1H, H5"), 5.26 ("dt", $J = 6.8$, 1.6 Hz, 1H, H3'), 6.05 (d, $J = 3.2$ Hz, 1H, furan), 6.37 (dd, $J = 8.8$, 6.1 Hz, 1H, H1'), 6.95 (d, $J = 3.3$ Hz, 1H, furan), 7.88 (s, 1H, H6), 9.00 (s, 1H, NH); HRMS calcd for $C_{42}H_{68}N_2NaO_8$ [M+Na]$^+$ 751.4873, found 751.4851.

5'-*O*-Undecanoyl-5-(fur-2-yl)uridine (119). *Step a*. DDC (516 mg, 1.25 mmol) was added to a stirred solution of 2',3'-*O*-isopropylideneuridine **116** (142 mg, 0.5 mmol), undecanoic acid (163 mg, 0.875 mmol), and 4-dimethylaminopyridine (91.6 mg, 0.375 mmol) in DMF (2 mL) at rt The resulting mixture was stirred at 60 °C overnight. Volatiles were evaporated and the residue was partitioned between EtOAc and 0.1 M HCl solution. The organic layer was washed with saturated solutions of NaHCO$_3$ and brine and then was column chromatographed (hexane/EtOAc, 50:50) to give 2',3'-*O*-isopropylidene-5'-*O*-undecanoyluridine (**117**; 203 mg, 90%) of sufficient purity to be used in next step: ^{1}H NMR δ 0.88 (t, $J = 7.1$ Hz, 3H, CH$_3$), 1.22-1.65 (m, 22H, 8 x CH$_2$, 2 x CH$_3$), 2.31 (t, $J = 7.5$ Hz, 2H, CH$_2$), 4.26-4.38 (m, 3H, H4',5',5"), 4.80 (dd, $J = 5.7$, 3.8 Hz, 1H, H3'), 4.98 (dd, $J = 6.2$, 1.4 Hz, 1H, H2'), 5.65 (d, $J = 1.3$ Hz, 1H, H1'), 5.72 (d, $J = 8.2$ Hz, 1H, H5), 7.28 (d,

$J = 8.2$ Hz, 1H, H6), 8.98 (s, 1H, NH). *Step b.* ICl (1M/CH$_2$Cl$_2$; 0.75 mL, 0.75 mmol) was added to a stirred solution of **117** (224 mg, 0.5 mmol) in CH$_2$Cl$_2$ (4.3 mL) at ambient temperature and the resulting mixture was stirred at 40 °C (oil-bath) overnight. The reaction solution was washed with 2% NaHSO$_3$ until the color turn into light yellow. The organic layer was washed with saturated solutions of NaHCO$_3$ and brine and then was column chromatographed (hexane/EtOAc, 60:40 → 10:90) to give 5'-*O*-undecanoyl-5-iodouridine (**118**; 66 mg, 25%): ^{1}H NMR δ 0.87 (t, $J = 6.6$ Hz, 3H, CH$_3$), 1.25-1.31 (m, 14H, 7 x CH$_2$), 1.67 (quin, $J = 7.0$ Hz, 2H, CH$_2$), 2.42-2.57 (m, 2H, CH$_2$), 4.22-4.48 (m, 5H, H2',3',4',5',5''), 5.91 (d, $J = 2.9$ Hz, 1H, H1'), 8.02 (s, 1H, H6), 10.69 (s, 1H, NH). *Step c.* Treatment of **118** (27 mg, 0.05 mmol) with furan by Procedure B (column chromatography; hexane/EtOAc, 20:80) gave **119** (15 mg, 63%); ^{1}H NMR δ 0.87 (t, $J = 6.7$ Hz, 3H, CH$_3$), 1.23-1.25 (m, 14H, 7 x CH$_2$), 1.59 (quin, $J = 6.8$, 2H, CH$_2$), 2.35 (t, $J = 7.5$ Hz, 2H, CH$_2$), 4.24 ("t", $J = 4.9$ Hz, 1H, H3'), 4.35-4.40 (m, 4H, H2',4',5',5''), 5.95 (d, $J = 4.1$ Hz, 1H, H1'), 6.40 (dd, $J = 3.3$, 1.8 Hz, 1H, furan), 6.97 (d, $J = 3.2$ Hz, 1H, furan), 7.27 ("s", 1H, furan), 7.96 (s, 1H, H6), 9.89 (s, 1H, NH); HRMS calcd for C$_{24}$H$_{35}$N$_2$O$_8$ [M+H]$^+$ 479.2388, found 479.2397

5'-*O*-Undecanoyl-5-(5-heptylfur-2-yl)uridine (120). Treatment of **118** (27 mg, 0.05 mmol) with 2-heptylfurane (96 μL, 83 mg, 0.5 mmol) by Procedure B (column chromatography; hexane/EtOAc, 30:70) gave **120** (13 mg, 44%): ^{1}H NMR (DMSO-*d$_6$*) δ 0.82-0.87 (m, 6H, 2 x CH$_3$), 1.18-1.30 (m, 22H, 11 x CH$_2$), 1.48 (quin, $J = 6.9$, 2H, CH$_2$), 1.58 (quin, $J = 7.2$, 2H, CH$_2$), 2.22-2.37 (m, 2H, CH$_2$), 2.58 (t, $J = 7.5$ Hz, 2H, CH$_2$), 3.95 (q, $J = 5.0$ Hz, 1H, H3'), 4.08-4.13 (m, 2H, H2',4'), 4.22 (dd, $J = 12.5$, 2.2 Hz, 1H, H5'), 4.30 (dd, $J = 12.5$, 5.6 Hz, 1H, H5''), 5.32 (d, $J = 5.9$ Hz, 1H, 3'-OH), 5.54 (d, $J = 5.0$ Hz, 1H, 2'-OH), 5.82 (d, $J = 5.3$ Hz, 1H, H1'), 6.14 (d, $J = 3.4$ Hz, 1H, furan), 6.77 (d, $J = 3.7$

Hz, 1H, furan), 7.78 (s, 1H, H6), 11.68 (s, 1H, NH); ^{13}C NMR (DMSO-d_6) δ 13.87 (CH$_3$), 13.90 (CH$_3$), 22.0, 24.4, 27.3, 27.4, 28.35, 28.37, 28.58, 28.61, 28.8, 28.9, 31.18, 31.23, 33.2 (CH$_2$), 63.4 (C5'), 69.9 (C3'), 73.3 (C2'), 81.5 (C4'), 88.9 (C1'), 101.1 (C5), 106.9 (furan), 109.2 (furan), 132.8 (C6), 144.3 (furan), 149.5 (furan), 154.7 (C2), 160.0 (C4), 172.6 (C=O); HRMS calcd for C$_{31}$H$_{49}$N$_2$O$_8$ [M+H]$^+$ 577.3483, found 577.3509

4.2. Polymerase-catalyzed synthesis of azidomethyl-modified DNA

Materials of enzymatic reactions

All DNA primers and templates were synthesized by Integrated DNA Technologies (Coralville, IA). The radionucleotides [γ-^{32}P] ATP (6000 mCi/mmol) was purchased from MP biomedicals Inc. (Santa Ana, CA). T4 polynucleotide kinase and deoxynucleoside 5'-triphosphates (dNTPs) were purchased from Thermo Scientific (Pittsburgh, PA). Micro Bio-Spin TM 6 Columns were from Bio-Rad (Hercules, CA). All other chemicals were from Thermo Scientific (Pittsburgh, PA) and Sigma-Aldrich (St. Louis, MO). Purified human DNA polymerase β (pol β), flap endonuclease 1 (FEN1) and DNA ligase I (LIG I) were purified according to the procedures described previously.[151,152] The Klenow fragment of *E. Coli* DNA polymerase I (Pol I) was purchased from New England Biolabs (Ipswitch, MA).

Oligonucleotide substrates

Substrates with an upstream primer annealed to the template strand were designated as open template substrates. The substrates were made by annealing an upstream primer (31nt) with the template strand (71 nt) at a molar ratio of 1:3. The substrate containing one-nucleotide gap were made by annealing an upstream primer and downstream primer (Table 12, Downstream primer 1) with the template strand at the molar ratio of 1:3:3. The open

113

template and one-nucleotide gap substrates were employed to mimic the intermediates formed during DNA replication. The substrate containing one-nucleotide gap with a 5'-sugar at the downstream strand were made by annealing an upstream primer, a downstream primer with a 5'-tetrahydrofuran (THF), an analogue of a sugar (Table 12, Downstream primer 2) with the template strand at a molar ratio of 1:3:3. Substrates were labeled with γ-^{32}P at the 5'-end of the upstream primers. Template 1 was designed for incorporation of AmdUTP **20**, whereas Template 2 was for AmdCTP **74**.

Table 12. Oligonucleotide Sequences of primers and templates for polymerase-catalyzed synthesis of azido-modified DNA

Oligonucleotide	nt	Sequence (5'-3')
Upstream primer	31	GCA GTC CTC TAG TCG TAG TAG CAG ATC ATC A
Downstream primer 1	39	CAA CCG GCA TTA GGT GTA GTA GCT AGA CTT ACT CAT TGC
Downstream primer 2	39	**THF** CAA CCG GCA TTA GGT GTA GTA GCT AGA CTT ACT CAT TGC
Template 1	71	GCA ATG AGT AAG TCT AGC TAC TAC ACC TAA TGC CGG TTG **A**TG ATG ATC TGC TAC TAC GAC TAG AGG ACT GC
Template 2	71	GCA ATG AGT AAG TCT AGC TAC TAC ACC TAA TGC CGG TTG **G**TG ATG ATC TGC TAC TAC GAC TAG AGG ACT GC

Note: THF denotes tetrahydrofuran, an abasic sugar analogue.

Enzymatic activity assay and BER reconstitution assay

Nucleotides incorporation by DNA polymerases was performed by incubating different concentrations of pol β or Klenow fragment with 25 nM ^{32}P labeled substrates at 37°C for 15 min. The enzymatic reactions were assembled with 50 μM AmdUTP **20** alone or with 50 μM AmdUTP **20** along with 50 μM dATP, 50 μM dCTP and 50 μM dGTP. To examine if an AmdUTP residue can be directly incorporated into a double-strand DNA through DNA lagging strand maturation and base excision repair (BER) via ligation, ligation reactions with the gapped substrates were performed in the presence of various concentrations of pol β or Klenow fragment and 10 nM LIG I along with 50 μM AmdUTP

20 and 50 μM dATP, 50 μM dCTP and 50 μM dGTP. BER was reconstituted by incubating 25 nM substrate containing a 5'-THF with 5 nM FEN1, 10 nM LIG I, 10 nM and 25 nM of pol β in the presence of 50 μM AmdUTP, 50 μM dATP, 50 μM dCTP and 50 μM dGTP. Reaction mixtures (20 μl) contained 5 mM Mg^{2+}, 50 mM Tris-HCl (pH 7.5), 50 mM KCl, 0.1 mg/ml BSA, 0.1 mM EDTA and 0.01% NP-40. For the reactions that contained LIG I, 2 mM ATP were included in the reaction mixtures. Reactions were terminated with 20 μl 2X stopping buffer contained 95 % formamide and 10 mM EDTA. Reaction mixtures were subsequently denatured at 95 °C for 10 min. DNA synthesis and ligation products were separated in a 15% urea denaturing polyacrylamide gel and were detected by Pharos FX Plus PhosphorImager (Bio-Rad Laboratory, CA).

Incorporation of a AmdCTP **74** by pol β was measured by incubating various concentrations of pol β (1 nM, 5 nM, 10 nM and 25 nM) with 25 nM open template substrate, one-nucleotide gap substrate and one-nucleotide gap substrate containing a 5'-THF along with 50 μM of a AmdCTP. Substrates were ^{32}P-labeled at the 5'-end of the upstream primer.

4.3. ESR studies of aminyl radical and its conversion to iminyl radical

Sample preparation and methods

As per the well-established methodologies,[42,73,153] transparent glassy samples of AmdU **18**, AmdC **42**, AvdU **21**, and AvdC **43** were prepared. Subsequently, γ-irradiation and ESR spectral analyses of these samples were performed.

Compounds purchased: Lithium chloride (LiCl) (ultra-dry, 99.995% (metals basis)) was obtained from Alfa Aesar (Ward Hill, MA, USA). Deuterium oxide (D_2O) (99.9 atom %

D) was purchased from Aldrich Chemical Company Inc. (Milwaukee, WI, USA). All compounds were used without further purification.

Glassy sample preparation:

(i) Preparation of homogeneous solutions: First, homogeneous solution was prepared by dissolving ca. 2.2 to 2.4 mg/mL of a compound (e.g., **18**) in either 7.5 M LiCl in D_2O. The native pH of 7.5 M LiCl in D_2O is ca. 5 and pH of these solutions was not adjusted.[73]

(ii) Preparation of glassy samples and their storage: Homogenous solutions of azido compounds were thoroughly bubbled with nitrogen gas. Subsequently, those solutions were immediately drawn into 4 mm Suprasil quartz tubes (Catalog no. 734-PQ-8, WILMAD Glass Co., Inc., Buena, NJ, USA). Thereafter, the quartz tubes containing these solutions were rapidly immersed in liquid nitrogen (77 K). Owing to rapid cooling at 77 K, the homogeneous liquid solutions formed transparent homogeneous glassy solutions. Subsequently, these transparent homogeneous glassy solutions of azido compounds were γ-irradiated at 77 K and were subjected to progressive annealing experiments along with ESR spectral studies. All glassy samples were stored in the dark at 77 K in Teflon containers prior to and after γ -irradiation.

γ-Irradiation of glassy samples and their storage: As per our well-established methodology of γ-irradiation of glassy samples of DNA and RNA-models,[42,73,153] the glassy samples were γ (^{60}Co)-irradiated (absorbed dose = 375-500 Gy (1.5 to 2 h)) at 77 K and stored at 77 K in Teflon containers in the dark. Owing to 2.2 to 2.4 mg per mL of 7.5 M LiCl glass (D_2O) and as per our previous work with 3′-AZT[42] and azidopentofuranoses,[73] the radiation-produced prehydrated electrons in the glass[153] are

scavenged by the azide solute and $Cl_2\bullet^-$ is formed owing to scavenging of radiation-induced holes by the matrix (7.5 M LiCl).[42,73,153]

Annealing of glassy samples: As per our previous studies,[42,73,153] a variable temperature assembly that passed liquid nitrogen cooled dry nitrogen gas past a thermister and over the glassy sample was employed for annealing. Stepwise (either 5 K or 10 K step) annealing of each glassy sample was conducted in the range (140 – 170) K for 15 min. The matrix radical, $Cl_2\bullet^-$, did not react with sample.[42,73,153] Thus, by employing ESR spectroscopy, we were able to study directly the formation of RNH• via reaction of radiation-produced prehydrated electron with azido compounds and subsequent reactions of RNH•.

Electron Spin Resonance: As per ongoing studies in our laboratory,[42,73,153] we used a Varian Century Series X-band (9.3 GHz) ESR spectrometer with an E-4531 dual cavity, 9-inch magnet, and a 200 mW Klystron. For the field calibration, Fremy's salt (g_{center} = 2.0056, A(N) = 13.09 G) was employed. All ESR spectra were recorded at 77 K and at 45 dB (6.3 µW) as well as 40 dB (20 µW). We note here that recording of ESR spectra at 77 K maximizes the signal height and allows for comparison of signal intensities.[73]

Employing the Bruker programs (WIN-EPR and SimFonia) and our ongoing studies on DNA and RNA-radicals,[73,153] anisotropic simulations of experimentally recorded ESR spectra were carried out. The ESR parameters (e.g., hyperfine coupling constant (HFCC) values, linwidth, etc.) were adjusted to obtain the "best fit" simulated spectrum that matched the experimental ESR spectrum well (see our previous works[42,73,153]). In addition, each ESR spectrum reported are obtained after subtraction of line components due to $Cl_2\bullet^-$.

Method of theoretical Calculations: Employing optimized geometries of radicals, energies of radicals and hyperfine coupling constant (HFCC) values were calculated using

DFT/B3LYP/6-31+G** method in Gaussian 09. Theoretically predicted HFCC values obtained employing B3LYP/6-31+G** method agree well with those obtained using experiment.[73,154] Jmol molecular modeling freeware was used to plot optimized molecular structures.[155,129]

4.4. Radiosensitizing effect of 5-azidomethyl and 5-azidovinyl pyrimidine nucleosides in aerobic and hypoxic cells

The radiation response of cells in the presence of azido-modified nucleosides in vitro was examined using exponentially growing monolayers in Perma-nox Contour dishes (Lux Scientific).[156] Clonogenic assay was used to do cell death assay. EMT6 mouse cells were allowed to grow for 1 day to produce cultures in mid exponential growth. For the tests in aerobic cells, the cultures were treated with 100 µM azido compounds in DMSO in small volumes or vehicles for 48 h. For the test in hypoxic cells, after the 44 h treatment under aerobic condition, hypoxia was produced by placing uncovered dishes, containing the monolayers overlaid with 2 mL of medium containing azido compounds or vehicle, into a pressure vessel and gassing the vessel at 37 $^{\circ}$C with a humidified mixture of 95% N_2/5% CO_2 for 4 h. The radiosensitizing effect tests were divided into following groups: (*a*) Control: without azido compounds and without irradiation treatment under aerobic or hypoxic condition. (*b*) Drug: the cultures were treated with 100 µM azido compounds in small volumes for 44 h under aerobic followed by 4 h under aerobic or hypoxic condition. (*c*) Drug and irradiation in aerobic cells: the cultures were treated with 100 µM azido compounds in small volumes or vehicles for 48 h and irradiated with 7.5 Gy radiation during the final few minutes of the 48 h incubation. Cells were irradiated with 320 kV X-rays produced by an XRAD irradiator (Precision X-ray, Branford CT, USA) at 12.5 mA,

2 mm Al filtration, and a dose rate of 2.4 Gy/min. (*d*) Drug and irradiation in hypoxic cells: the cultures were treated with 100 μM azido compounds in small volumes or vehicles for 44 h under aerobic condition and then 4 h under hypoxia condition. Cultures were irradiated with 7.5 GY radiation. Cells were irradiated with 320 kV X-rays produced by an XRAD irradiator at 12.5 mA, 2 mm Al filtration, and a dose rate of 1.9 Gy/min.

4.5. Fluorescent properties of triazolyl nucleosides

The fluorescent properties of the four *N*-unsubstituted triazolyl nucleosides (8-TrzdA **46**, 8-TrzdG **47**, 5-TrzdC **48**, and 5-TrzdU **39**) and their lipophilic analogues (diTBDMS-8-TrzdA **88**, diAc-5-TrzdU **84**, and diAc-5-TrzdC **83**) were determined following the general procedure reported in the paper reported from our group.[51] Triazoles samples were tested with varying concentration. The whose absorbance at the excitation wavelength did not exceed 0.1 absorbance units. For determination of quantum yield Φ_F, the absorbance of the sample solution was kept below 0.06. Quinine sulfate ($\Phi_F = 0.55$) in 100 mM H_2SO_4 was used as reference standard to quantify the quantum yield. All the triazoles were soluble enough in the methanol and thus were prepared in HPLC grade methanol. The test was performed in a 2×10 mm quartz cuvette at room temperature. Absorption spectra were measured using Cary 100Bio UV-Visible Spectrophotometer. Steady-state excitation and emission spectra were investigated on a PC1 spectrofluorometer with bandwidth and slit width for ex/em set at 2 nm. Frequency-domain fluorescence lifetime were measured using a ChronosFD spectrofluorometer. Sample solutions were excited using a frequency modulated 280 nm LED. The emission was gathered with a 305 nm long-pass filter (Andover). 2,5-diphenyloxazole ($\tau = 1.4$ ns) solution in EtOH was employed as a lifetime reference. A multiple-exponential decay model employing GlobalsWE software were used

to fit the modulation phase data. The residual and $\chi 2$ parameter were employed as criteria for goodness of fit.

4.6. Cell microscopy studies of triazoles

4.6.1. Using primary mouse astrocytes

Primary mouse astrocytes were plated on coverslips and acclimated for 24 hours. 1 M stock solution of compounds were prepared in DMSO. The cells were treated with the vehicle (0.05% DMSO) or 10 uM, 100 uM, 1 mM of compounds (each with 0.05% DMSO) in 10% FBS P-S DMEM F-12 media for 24 hours. The cells were mounted using Prolong Mounting Medium. Nail polish was used to seal. The live cells were imaged using FV10i Confocal Laser Scanning Microscope from Olympus (10x & 60x objectives with 405 laser and phase contrast).

4.6.2. Using mouse pre-adipocytes transfected with pMX-puro-GFP

cDNA Construction and cell transfection.

cDNA of GFP was cloned into the pMX-puro vector at EcoRI and NotI restriction sites and plasmid DNA was purified according to the QIAprep Spin Miniprep Kit. The pMX-puro-GFP vector was then transfected into the Plat-A (Cell Biolabs, INC. # RV-102) monolayer using Lipofectamine® 2000 Transfection Reagent (Thermo Fisher Scientific). Plat-A cells were grown in Plat-A growth media (1% penicillin/streptomycin, 1 µg/mL puromycin, 10 µg/mL blasticidin and 10% fetal bovine serum in Dulbecco's modified Eagle's medium (DMEM)) and incubated under a humid atmosphere containing 5% CO_2 under 37°C. 48h after transfection, the supernatant of Plat-A media was filtered with 0.2 nm filter and applied to 90% confluent 3T3-L1 cells grown in 3T3-L1 growth media (1% penicillin/streptomycin, 1% L-glutamine and 10% FBS in DMEM). After 24h

of incubation, 3T3-L1 cells been transfected with pMX-puro-GFP will be selected with the 3T3-L1 selection media (5µg/mL puromycin in 3T3-L1 growth media).

Confocal Microscopy. 3T3-L1 mouse pre-adipocytes (Zen-bio #SP-L1-F) that have been transfected with pMX-puro-GFP were seeded on glass coverslips at 1.0×10^5 per 3.8 cm^2 well for 24 hours in 3T3-L1 selection media. Stock solution of 8-TrzdA **46** and 5-TrzdU **39** were prepared in DMSO. Then the cells were treated with the vehicle (0.05% DMSO), 200 uM of 8-TrzdA, or 200 uM of 5-TrzdU (with 0.05% DMSO) in 3T3-L1 selection media for 24 hours. After the 24h incubation, cells were washed with PBS and fixed in 4% paraformaldehyde for 20 minutes. Fixed cells were mounted with ProLong™ Gold Antifade Mountant (Thermo Fisher Scientific) and observed under the Olympus FV 1200 confocal microscope. Ex/Em = 473/519 nm were used for imaging of GFP and Ex/Em = 405/461 nm were used for imaging of the triazoles, respectively.

4.7. Proliferation Assays

Human cervical carcinoma (HeLa) cells were seeded in 96-well plates at 15,000 cells/well in the presence of 5-fold dilutions of the compounds. After 4 days of incubation, the cells were trypsinized and counted by means of a Coulter counter (Analis, Belgium). Suspension cells (Mouse leukemia L1210 and human lymphoid CEM cells) were seeded in 96-well plates at 60,000 cells/well in the presence of the compounds. L1210 and CEM cells were allowed to proliferate for 48 h or 96 h, respectively and then counted. The 50% inhibitory concentration (IC$_{50}$) was defined as the compound concentration required to reduce cell proliferation by 50%.

4.8. Antiviral Assays

The compounds were evaluated against the following viruses: herpes simplex virus type 1 (HSV-1) strain KOS, thymidine kinase-deficient (TK⁻) HSV-1 KOS strain resistant to ACV (ACVʳ), herpes simplex virus type 2 (HSV-2) strain G, varicella-zoster virus (VZV) strain Oka, TK⁻ VZV strain 07-1, human cytomegalovirus (HCMV) strains AD-169 and Davis, vaccinia virus Lederle strain, respiratory syncytial virus (RSV) strain Long, vesicular stomatitis virus (VSV), Coxsackie B4, parainfluenza 3, influenza virus A (subtypes H1N1, H3N2), influenza virus B, Sindbis, reovirus-1, Punta Toro, human immunodeficiency virus type 1 strain IIIB and human immunodeficiency virus type 2 strain ROD. The antiviral, other than anti-HIV, assays were based on inhibition of virus-induced cytopathicity or plaque formation in human embryonic lung (HEL) fibroblasts, African green monkey cells (Vero), human epithelial cells (HeLa) or Madin-Darby canine kidney cells (MDCK). Confluent cell cultures in microtiter 96-well plates were inoculated with 100 CCID50 of virus (1 $CCID_{50}$ being the virus dose to infect 50% of the cell cultures) or with 20 or 100 plaque forming units (PFU) (VZV or HCMV) in the presence of varying concentrations of the test compounds. Viral cytopathicity or plaque formation was recorded as soon as it reached completion in the control virus-infected cell cultures that were not treated with the test compounds. Antiviral activity was expressed as the EC_{50} or compound concentration required to reduce virus-induced cytopathogenicity or viral plaque formation by 50%. Cytotoxicity of the test compounds was expressed as the minimum cytotoxic concentration (MCC) or the compound concentration that caused a microscopically detectable alteration of cell morphology.

5. CONCLUSION

In this dissertation, I explored the C5 azido-modified pyrimidine nucleosides (AmdU **18**, AvdU **21**, AmdC **42**, and AvdC **43**) as potential radiosensitizer under normoxic and hypoxic environment. I also synthesized 2-azido-2'-deoxyinosine (2-N$_3$dI, **44**) for the site-specific formation and characterization of the elusive 2'-deoxyguanosin-N2-yl radical (dG(N2-H)•, **45**) to investigate the nucleic acid damage pathways induced by γ-radiolysis. Moreover, novel fluorescent *N*-unsubstituted 1,2,3-triazol-4-yl nucleosides (5-TrzdU **39**, 8-TrzdA **46**, 8-TrzdG **47**, and 5-TrzdC **48**) were designed and synthesized as potential tools for investigating the perturbations to nucleic acids.

Two classes of C5 azido-modified pyrimidine nucleosides were synthesized and explored as radiosensitizers. 5-Azidomethyl-2'-deoxyuridine (AmdU, **18**) was prepared from thymidine and was converted to its cytosine counterpart (AmdC, **42**). The 5-(1-azidovinyl)-2'-deoxyuridine (AvdU, **21**) and 5-(1-azidovinyl)-2'-deoxycytidine (AvdC, **43**) have been prepared by the regioselective Ag-catalyzed hydroazidation of the 5-ethynyl substrates with TMSN$_3$. Using Yoshikawa protocol followed by coupling with pyrophosphate, the AmdU **18** and AmdC **43** were converted to their 5'-triphosphate, *i.e.* AmdUTP **20** and AmdCTP **74**, which were enzymatically incorporated into DNA fragment during DNA replication and base excision repair (BER). γ-Irradiation-mediated prehydrated electrons formed in homogeneous aqueous glassy (7.5 M LiCl) systems in the absence of oxygen at 77 K led to site-specific formation of novel and neutral π-type aminyl radicals (RNH•) from AmdU **18**, AmdC **42**, AvdU **21**, and AvdC **43**. The ESR spectral studies and DFT calculations showed that RNH• undergo facile conversion to thermodynamically more stable σ-type iminyl radicals, R=N•. For AmdU **18** and AmdC

42, conversion of aminyl RNH• to iminyl radiacl R=N• was found to be bimolecular involving an α-azidoalkyl radical as intermediate. On the other hand, aminyl radicals RNH• derived from AvdU **21** and AvdC **43** tautomerized to the iminyl radical R=N•. Our work provides the first evidence for the formation of aminyl radical RNH• attached to C5 position of azidopyrimidine nucleoside and its facile conversion to R=N• under a reductive environment. These aminyl and iminyl radicals can generate DNA damage via oxidative pathways. Owing to the high free radical scavenger concentrations in cells, the bimolecular conversion of the π-type RNH• to σ-type iminyl radical from **18** and **42** should not take place. However, the facile unimolecular tautomerization of the π-type RNH• to σ-type iminyl radical from **21** and **43** should occur. Therefore, it is expected that the π-type RNH• from **18** and **42** should augment the radiation damage more effectively than the σ-type iminyl radical from **21** and **43**, which was proved by the radiosensitizing effect tests. AmdU **18** showed radiosensitizing effect under both normoxic and hypoxic environment with $SER_{SF7.5}$ of 4.57 and 4.10, respectively. Other azido-modified nucleosides tested showed lower radiosensitizing effect with $SER_{SF7.5}$ of 1.35 for AmdC **42** under hypoxic cells and 1.37 for AvdC **43** under aerobic cells.

To explore the generation and reactivity of 2'-deoxyguanosin-N2-yl radical (dG(N2-H)•) postulated to be generated during the ambidient reactivity of the guanine moiety in 2'-deoxyguanosine towards hydroxyl radicals (HO•), I prepared 2-azido-2'-deoxyinosine (2-N_3dI, **44**) serving as convenient substrate to generate site-specific elusive guaninyl aminyl radical. Using ESR, the structure of guaninyl aminyl radical and its subsequent reactions as well as DNA-hole transfer processes were investigated to understand nucleic acid damage pathways induced by γ-radiolysis. I synthesized the

2-azido-2'-deoxyinosine **44** by conversion of 2-amino group in the protected 2'-deoxyguanosine into 2-azido group via diazotization reaction with tert-butyl nitrite followed by nucleophilic displacement with azide and deprotection.

The fluorescent *N*-unsubstituted 1,2,3-triazol-4-yl analogues of the four natural bases of DNA (*i.e.* 5-TrzdU **39**, 5-TrzdC **48**, 8-TrzdA **46**, and 8-TrzdG **47**) have been synthesized by metal-catalyzed reactions between the 5-ethynylpyrimidine or 8-ethynylpurine nucleosides with trimethylsilyl azide (TMSN$_3$). CuI catalyzed cycloaddition (DMF/H$_2$O, 90 ^{o}C, 5 h) gave 1,2,3-triazoles as sole products however in low to moderate yield (10% for 5-TrzdC to 50% for 5-TrzdU) due to the oxidation of Cu (I) to Cu (II) during the reaction. Combination of CuSO$_4$/sodium ascorbate gave triazoles in improved yields (38% for 5-TrzdC to 52% for 5-TrzdU). Interestingly, Ag$_2$CO$_3$ catalyzed cycloaddition (DMF, 2 eq. H$_2$O, 80 ^{o}C, 1 h) of 8-ethynylpurine nucleosides with TMSN$_3$ produced 8-triazolylpurines as sole products in good yields (8-TrzdG, 55%), while analogous cycloadditions of 5-ethynylpyrimidine nucleosides produced mixture of 5-triazolylpyrimidine nucleosides (5-TrzdC, 7%) and the corresponding 5-(1-azidovinyl)pyrimidine byproducts (5-(1-azidovinyl)-2'-deoxycytidine, 48%). The novel *N*-unsubstituted 1,2,3-triazol-4-yl nucleoside analogues showed excellent fluorescent properties in MeOH. The 8-purine analogue 8-TrzdA **46** exhibits the highest quantum yield of 44% while the 8-TrzdG **47** had quantum yield of 9%. In contrast, the 5-pyrimidine analogues 5-TrzdU **39** and 5-TrzdC **48** showed a large Stokes shift of ~110 nm with the maximum emission approximately at 408 nm and quantum yield of 2%. The fluorescent triazoles could enter living cells (primary mouse astrocytes and pre-adipocytes transfected with PMX-puro-GFG) and show fluorescence in the cytosol.

Transition metal-catalyzed halosulfonylation of 5-ethynyl uracil nucleosides provided (E)-5-(1-chloro-2-tosylvinyl)uridines. Tetrabutylammonium fluoride-mediated direct C-H arylation of 5-iodouracil nucleosides with furan or 2-heptylfuran gave 5-furyl-substituted nucleosides without the necessity of using the organometallic substrates. These two classes of 5-substituted uracil nucleosides as well their corresponding ester derivatives were tested against a broad range of DNA and RNA viruses and the human immunodeficiency virus (HIV). The 3',5'-di-*O*-acetyl-5-(*E*)-(1-chloro-2-tosylvinyl)-2'-deoxyuridine **122** inhibited the growth of L1210, CEM and HeLa cancer cells in the lower micromolar range. The (β-chloro)-vinyl sulfone **122** and 5-(5-heptylfur-2-yl)-2'-deoxyuridine **108** displayed micromolar activity against varicella zoster virus (VZV). The 5-(5-heptylfur-2-yl) analog **108** and its 3',5'-di-*O*-acetyl-protected derivative showed similar activity against the cytomegalovirus (CMV). The 5-(fur-2-yl) derivatives of 2'-deoxyuridine and arabino-uridine inhibited the replication of herpes simplex virus (HSV) TK$^+$ strains while the 5-(5-heptylfur-2-yl) derivative **108** displayed antiviral activity against the parainfluenza virus.

REFERENCES

(1)   *American Cancer Society. Cancer Facts & Figures* **2018**

(2)   Jordheim, L. P.; Durantel, D.; Zoulim, F.; Dumontet, C. *Nat. Rev. Drug Discov.* **2013**, *12*, 447-464.

(3)   Lawrence, T. S.; Blackstock, A. W.; McGinn, C. *Semin. Radiat. Oncol.* **2003**, *13*, 13-21.

(4)   Barton, M. B.; Jacob, S.; Shafiq, J.; Wong, K.; Thompson, S. R.; Hanna, T. P.; Delaney, G. P. *Radiother. Oncol.* **2014**, *112*, 140-144.

(5)   Polgár, C.; Ott, O. J.; Hildebrandt, G.; Kauer-Dorner, D.; Knauerhase, H.; Major, T.; Lyczek, J.; Guinot, J. L.; Dunst, J.; Miguelez, C. G.; Slampa, P.; Allgäuer, M.; Lössl, K.; Polat, B.; Kovács, G.; Fischedick, A.-R.; Fietkau, R.; Resch, A.; Kulik, A.; Arribas, L.; Niehoff, P.; Guedea, F.; Schlamann, A.; Pötter, R.; Gall, C.; Uter, W.; Strnad, V. *Lancet Oncol.* **2017**, *18*, 259-268.

(6)   Types of Cancer Treatment. NCI/NIH: https://www.cancer.gov/about-cancer/treatment/types

(7)   Schurmann, R.; Vogel, S.; Ebel, K.; Bald, I. *Chemistry* **2018**.

(8)   Wang, H.; Mu, X.; He, H.; Zhang, X.-D. *Trends Pharmacol. Sci.* **2018**, *39*, 24-48.

(9)   Sonntag, C. v. *Free-radical-induced DNA Damage and Its Repair*; Springer-Verlag: Springer-Verlag: Berlin, 2006.

(10)   Nguyen, J.; Ma, Y.; Luo, T.; Bristow, R. G.; Jaffray, D. A.; Lu, Q.-B. *Proc. Natl. Acad. Sci. U. S. A.* **2011**, *108*, 11778-11783.

(11)   Jones, G. D. D.; Symonds, P. *Molecular, cellular and tissue effects of radiotherapy. https://radiologykey.com/molecular-cellular-and-tissue-effects-of-radiotherapy/.*

(12)   Hatzi, V. I.; Laskaratou, D. A.; Mavragani, I. V.; Nikitaki, Z.; Mangelis, A.; Panayiotidis, M. I.; Pantelias, G. E.; Terzoudi, G. I.; Georgakilas, A. G. *Cancer Lett.* **2015**, *356*, 34-42.

(13)   Sridharan, D. M.; Asaithamby, A.; Bailey, S. M.; Costes, S. V.; Doetsch, P. W.; Dynan, W. S.; Kronenberg, A.; Rithidech, K. N.; Saha, J.; Snijders, A. M.; Werner, E.; Wiese, C.; Cucinotta, F. A.; Pluth, J. M. *Radiat. Res.* **2015**, *183*, 1-26.

(14)   Roos, W. P.; Kaina, B. *Trends Mol. Med.* **2006**, *12*, 440-450.

(15)   Markus, L.; Jürgen, K. *Int. J. Cancer* **2006**, *118*, 2652-2656.

(16)   Wardman, P. *Clin. Oncol.* **2007**, *19*, 397-417.

(17)   Rak, J.; Chomicz, L.; Wiczk, J.; Westphal, K.; Zdrowowicz, M.; Wityk, P.; Żyndul, M.; Makurat, S.; Golon, Ł. *J. Phys. Chem. B* **2015**, *119*, 8227-8238.

(18)   Baccarelli, I.; Bald, I.; Gianturco, F. A.; Illenberger, E.; Kopyra, J. *Phys. Rep.* **2011**, *508*, 1-44.

(19)   Lehnert, S. *Radiosensitizers and Radiochemotherapy in the Treatment of Cancer*; CRC Press, Taylor & Francis Group: Boca Raton 2015, 93-118.

(20)   Rich, T. A. *Oncology (Williston Park)* **1999**, *13*, 131-134.

(21)   Whittington, R.; Neuberg, D.; Tester, W. J.; 3rd, A. B. B.; Haller, D. G. *J. Clin. Oncol.* **1995**, *13*, 227-232.

(22)   Sawada, N.; Ishikawa, T.; Sekiguchi, F.; Tanaka, Y.; Ishitsuka, H. *Clin. Cancer Res.* **1999**, *5*, 2948-2953.

(23)   British national formulary : BNF 69 (69 ed.). British Medical Association. 2015. pp. 585, 588. ISBN 9780857111562

(24)   Shewach, D. S.; Hahn, T. M.; Chang, E.; Hertel, L. W.; Lawrence, T. S. *Cancer Res.* **1994**, *54*, 3218-3223.

(25)   Ma, P. a.; Xiao, H.; Li, C.; Dai, Y.; Cheng, Z.; Hou, Z.; Lin, J. *Mater. Today* **2015**, *18*, 554-564.

(26)   Richmond, R. C. *Radiat. Res.* **1984**, *99*, 596-608.

(27)   Yang, L.-x.; Douple, E. B.; Wang, H.-j. *Int. J. Radiat. Oncol. Biol. Phys.* **1995**, *33*, 641-646.

(28)   Amorino, G. P.; Freeman, M. L.; Carbone, D. P.; Lebwohl, D. E.; Choy, H. *Int. J. Radiat. Oncol. Biol. Phys.* **1999**, *44*, 399-405.

(29)   Dewhirst, M. W. *Radiat. Res.* **2009**, *172*, 653-665.

(30)   Brown, J. M.; Wilson, W. R. *Nat. Rev. Cancer* **2004**, *4*, 437-447.

(31)   Wilson, W. R.; Hay, M. P. *Nat. Rev. Cancer* **2011**, *11*, 393-410.

(32)   Thomlinson, R. H.; Gray, L. H. *Br. J. Cancer* **1955**, *9*, 539-549.

(33)   Peters, K. B.; Brown, J. M. *Cancer Res.* **2002**, *62*, 5248-5253.

(34)   Ahn, G. O.; Ware, D. C.; Denny, W. A.; Wilson, W. R. *Radiat. Res.* **2004**, *162*, 315-325.

(35)   Kriste, A. G.; Tercel, M.; Anderson, R. F.; Ferry, D. M.; Wilson, W. R. *Radiat. Res.* **2002**, *158*, 753-762.

(36)   Shibamoto, Y.; Zhou, L.; Hatta, H.; Mori, M.; Nishimoto, S.-i. *Jpn. J. Cancer Res.* **2000**, *91*, 433-438.

(37)   Brase, S.; Gil, C.; Knepper, K.; Zimmermann, V. *Angew. Chem. Int. Ed. Engl.* **2005**, *44*, 5188-5240.

(38)   Chen, Y.; Kamlet, A. S.; Steinman, J. B.; Liu, D. R. *Nat. Chem.* **2011**, *3*, 146-153.

(39)   Amblard, F.; Cho, J. H.; Schinazi, R. F. *Chem. Rev. (Washington, DC, U. S.)* **2009**, *109*, 4207-4220.

(40)   Neef, A. B.; Luedtke, N. W. *ChemBioChem* **2014**, *15*, 789-793.

(41)   Shiau, G. T.; Schinazi, R. F.; Chen, M. S.; Prusoff, W. H. *J. Med. Chem.* **1980**, *23*, 127-133.

(42)   Adhikary, A.; Khanduri, D.; Pottiboyina, V.; Rice, C. T.; Sevilla, M. D. *J. Phys. Chem. B* **2010**, *114*, 9289-9299.

(43)   Prescher, J. A.; Bertozzi, C. R. *Nat. Chem. Biol.* **2005**, *1*, 13-21.

(44)   Rostovtsev, V. V.; Green, L. G.; Fokin, V. V.; Sharpless, K. B. *Angew. Chem. Int. Ed.* **2002**, *41*, 2596-2599.

(45)   Tornøe, C. W.; Christensen, C.; Meldal, M. *J. Org. Chem.* **2002**, *67*, 3057-3064.

(46)   Agard, N. J.; Prescher, J. A.; Bertozzi, C. R. *J. Am. Chem. Soc.* **2004**, *126*, 15046-15047.

(47)   Chang, P. V.; Prescher, J. A.; Sletten, E. M.; Baskin, J. M.; Miller, I. A.; Agard, N. J.; Lo, A.; Bertozzi, C. R. *Proc. Natl. Acad. Sci. U. S. A.* **2010**, *107*, 1821-1826.

(48)   Hein, C. D.; Liu, X.-M.; Wang, D. *Pharm. Res.* **2008**, *25*, 2216-2230.

(49)   Nwe, K.; Brechbiel, M. W. *Cancer Biother. Radiopharm.* **2009**, *24*, 289-302.

(50)   Yang, P.-Y.; Wang, M.; He, C. Y.; Yao, S. Q. *Chem. Commun. (Cambridge, U. K.)* **2012**, *48*, 835-837.

(51)   Zayas, J.; Annoual, M.; Das, J. K.; Felty, Q.; Gonzalez, W. G.; Miksovska, J.; Sharifai, N.; Chiba, A.; Wnuk, S. F. *Bioconjug. Chem.* **2015**, *26*, 1519-1532.

(52)   Gourdain, S.; Martinez, A.; Petermann, C.; Harakat, D.; Clivio, P. *J. Org. Chem.* **2009**, *74*, 6885-6887.

(53)   Liu, Y.; Wang, X.-F.; Chen, Y.; Zhang, L.-H.; Yang, Z.-J. *MedChemComm* **2012**, *3*, 506-511.

(54)   Krim, J.; Taourirte, M.; Grünewald, C.; Krstic, I.; Engels, J. W. *Synthesis* **2013**, *45*, 396-405.

(55)   Xu, X.; Yan, S.; Hu, J.; Guo, P.; Wei, L.; Weng, X.; Zhou, X. *Tetrahedron* **2013**, *69*, 9870-9874.

(56)   Haque, M. M.; Sun, H.; Liu, S.; Wang, Y.; Peng, X. *Angew. Chem., Int. Ed. Engl.* **2014**, *53*, 7001-7005.

(57)   Ren, X.; El-Sagheer, A. H.; Brown, T. *Analyst* **2015**, *140*, 2671-2678.

(58)   Horwitz, J. P.; Chua, J.; Noel, M. *J. Org. Chem.* **1964**, *29*, 2076-2078.

(59)   Tárkányi, I.; Aradi, J. *Biochimie* **2008**, *90*, 156-172.

(60)   Housri, N.; Yarchoan, R.; Kaushal, A. *Cancer* **2010**, *116*, 273-283.

(61)   Kampf, A.; Barfknecht, R. L.; Shaffer, P. J.; Osaki, S.; Mertes, M. P. *J. Med. Chem.* **1976**, *19*, 903-908.

(62)   Balzarini, J.; De Clercq, E.; Mertes, M. P.; Shugar, D.; Torrence, P. F. *Biochem. Pharmacol.* **1982**, *31*, 3673-3682.

(63)   Kampf, A.; Pillar, C. J.; Woodford, W. J.; Mertes, M. P. *J. Med. Chem.* **1976**, *19*, 909-915.

(64)   Balzarini, J.; De Clercq, E.; Torrenc, P. F.; Mertes, M. P.; Park, J. S.; Schmidt, C. L.; Shugar, D.; Barra, P. J.; Jones, A. S.; Verhelst, G.; Walker, R. T. *Biochem. Pharmacol.* **1982**, *31*, 1089-1095.

(65)   Reefschläger, J.; Bärwolff, D.; Engelmann, P.; Langen, P.; Rosenthal, H. A. *Antiviral Res.* **1982**, *2*, 41-52.

(66)   De clercq, E.; Descamps, J.; Schmidt, C. L.; Mertes, M. P. *Biochem. Pharmacol.* **1979**, *28*, 3249-3254.

(67)   Kumar, P.; Hornum, M.; Nielsen, L. J.; Enderlin, G.; Andersen, N. K.; Len, C.; Hervé, G.; Sartori, G.; Nielsen, P. *J. Org. Chem.* **2014**, *79*, 2854-2863.

(68)   Balzarini, J.; Andrei, G.; Kumar, R.; Knaus, E. E.; Wiebe, L. I.; De Clercq, E. *FEBS Lett.* **1995**, *373*, 41-44.

(69)   Srivastav, N. C.; Manning, T.; Kunimoto, D. Y.; Kumar, R. *Med. Chem.* **2006**, *2*, 287-293.

(70)   Zhou, F.-X.; Liao, Z.-K.; Dai, J.; Xiong, J.; Xie, C.-H.; Luo, Z.-G.; Liu, S.-Q.; Zhou, Y.-F. *Biochem. Biophys. Res. Commun.* **2007**, *354*, 351-356.

(71)   Liao, Z. K.; Zhou, F. X.; Luo, Z. G.; Zhang, W. J.; Xiong, J.; Bao, J.; Han, G.; Zhang, M. S.; Xie, C. H.; Zhou, Y. F. *Oncol. Rep.* **2008**, *19*, 281-286.

(72)   Coucke, P. A.; Cottin, E.; Decosterd, L. A. *Acta Oncol.* **2007**, *46*, 612-620.

(73)   Mudgal, M.; Rishi, S.; Lumpuy, D. A.; Curran, K. A.; Verley, K. L.; Sobczak, A. J.; Dang, T. P.; Sulimoff, N.; Kumar, A.; Sevilla, M. D.; Wnuk, S. F.; Adhikary, A. *J. Phys. Chem. B* **2017**, *121*, 4968-4980.

(74)   Greenberg, M. M. *Acc. Chem. Res.* **2012**, *45*, 588-597.

(75)   Jagetia, G. C.; Aruna, R. *Toxicol. Lett.* **2003**, *139*, 33-43.

(76)   Erik, H. R.; J., D. P.; K., B. J. *Angew. Chem. Int. Ed.* **1997**, *36*, 2714-2730.

(77)   Chatgilialoglu, C.; Caminal, C.; Altieri, A.; Vougioukalakis, G. C.; Mulazzani, Q. G.; Gimisis, T.; Guerra, M. *J. Am. Chem. Soc.* **2006**, *128*, 13796-13805.

(78)   Candeias, L. P.; Steenken, S. *J. Am. Chem. Soc.* **1989**, *111*, 1094-1099.

(79)   Steenken, S. *Chem. Rev. (Washington, DC, U. S.)* **1989**, *89*, 503-520.

(80)   P., C. L.; Steen, S. *Chem. Eur. J.* **2000**, *6*, 475-484.

(81)   Chatgilialoglu, C.; D'Angelantonio, M.; Guerra, M.; Kaloudis, P.; Mulazzani, Q. G. *Angew. Chem. Int. Ed.* **2009**, *48*, 2214-2217.

(82)   Mundy, C. J.; Colvin, M. E.; Quong, A. A. *J. Phys. Chem. A* **2002**, *106*, 10063-10071.

(83) Chryssostomos, C.; Clara, C.; Maurizio, G.; G., M. Q. *Angew. Chem.* **2005**, *117*, 6184-6186.

(84) Chryssostomos, C.; Clara, C.; Maurizio, G.; G., M. Q. *Angew. Chem. Int. Ed.* **2005**, *44*, 6030-6032.

(85) Zheng, L.; Lin, L.; Qu, K.; Adhikary, A.; Sevilla, M. D.; Greenberg, M. M. *Org. Lett.* **2017**, *19*, 6444-6447.

(86) Daniels, M.; Hauswirth, W. *Science* **1971**, *171*, 675-677.

(87) Greco, N. J.; Tor, Y. *J. Am. Chem. Soc.* **2005**, *127*, 10784-10785.

(88) Holz, B.; Klimasauskas, S.; Serva, S.; Weinhold, E. *Nucleic Acids Res.* **1998**, *26*, 1076-1083.

(89) Srivatsan, S. G.; Tor, Y. *J. Am. Chem. Soc.* **2007**, *129*, 2044-2053.

(90) Srivatsan, S. G.; Tor, Y. *Tetrahedron* **2007**, *63*, 3601-3607.

(91) Tanpure, A. A.; Pawar, M. G.; Srivatsan, S. G. *Isr. J. Chem.* **2013**, *53*, 366-378.

(92) Wilhelmsson, L. M. *Q. Rev. Biophys.* **2010**, *43*, 159-183.

(93) Xu, W.; Chan, K. M.; Kool, E. T. *Nat. Chem.* **2017**, *9*, 1043.

(94) Seo, Y. J.; Ryu, J. H.; Kim, B. H. *Org. Lett.* **2005**, *7*, 4931-4933.

(95) Ozols, K.; Cīrule, D.; Novosjolova, I.; Stepanovs, D.; Liepinsh, E.; Bizdēna, Ē.; Turks, M. *Tetrahedron Lett.* **2016**, *57*, 1174-1178.

(96) Kavoosi, S.; Rayala, R.; Walsh, B.; Barrios, M.; Gonzalez, W. G.; Miksovska, J.; Mathivathanan, L.; Raptis, R. G.; Wnuk, S. F. *Tetrahedron Lett.* **2016**, *57*, 4364-4367.

(97) Lawson, C. P.; Dierckx, A.; Miannay, F.-A.; Wellner, E.; Wilhelmsson, L. M.; Grotli, M. *Org. Biomol. Chem.* **2014**, *12*, 5158-5167.

(98) Dyrager, C.; Börjesson, K.; Dinér, P.; Elf, A.; Albinsson, B.; Wilhelmsson, L. M.; Grøtli, M. *Eur. J. Org. Chem.* **2009**, *2009*, 1515-1521.

(99) Redwan, I. N.; Bliman, D.; Tokugawa, M.; Lawson, C.; Grøtli, M. *Tetrahedron* **2013**, *69*, 8857-8864.

(100) Kočalka, P.; Andersen, N. K.; Jensen, F.; Nielsen, P. *ChemBioChem* **2007**, *8*, 2106-2116.

(101) Hatano, A.; Kurosu, M.; Yonaha, S.; Okada, M.; Uehara, S. *Org. Biomol. Chem.* **2013**, *11*, 6900-6905.

(102) Jin, T.; Kamijo, S.; Yamamoto, Y. *Eur. J. Org. Chem.* **2004**, *2004*, 3789-3791.

(103) Barluenga, J.; Valdés, C.; Beltrán, G.; Escribano, M.; Aznar, F. *Angew. Chem. Int. Ed.* **2006**, *45*, 6893-6896.

(104) Quan, X.-J.; Ren, Z.-H.; Wang, Y.-Y.; Guan, Z.-H. *Org. Lett.* **2014**, *16*, 5728-5731.

(105) Kalisiak, J.; Sharpless, K. B.; Fokin, V. V. *Org. Lett.* **2008**, *10*, 3171-3174.

(106) Cha, H.; Lee, K.; Chi, D. Y. *Tetrahedron* **2017**, *73*, 2878-2885.

(107) Hicks, K. O.; Pruijn, F. B.; Sturman, J. R.; Denny, W. A.; Wilson, W. R. *A Pharmacokinetic/Pharmacodynamic Study in HT29 Multicellular Layer Cultures* **2003**, *63*, 5970-5977.

(108) Huttunen, K. M.; Raunio, H.; Rautio, J. *Pharmacol. Rev.* **2011**, *63*, 750-771.

(109) Pradere, U.; Garnier-Amblard, E. C.; Coats, S. J.; Amblard, F.; Schinazi, R. F. *Chem. Rev. (Washington, DC, U. S.)* **2014**, *114*, 9154-9218.

(110) Liang, Y.; Suzol, S. H.; Wen, Z.; Artiles, A. G.; Mathivathanan, L.; Raptis, R. G.; Wnuk, S. F. *Org. Lett.* **2016**, *18*, 1418-1421.

(111) Liang, Y.; Gloudeman, J.; Wnuk, S. F. *J. Org. Chem.* **2014**, *79*, 4094-4103.

(112) Zhang, X.; Yang, H.; Tang, P. *Org. Lett.* **2015**, *17*, 5828-5831.

(113) Fan, X.; Zhang, X.; Zhou, L.; Keith, K. A.; Kern, E. R.; Torrence, P. F. *J. Med. Chem.* **2006**, *49*, 3377-3382.

(114) Fomich, M. A.; Kvach, M. V.; Navakouski, M. J.; Weise, C.; Baranovsky, A. V.; Korshun, V. A.; Shmanai, V. V. *Org. Lett.* **2014**, *16*, 4590-4593.

(115) Liu, Z.; Liao, P.; Bi, X. *Org. Lett.* **2014**, *16*, 3668-3671.

(116) Kumar, R.; Wiebe, L. I.; Knaus, E. E. *Can. J. Chem.* **1996**, *74*, 1609-1615.

(117) Fu, J.; Zanoni, G.; Anderson, E. A.; Bi, X. *Chem. Soc. Rev.* **2017**, *46*, 7208-7228.

(118) Robins, M. J.; Barr, P. J. *J. Org. Chem.* **1983**, *48*, 1854-1862.

(119) Suzol, S. H.; Howlader, A. H.; Wen, Z.; Ren, Y.; Laverde, E. E.; Garcia, C.; Liu, Y.; Wnuk, S. F. *ACS Omega* **2018**, *3*, 4276-4288.

(120) Guan, L.; van der Heijden, G. W.; Bortvin, A.; Greenberg, M. M. *ChemBioChem* **2011**, *12*, 2184-2190.

(121) Hu, B.; DiMagno, S. G. *Org. Biomol. Chem.* **2015**, *13*, 3844-3855.

(122) Hoard, D. E.; Ott, D. G. *J. Am. Chem. Soc.* **1965**, *87*, 1785-1788.

(123) Kovács, T.; Ötvös, L. *Tetrahedron Lett.* **1988**, *29*, 4525-4528.

(124) von Watzdorf, J.; Leitner, K.; Marx, A. *Angew. Chem. Int. Ed.* **2016**, *55*, 3229-3232.

(125) Röthlisberger, P.; Levi-Acobas, F.; Hollenstein, M. *Bioorg. Med. Chem. Lett.* **2017**, *27*, 897-900.

(126) Bernhard, W. A. *Wiley Ser. React. Intermed. Chem. Biol.* **2009**, *2*, 41-68.

(127) Sagstuen, E.; Hole, E. O.; John Wiley & Sons, Inc.: 2009, p 325-382.

(128) Close, D. Radiation Induced Molecular Phenomena in Nucleic Acids; Shukla, M., Leszczynski, J., Eds.; Springer Netherlands: 2008; Vol. 5, p 493-529.

(129) Wen, Z.; Peng, J.; Tuttle, P.; Debnath, D.; Rishi, S.; Hanson, C.; Ward, S.; Ren, Y.; Garcia, C.; Liu, Y.; Liu, Y.; Zhao, W.; Glazer, P. M.; Kumar, A.; Sevilla, M. D.; Adhikary, A.; Wnuk, S. F. Radiation Damage to Hypoxic Cells Augmented by Aminyl Radicals Formed via Electron Addition to 5-Azido-modified Pyrimidine Nucleosides. *To be submitted.*

(130) Adhikary, A.; Kumar, A.; Bishop, C. T.; Wiegand, T. J.; Hindi, R. M.; Adhikary, A.; Sevilla, M. D. *J. Phys. Chem. B* **2015**, *119*, 11496-11505.

(131) Mandel, S. M.; Singh, P. N. D.; Muthukrishnan, S.; Chang, M.; Krause, J. A.; Gudmundsdóttir, A. D. *Org. Lett.* **2006**, *8*, 4207-4210.

(132) Bencivenni, G.; Lanza, T.; Leardini, R.; Minozzi, M.; Nanni, D.; Spagnolo, P.; Zanardi, G. *J. Org. Chem.* **2008**, *73*, 4721-4724.

(133) *Electron Spin Resonace*; Ayscough, P. B., Ed.

(134) Dextraze, M. E.; Wagner, J. R.; Hunting, D. J. *Biochemistry* **2007**, *46*, 9089-9097.

(135) Greenberg, M. M. *Radiat. Phys. Chem.* **2016**, *128*, 82-91.

(136) McGinn, C. J.; Shewach, D. S.; Lawrence, T. S. *J. Natl. Cancer Inst.* **1996**, *88*, 1193-1203.

(137) A. Gottinger, H.; E. Zubarev, V.; Brede, O. *J. Chem. Soc., Perkin Trans. 2* **1997**, 2167-2172.

(138) Hohman, W. F.; Palcic, B.; Skarsgard, L. D. *Int. J. Radiat. Biol. Relat. Stud. Phys. Chem. Med.* **1976**, *30*, 247-261.

(139) Millar, B. C.; Fielden, E. M.; Smithen, C. E. *Br. J. Cancer Suppl.* **1978**, *3*, 73-79.

(140) Dodd, D. W.; Swanick, K. N.; Price, J. T.; Brazeau, A. L.; Ferguson, M. J.; Jones, N. D.; Hudson, R. H. E. *Org. Biomol. Chem.* **2010**, *8*, 663-666.

(141) Reddy, M. R.; Shibata, N.; Kondo, Y.; Nakamura, S.; Toru, T. *Angew. Chem.* **2006**, *118*, 8343-8346.

(142) Shinohara, Y.; Matsumoto, K.; Kugenuma, K.; Morii, T.; Saito, Y.; Saito, I. *Bioorg. Med. Chem. Lett.* **2010**, *20*, 2817-2820.

(143) Sheehan, J. C.; Robinson, C. A. *J. Am. Chem. Soc.* **1949**, *71*, 1436-1440.

(144) Journet, M.; Cai, D.; Kowal, J. J.; Larsen, R. D. *Tetrahedron Lett.* **2001**, *42*, 9117-9118.

(145) Salic, A.; Mitchison, T. J. *Proc. Natl. Acad. Sci. U. S. A.* **2008**, *105*, 2415-2420.

(146) Neef, A. B.; Luedtke, N. W. *Proc. Natl. Acad. Sci. U. S. A.* **2011**, *108*, 20404-20409.

(147) Wen, Z.; Suzol, S. H.; Peng, J.; Liang, Y.; Snoeck, R.; Andrei, G.; Liekens, S.; Wnuk, S. F. *Arch. Pharm.* **2017**, e1700023-n/a.

(148) Acedo, M.; Fàbrega, C.; Aviño, A.; Goodman, M.; Fagan, P.; Wemmer, D.; Eritja, R. *Nucleic Acids Res.* **1994**, *22*, 2982-2989.

(149) Fabrega, C.; Guimil Garcia, R.; Diaz, A. R.; Eritja, R. *Biol. Chem.* **1998**, *379*, 527-533.

(150) Claudio-Montero, A.; Pinilla-Macua, I.; Fernández-Calotti, P.; Sancho-Mateo, C.; Lostao, M. a. P.; Colomer, D.; Grandas, A.; Pastor-Anglada, M. *Mol. Pharm.* **2015**, *12*, 2158-2166.

(151) Liu, Y.; Prasad, R.; Beard, W. A.; Hou, E. W.; Horton, J. K.; McMurray, C. T.; Wilson, S. H. *J. Biol. Chem.* **2009**, *284*, 28352-28366.

(152) Xu, M.; Lai, Y.; Torner, J.; Zhang, Y.; Zhang, Z.; Liu, Y. *Nucleic Acids Res.* **2014**, *42*, 3675-3691.

(153) Petrovici, A.; Adhikary, A.; Kumar, A.; Sevilla, M. *Molecules* **2014**, *19*, 13486.

(154) Adhikary, A.; Becker, D.; Sevilla, M. D. In Applications of EPR in Radiation Research; Lund, A., Shiotani, M., Eds.; Springer International Publishing: 2014, p 299-352.

(155) http://jmol.sourceforge.net

(156) Rockwell, S.; Keyes, S. R.; Sartorelli, A. C. *Radiat. Res.* **1988**, *116*, 100-113.

VITA

ZHIWEI WEN

Born, Quanzhou, China

2018	FIU Graduate School, Dissertation Year Fellowship
2013-2018	Ph.D. candidate, Organic Chemistry Florida International University Miami, Florida, U.S.
2009-2012	Master, Analytical Chemistry CIAC, Chinese Academy of Sciences Changchun, P. R. China
2005-2009	Bachelor, Chemistry Fuzhou University Fuzhou, P. R. China

PUBLICATIONS (Citations: 537, Web of Science 03/30/2018)

1. Z. Wen, J. Peng, P. Tuttle, A. Petrovici, S. Rishi, C. Hanson, Y. Ren, C. Garcia, Y. Liu, M. D. Sevilla, A. Adhikary, and S. F. Wnuk. Radiation Damage to Cells Augmented by Electron-induced Aminyl Radicals in 5-Azido-modified Pyrimidine Nucleosides Incorporated into DNA-fragments. *Submitted to JACS.*

2. Z. Wen, P. Tuttle, A. Vasilyeva, A. Tangar, J. Miksovska, and S. F. Wnuk. 5-Pyrimidine and 8-Purine Nucleosides Modified with *N*-unsubstituted 1,2,3-Triazol-4-yl: Synthesis and Fluorescent Properties. *To be submitted to Org. Lett.*

3. M.L.S. Guther, R. Lowden, Z. Wen, L. Stojanovski, K. Read, S. F. Wnuk, and M.A.J. Ferguson. In Vivo and in Vitro Studies with 6'-*E*-Chlorohomovinyladenosine Aiming Treatment of Human African Sleeping Sickness, Leishmaniasis and Chagas Disease. *In preparation*.

4. S. H. Suzol, A. H. Howlader, Z. Wen, Y. Ren, E. E. Laverde, C. Garcia, Yuan Liu, and S. F. Wnuk. *ACS Omega* 2018, (3), 4276-4288

5. Z. Wen, S. H. Suzol, J. Peng, Y. Liang, R. Snoeck, G. Andrei, S. Liekens, and S. F. Wnuk. *Arch. Pharm. (Weinheim, Ger.)* 2017, e1700023-n/a.

6. Y. Liang, S. H. Suzol, Z. Wen, A. G. Artiles, L. Mathivathanan, R. G. Raptis, and S. F. Wnuk. *Org. Lett.* 2016 (18): 1418-1421.

7. Y. Sun, Z. Wen, F. Xu, Y. Zhang, Y. Shi, H. Dai, and Z. Li. *Anal. Methods.* 2014 (6): 337-340.

8. Y. Shi, J. Wu, Y. Sun, Y. Zhang, Z. Wen, H. Dai, H. Wang, and Z. Li. *Biosens. Bioelectron.* 2012 (38): 31-36.

9. F. Xu, Y. Zhang, Y. Sun, Y. Shi, <u>Z. Wen</u>, and Z. Li. *J. Phys. Chem. C* 2011 (115): 9977-9983.

10. F. Xu, Y. Sun, Y. Zhang, Y. Shi, <u>Z. Wen</u>, and Z. Li. *Electrochem. Commun.* 2011 (13): 1131-1134.

11. Y. Zhang, F. Xu, Y. Sun, Y. Shi, <u>Z. Wen</u>, and Z. Li. *J. Mater. Chem.* 2011 (21): 16949-16954.

12. Y. Sun, F. Xu, Y. Zhang, Y. Shi, <u>Z. Wen</u>, and Z. Li. *J. Mater. Chem.* 2011 (21): 16675-16685.

13. Y. Shi, C. Guo, Y. Sun, Z. Liu, F. Xu, Y. Zhang, <u>Z. Wen</u>, and Z. Li. *Biomacromolecules* 2011 (12): 797-803.

14. Y. Zhang, Y. Sun, Z. Liu, F. Xu, K. Cui, Y. Shi, <u>Z. Wen</u>, and Z. Li. *J. Electroanal. Chem.* 2011 (656): 23-28.

15. Y. Shi, Z. Liu, B. Zhao, Y. Sun, F. Xu, Y. Zhang, <u>Z. Wen</u>, H. Yang, and Z. Li. *J. Electroanal. Chem.* 2011 (656): 29-33.

16. Y. Zhang, F. Xu, Y. Sun, C. Guo, Y. Shi, <u>Z. Wen</u>, and Z. Li. *Chem-Eur. J.* 2010 (16): 9248-9256.

17. Z. Li, <u>Z. Wen</u>, Y. Zhang, F. Xu, Y. Sun, Y. Shi, H. Dai. Surface Enhanced Raman Scattering (SERS) Substrate and Preparation Method Thereof. 2014. China. CN102608103 B. CN 201210091092.

18. Z. Li, F. Xu, Y. Sun, Y. Zhang, Y. Shi, <u>Z. Wen</u>. Method for Detecting Melamine. 2011. China. CN102156118 A. CN 201110068576.

19. Z. Li, F. Xu, Y. Zhang, Y. Sun, Y. Shi, <u>Z. Wen</u>. Substrate for Surface Enhanced Raman Scattering and Preparation Method Thereof. 2011. China. CN102156117 A. CN 201110068574.

20. <u>Z. Wen</u>, P. Tuttle, A. Vasilyeva, A. Tangar, J. Miksovska, and S. F. Wnuk. 255th ACS national meeting (oral presentation). Mar. 2018, New Orleans.

21. P. Tuttle, <u>Z. Wen</u>, A. Vasilyeva, and S. F. Wnuk. 255th ACS national meeting (poster). Mar. 2018, New Orleans.

22. <u>Z. Wen</u>, J. Peng, P. Tuttle, Y. Liang, S. Rishi, A. Adhikary, M. D. Sevilla, C. Garcia, Y. Ren, Y. Liu, and S. F. Wnuk. 253rd ACS national meeting (oral presentation). Apr. 2017, San Francisco.

23. C. Garcia, Y. Ren, <u>Z. Wen</u>, S. F. Wnuk, and Y. Liu. 253rd ACS national meeting (poster). Apr. 2017, San Francisco.

24. S. F. Wnuk, M. Mudgal, <u>Z. Wen</u>, A. Adhikary, and M.D. Sevilla. 22nd International Round Table Symposium: Nucleosides, Nucleotides and their Biological Applications (poster presentation). Jul. 2016, Paris, France.

25. Y. Liang, S. H. Suzol, <u>Z. Wen</u>, A. Artiles, I. Jesus da Silva, M. Dinh, A. Akinniyi, and S. F. Wnuk. 251st ACS national meeting (oral presentation). 2016, San Diego.

26. <u>Z. Wen</u>, F. Xu, Y. Zhang, Y. Sun, Y. Shi, H. Dai and Z. Li. The 13th International Symposium on Electroanalytical Chemistry (poster). 2011, 193. Changchun.

27. F. Xu, <u>Z. Wen</u>, Y. Sun, Y. Zhang, Y. Shi, Z. Li. The 13th International Symposium on Electroanalytical Chemistry (poster). 2011, 114. Changchun.